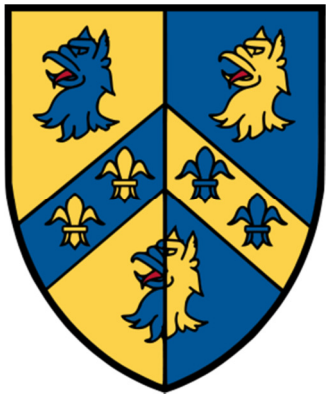
Potential Mechanisms Underlying Impaired Left Ventricular Function in Atrial Fibrillation: Insights from Multi-Parametric Cardiac Magnetic Resonance

Rohan S. Wijesurendra
MB BChir, MA (Cantab), MRCP (UK)





Trinity College
Division of Cardiovascular Medicine
Radcliffe Department of Medicine
Oxford Centre for Clinical Magnetic Resonance Research
University of Oxford

A thesis submitted for the degree of Doctor of Philosophy in Cardiovascular Medicine

Trinity Term 2017

Acknowledgements

The work presented in this thesis would not have been possible without an outstanding group of colleagues, collaborators, and mentors. I feel enormously privileged to be able to continue to work in such a multi-disciplinary and stimulating environment.

I am particularly grateful to my supervisors, Barbara Casadei, Stefan Neubauer, and Vanessa Ferreira. Each of you has been a tremendous source of encouragement, insight, and direction. Perhaps most importantly, as incredible role models, you have inspired me to pursue a career in clinical academia.

I sincerely thank the patients and volunteers who so generously gave up their time to participate in these studies. I also acknowledge the Oxford British Heart Foundation Centre for Research Excellence, the British Heart Foundation, and the National Institute for Health Research Oxford Biomedical Research Centre, for supporting this research.

Above all, my deepest thanks to Dalia, for your love, patience, and support, and to my parents, for your lifelong love and encouragement.

This thesis is dedicated to my children, Rahul and Alyssa.

Abstract

Atrial fibrillation (AF) is the most common sustained arrhythmia and is associated with significant cardiovascular complications, including stroke, myocardial infarction, heart failure, and premature death. The presence of subtle left ventricular (LV) dysfunction is increasingly recognised in patients with AF, raising questions regarding the underlying pathophysiology and potential treatment strategies. I used advanced and multiparametric cardiac magnetic resonance (CMR) methods to investigate potential mechanisms that could contribute to LV dysfunction in patients with AF, controlled ventricular rate and no significant cardiovascular comorbidities (i.e., with so-called "lone" AF). Patients were evaluated before and after catheter ablation, allowing examination of the effect of restoration of sinus rhythm and reduction in AF burden on LV structure, function, energetics, tissue characteristics, and perfusion.

I demonstrated for the first time that patents with lone AF before ablation have significantly impaired ventricular energetics and a subtle reduction in LV systolic function compared to control subjects in sinus rhythm. Furthermore, there was only modest improvement (but not normalisation) in LV function following successful ablation, and myocardial energetics remained impaired despite a significant and sustained reduction in AF burden. These findings imply that lone AF may actually be the consequence (rather than the cause) of an underlying cardiomyopathy.

Next, to interrogate advanced ventricular tissue characteristics (such as diffuse myocardial fibrosis) in patients with tachyarrhythmia, I developed a novel CMR method involving a systolic readout T1-mapping sequence. Methodological work in volunteers

and patients with tachyarrhythmia demonstrated that this method reports clinically equivalent T1 values to the conventional diastolic readout in healthy volunteers, and was feasible in tachyarrhythmia, producing excellent quality T1 maps. When applied to the investigation of patients with AF, I demonstrated that subtle LV dysfunction in lone AF occurs in the absence of CMR evidence of diffuse myocardial fibrosis, suggesting that LV dysfunction may be reversible with appropriate and targeted therapeutic strategies initiated prior to the development of structural LV remodelling.

Finally, I used quantitative perfusion imaging to determine absolute myocardial blood flow and coronary reserve in patients with AF, and determine whether microvascular coronary dysfunction could underlie impaired LV function and energetics in patients with AF. I found that myocardial perfusion is significantly reduced in patients with AF in the absence of significant epicardial coronary artery disease, both at baseline and under conditions of vasodilator stress. Lower baseline blood flow was related to reduced LV performance, and there was no significant change in perfusion after successful AF ablation. These novel findings indicate that coronary microvascular dysfunction may be an important pathophysiological mechanism in lone AF, and at least partially responsible for LV dysfunction.

Overall, the findings reported in this thesis have potentially far-reaching implications for the management of patients with AF. They suggest that approaches that predominantly target rhythm control (including anti-arrhythmic medications and ablation) are insufficient to normalise the systemic and cardiometabolic phenotype in patients with AF. Further studies are needed to investigate whether novel approaches that target microvascular and energetic dysfunction in patients with AF can contribute to durable restoration of sinus rhythm and improve clinical outcomes.

List of Publications, Prizes, and Awards

Manuscripts Contributing to D. Phil. Thesis

1. **Wijesurendra RS**, Casadei B. Atrial fibrillation: effects beyond the atrium? *Cardiovasc Res* 2015 Mar 1;105 (3):238-47

2. **Wijesurendra RS**, Liu A, Eichhorn C, Ariga R, Levelt E, Clarke WT, Rodgers CT, Karamitsos TD, Bashir Y, Ginks M, Rajappan K, Betts T, Ferreira VM, Neubauer S, Casadei B. "Lone" atrial fibrillation is associated with impaired left ventricular energetics that persist despite successful catheter ablation. *Circulation* 2016 Oct;134(15):1068-1081. doi: 10.1161/CIRCULATIONAHA.116.022931

3. Ferreira VM*, **Wijesurendra RS* [*equal contribution],** Liu A, Greiser A, Casadei B, Robson MD, Neubauer S, Piechnik SK. Systolic ShMOLLI myocardial T1 mapping for improved robustness to partial-volume effects and applications in tachyarrhythmias. *J Cardiovasc Magn Reson* 2015; 17(1):77. doi: 10.1186/s12968-015-0182-5.

4. **Wijesurendra RS**, Liu A, Eichhorn C, Karamitsos TD, Bashir Y, Ginks M, Rajappan K, Betts T, Piechnik SK, Neubauer S, Casadei B, Ferreira VM. Early Left Ventricular Dysfunction in Lone Atrial Fibrillation is Independent of Diffuse Myocardial Fibrosis. *In Preparation.*

5. **Wijesurendra RS**, Liu A, Notaristefano F, Jerosch-Herold M, Eichhorn C, Ntusi N, Karamitsos TD, Bashir Y, Ginks M, Rajappan K, Betts T, Ferreira VM, Neubauer S,

Casadei B. Reduced Myocardial Perfusion Relates to Left Ventricular Dysfunction in Atrial Fibrillation. *J Am Heart Assoc* 2018 (accepted)

Other Publications During D. Phil.

1. **Wijesurendra RS**, Liu A, Ferreira VM, Neubauer S, Casadei B. Histopathological and Immunological Characeteristics of Tachycardia-Induced Cardiomyopathy. [Letter to the Editor] *J Am Coll Cardiol*. 2017 Sep 26;70(13):1686. doi: 10.1016/j.jacc.2017.05.083.
2. **Wijesurendra RS**, Casadei B. Seek and ye shall find: subclinical atrial fibrillation in high-risk elderly patients. [Invited Editorial] *Circulation*. 2017 Oct 3;136(14):1284-1287. doi: 10.1161/CIRCULATIONAHA.117.029397
3. **Wijesurendra RS**, Sheppard KA, Westaby S, Ormerod O, Myerson SG. The Many Faces of Cardiac Lipoma – an Egg in the Heart! *Eur Heart J Cardiovasc Imaging*. 2017 Jul 1;18(7):821. doi: 10.1093/ehjci/jex048
4. **Wijesurendra RS**, Rider OJ, Neubauer S. Left Atrial Volumes in Health and Disease Measured Using Cardiac Magnetic Resonance. [Invited Editorial] *Circ Cardiovasc Imaging.* 2017 Feb;10(2). pii: e006124. doi: 10.1161/CIRCIMAGING.117.006124.
5. **Wijesurendra RS**, Rider OJ. Atrial remodeling in obesity and hypertension - what can we learn from the ECG? [Invited Editorial] *Obesity (Silver Spring)* 2016 Dec;24(12):2448. doi: 10.1002/oby.21689.
6. **Wijesurendra R**, Casadei B. Atrial supply-demand mismatch in atrial fibrillation: The missing link between rapid rate and atrial remodeling? [Invited Editorial] *Heart Rhythm* 2015 May;12(5):1001-2. doi: 10.1016/j.hrthm.2015.01.036.

7. **Wijesurendra RS**, Carey M, Butterworth RJ, Khiani R. Pause for thought? Syncope and sinus arrest as the presenting feature of temporal lobe epilepsy. *Acute Med.* 2014; 13(2):65-7.

8. Liu A, **Wijesurendra RS**, Ariga R, Mahmod M, Levelt E, Greiser A, Petrou M, Krasopoulos G, Forfar JC, Kharbanda RK, Channon KM, Neubauer S, Piechnik SK, Ferreira VM. Splenic T1-mapping: a novel quantitative method for assessing adenosine stress adequacy for cardiovascular magnetic resonance. *J Cardiovasc Magn Reson* 2017 Jan 13;19(1):1. doi: 10.1186/s12968-016-0318-2.

9. Liu A, **Wijesurendra RS**, Francis JM, Robson MD, Neubauer S, Piechnik SK, Ferreira VM. Adenosine Stress and Rest T1 Mapping Can Differentiate Between Ischemic, Infarcted, Remote, and Normal Myocardium Without the Need for Gadolinium Contrast Agents. *JACC Cardiovasc Imaging* 2016 Jan;9(1):27-36. doi: 10.1016/j.jcmg.2015.08.018.

10. Cahill TJ, **Wijesurendra RS**, Casadei B. Rivaroxaban in Stable Cardiovascular Disease. [Letter to the Editor] *N Engl J Med*. 2018 Jan 25;378(4):397. doi: 10.1056/NEJMc1714934

11. Levelt E, Piechnik SK, Liu A, **Wijesurendra RS**, Mahmod M, Ariga R, Francis JM, Greiser A, Clarke K, Neubauer S, Ferreira VM, Karamitsos TD. Adenosine stress CMR T1-mapping detects early microvascular dysfunction in patients with type 2 diabetes mellitus without obstructive coronary artery disease. *J Cardiovasc Magn Reson.* 2017 Oct 25;19(1):81. doi: 10.1186/s12968-017-0397-8. Erratum in: *J Cardiovasc Magn Reson*. 2017 Dec 7;19(1):99.

12. Liu D, Borlotti A, Viliani D, Jerosch-Herold M, Alkhalil M, De Maria GL, Fahrni G, Dawkins S, **Wijesurendra R**, Francis J, Ferreira V, Piechnik S, Robson MD, Banning A, Choudhury R, Neubauer S, Channon K, Kharbanda R, Dall'Armellina E. CMR Native T1 Mapping Allows Differentiation of Reversible Versus Irreversible Myocardial Damage in ST-Segment-Elevation Myocardial Infarction: An OxAMI Study (Oxford Acute Myocardial Infarction). *Circ Cardiovasc Imaging* 2017 Aug;10(8). pii: e005986. doi: 10.1161/CIRCIMAGING.116.005986.

13. Werys K, Petryka-Mazurkiewicz J, Błaszczyk Ł, Miśko J, Śpiewak M, Małek ŁA, Mazurkiewicz Ł, Miłosz-Wieczorek B, Marczak M, Kubik A, Dąbrowska A, Piątkowska-Janko E, Sawionek B, **Wijesurendra R**, Piechnik SK, Bogorodzki P. Cine dyscontractility index: A novel marker of mechanical dyssynchrony that predicts response to cardiac resynchronization therapy. *J Magn Reson Imaging* 2016 Dec;44(6):1483-1492. doi: 10.1002/jmri.25295.

14. Levelt E, Rodgers CT, Clarke WT, Mahmod M, Ariga R, Francis JM, Liu A, **Wijesurendra RS**, Dass S, Sabharwal N, Robson MD, Holloway CJ, Rider OJ, Clarke K, Karamitsos TD, Neubauer S. Cardiac energetics, oxygenation, and perfusion during increased workload in patients with type 2 diabetes mellitus. *Eur Heart J* 2016 Dec 7;37(46):3461-3469. doi: 10.1093/eurheartj/ehv442.

15. Reilly SN, Liu X, Carnicer R, Recalde A, Muszkiewicz A, Jayaram R, Carena MC, **Wijesurendra R**, Stefanini M, Surdo NC, Lomas O, Ratnatunga C, Sayeed R, Krasopoulos G, Rajakumar T, Bueno-Orovio A, Verheule S, Fulga TA, Rodriguez B, Schotten U, Casadei B. Up-regulation of miR-31 in human atrial fibrillation begets the arrhythmia by depleting dystrophin and neuronal nitric oxide synthase. *Sci Transl Med* 2016 May 25;8(340):340ra74. doi: 10.1126/scitranslmed.aac4296.

Prizes and Awards During D. Phil.

1. **Melvin Judkins Young Investigator Award – Winner**

   "Reduced Absolute Myocardial Perfusion Relates to Left Ventricular Dysfunction in Lone Atrial Fibrillation Before and After Successful Catheter Ablation."

   American Heart Association, November 2017

2. **Travel Bursary** [to present oral abstract of D. Phil work, ESC Congress Barcelona]

   British Cardiovascular Society, August 2017

3. **Young Investigators E-Poster Award – 1st Prize**

   "The interplay between left ventricular function, tissue characterisation, and perfusion reserve in atrial fibrillation: insights from a longitudinal multiparametric cardiac magnetic resonance study"

   British Society for Cardiovascular Magnetic Resonance, April 2017

4. **Graduate Prize** [for work done during D. Phil]

   Radcliffe Department of Medicine, University of Oxford, September 2016

5. **Graduate Prize** [for work done during D. Phil]

   Trinity College, University of Oxford, September 2016

6. **Young Investigator Award in Clinical Science – Winner**

   "Atrial fibrillation is associated with impaired left ventricular energetics that persist despite successful catheter ablation"

   European Society of Cardiology, August 2016

7. **Investigator's Award – 1st Prize**

   "Atrial fibrillation is associated with impaired left ventricular energetics that persist after successful catheter ablation: is atrial fibrillation more than a rhythm problem?"

   British Society for Cardiovascular Magnetic Resonance, April 2016

8. **Clinical Early Career Award - Finalist**

   "Successful ablation of atrial fibrillation does not normalise left ventricular function, reverse impaired myocardial energetics or increase perfusion reserve: novel mechanistic insights with clinical implications"

   Society of Cardiovascular Magnetic Resonance, January 2016

9. **Regional Scholarship Award** [to present D.Phil work at SCMR, Los Angeles]

   Society of Cardiovascular Magnetic Resonance Scientific Sessions, January 2016

10. **Graduate Scholarship** [for work done during D. Phil]

    Trinity College, University of Oxford, September 2015

Table of Contents

Acknowledgements ..... ***ii***

Abstract ..... ***iii***

List of Publications, Prizes, and Awards ..... ***v***

Table of Contents ..... ***xi***

Abbreviations ..... ***xvii***

Chapter 1 ..... ***1***

Introduction ***1***

1.1 Overview 1

1.2 Potential mechanisms underlying impaired left ventricular function in AF 4

1.2.1 Ventricular remodelling and dysfunction 6

1.2.2 Adverse haemodynamics 9

1.2.3 Ventricular fibrosis 11

1.2.3.1 Histological studies 11

1.2.3.2 Cardiac magnetic resonance fibrosis assessment 11

1.2.3.3 CMR studies assessing fibrosis in patients with AF 13

1.2.3.4 Role of ventricular rate in development of LV fibrosis 13

1.2.3.5 Mechanisms regulating myocardial fibrosis in AF 15

1.2.3.6 Prognostic importance of LV fibrosis in AF 16

1.2.4 Impaired ventricular perfusion / perfusion reserve in AF 17

1.2.5 Microvascular/endothelial dysfunction and inflammation in AF 21

1.2.6 Oxidative stress 24

1.2.7 Abnormal calcium handling 25

1.2.8 Unexplored potential mechanisms 29

1.3 Current knowledge gaps 29

1.4 Questions addressed in this Thesis 30

1.5 Rationale for study design 30

1.6 Overview of Thesis 31

Chapter 2 33

Methods 33

2.1 Ethical Considerations 33
2.2 Study Participants 33
2.2.1 Inclusion Criteria 34
2.2.2 Exclusion Criteria 35
2.3 Study Timeline 36
2.4 Clinical Assessment 37
2.5 CMR Scan Protocols 37
2.5.1 Phosphorus-31 MR spectroscopy (^{31}P-MRS) 41
2.5.2 Cine imaging 42
2.5.3 Choice of short axis slice positions 45
2.5.4 T1 mapping (native) 45
2.5.5 Post-contrast T1 mapping and ECV estimation 47
2.5.6 Tagging assessment of myocardial strain 48
2.5.7 Adenosine stress/rest perfusion 49
2.5.8 Late gadolinium enhancement (LGE) imaging 52
2.6 Echocardiography 52
2.7 Blood Collection, Handling, Storage and Analysis 53
2.8 Rhythm Monitoring 53
2.8.1 Assessment of change in AF burden by Holter monitoring 53
2.8.2 Event monitoring 54
2.8.3 Classification of patients post-ablation 54
2.9 Data Blinding for Analysis 55

Chapter 3 56

Left ventricular function and energetics in atrial fibrillation 56

3.1 Abstract 56
3.1.1 Background 56
3.1.2 Methods 56
3.1.3 Results 57
3.1.4 Conclusions 58
3.2 Introduction 58

3.3 Methods 60
3.3.1 Patient population 60
3.3.2 Control group 61
3.3.3 Study protocol 61
3.3.4 Cardiac magnetic resonance and echocardiography 61
3.3.5 Statistical analysis 62
3.4 Results 63
3.4.1 Results in control subjects and patients with AF before ablation 66
3.4.2 Outcomes following ablation 72
3.4.3 Early effect of ablation on LV function 73
3.4.4 Late effect of ablation on LV function and myocardial energetics 75
3.4.5 Effect of Medications 78
3.5 Discussion 81
3.5.1 Left ventricular function in AF 81
3.5.2 Myocardial energetics in AF 85
3.5.3 Clinical implications and future directions 86
3.5.4 Limitations 87
3.6 Conclusion 88

Chapter 4 89

Systolic T1 mapping for application in tachyarrhythmia 89

4.1 Abstract 89
4.1.1 Background 89
4.1.2 Methods 89
4.1.3 Results 90
4.1.4 Conclusions 90
4.2 Introduction 91
4.3 Methods 92
4.3.1 Volunteer experiments 93
4.3.1.1 MR acquisition parameters 93
4.3.1.2 Pilot Experiments 95
4.3.1.3 CMR Scan Protocol 95
4.3.1.4 Image post-processing 96
4.3.2 Validation in patients 97

4.3.3 Statistical analysis 98
4.4 Results 99
4.4.1 Volunteer experiments 99
4.4.1.1 Effect of TD and normal/short readout on trigger time and myocardial thickness 100
4.4.1.2 Effect of TD and normal/short readout on fit quality, T1 values and variability 101
4.4.1.2.1 Fit quality 101
4.4.1.2.2 T1 values 102
4.4.1.2.3 T1 variability 102
4.4.1.3 Partial-volume effects 104
4.4.1.4 Effects of gender 106
4.4.2 Validation in patients 108
4.5 Discussion 110
4.5.1 Variation of T1 values within the cardiac cycle 110
4.5.2 Potential advantages of systolic T1 mapping and future directions 113
4.5.3 Limitations 115
4.6 Conclusions 116

Chapter 5 118

Diffuse myocardial fibrosis in atrial fibrillation 118

5.1 Abstract 118
5.1.1 Introduction 118
5.1.2 Methods 118
5.1.3 Results 119
5.1.4 Conclusion 119
5.2 Introduction 119
5.3 Methods 121
5.3.1 Study population 121
5.3.2 Study protocol 122
5.3.3 Cardiac magnetic resonance protocol and analysis 122
5.3.4 Statistical analysis 123
5.4 Results 123
5.4.1 Pre-ablation left ventricular indices 124
5.4.2 Pre-ablation LV tissue characterisation 126

5.4.3 Outcomes after ablation 133
5.4.4 Post-ablation left ventricular indices and tissue characterisation 133
5.5 Discussion 135
5.5.1 Diffuse ventricular fibrosis in AF 136
5.5.2 T1-mapping in AF 138
5.5.3 Clinical implications and future directions 139
5.5.4 Limitations 140
5.6 Conclusion 141

Chapter 6 142

Myocardial perfusion in atrial fibrillation 142

6.1 Abstract 142
6.1.1 Introduction 142
6.1.2 Methods 142
6.1.3 Results 143
6.1.4 Conclusion 143
6.2 Introduction 143
6.3 Methods 145
6.3.1 Study Population 145
6.3.2 Study Protocol 145
6.3.3 Cardiac Magnetic Resonance Protocol and Analysis 146
6.3.4 Statistical Analysis 146
6.4 Results 147
6.4.1 Pre-ablation LV function, hemodynamic data, and perfusion reserve 148
6.4.2 Absolute myocardial blood flow is impaired in patients with AF pre-ablation 151
6.4.3 Relationship between LV myocardial blood flow and function 153
6.4.4 MBF is unaffected despite reduction in AF burden after ablation 157
6.5 Discussion 162
6.5.1 Myocardial perfusion in patients with AF 162
6.5.2 Impaired LV perfusion and function in AF 164
6.5.3 Clinical implications and future directions 166
6.5.4 Limitations 167
6.6 Conclusion 168

Chapter 7 169

General conclusions *169*

Bibliography..... *173*

Abbreviations

AF	= atrial fibrillation
bpm	= beats per minute
BMI	= body mass index
CMR	= cardiovascular magnetic resonance
CNR	= contrast-to-noise ratio
DMF	= diffuse myocardial fibrosis
ECG	= electrocardiogram
EDV	= end-diastolic volume
EF	= ejection fraction
ESV	= end-systolic volume
FOV	= field of view
Gd-DPTA	= gadolinium-diethylene triamine pentaacetic acid
GRAPPA	= generalised autocalibrating partially parallel acquisition
IQR	= interquartile range
IR	= inversion recovery
LA	= left atrium/atrial

LGE = late gadolinium enhancement

LV = left ventricle/ventricular

LVOT = left ventricular outflow tract

MBF = myocardial blood flow

MI = myocardial infarction

MOLLI = Modified Look-Locker Inversion Recovery

MPR = myocardial perfusion reserve

MRS = magnetic resonance spectroscopy

RF = radiofrequency

ROC = receiver operator characteristic

ROI = region of interest

SD = standard deviation

ShMOLLI = Shortened Modified Look-Locker Inversion Recovery

SI = signal intensity

SNR = signal-to-noise ratio

SR = sinus rhythm

SSFP = steady-state free precession

ST = sinus tachycardia

SV = stroke volume

T	= Tesla
T1	= longitudinal or spin-lattice relaxation
T2	= transverse or spin-spin relaxation
TD	= trigger delay
TE	= echo time
TI	= inversion time
TR	= repetition time
TSE	= turbo spin echo
TT	= trigger time

Chapter 1

Introduction

1.1 **Overview**

Atrial fibrillation (AF) is the most common sustained arrhythmia[1]. Its incidence is strongly associated with increasing age[2] and comorbidity[3], although up to a third of cases occur in the absence of identifiable underlying cardiovascular disease, and have been termed "lone" AF[3]. Regardless of aetiology, AF is associated with a significantly increased risk of heart failure[4], stroke[5], myocardial infarction[6], sudden cardiac death[4] and an estimated two-fold increase in premature death[7].

Efforts to increase pathophysiologic understanding of AF have focused on unravelling the mechanisms and implications of electrical and structural atrial remodelling[8]. However, it is now increasingly recognised that AF can also adversely affect ventricular function[9, 10]. Whilst some patients develop overt left ventricular (LV) dysfunction and heart failure, others present with subclinical alterations in ventricular structure and systolic and diastolic function which may only be revealed by detailed investigation[11-13].

AF is common in heart failure, with a reported prevalence ranging from 13-27%[14]. It is also associated with heart failure severity - up to 50% of patients with severe heart failure are affected by AF[15]. Furthermore, AF is clearly associated with adverse prognosis (including premature mortality) in heart failure trials[16-18], although it remains controversial whether this effect is truly independent[14].

In clinical practice, significant improvement in ventricular function following restoration of sinus rhythm (SR) is perhaps the best identifier of a causal role of AF in the associated LV dysfunction, demonstrating that ventricular impairment is a reversible secondary effect. However, achievement of durable rhythm control was extremely challenging in the cardioversion and anti-arrhythmic drug era. Large randomized studies such as AFFIRM[19], RACE[20] and AF-CHF[21] showed no benefit of rhythm control over rate control on clinical outcomes (such as overall or cardiovascular mortality, stroke and worsening heart failure), perhaps reflecting the high rate of AF recurrence and the toxic side-effects of antiarrhythmic medications.

The relatively novel technique of catheter ablation may offer a safer and more effective method for sustained rhythm control. Catheter ablation has evolved rapidly since the landmark observations by Haïssaguerre et al. that ectopic beats originating in the pulmonary veins are frequently the trigger for initiation of arrhythmia in paroxysmal AF[22]. The technique is now established in clinical guidelines[23], with the primary indication being symptomatic AF in

patients refractory or intolerant to at least one antiarrhythmic medication. Ongoing studies are addressing the hypothesis that catheter ablation may improve cardiovascular outcomes compared to medical therapy in selected patient populations[24]. Nevertheless, it remains the case that at present there are no randomized, clinical data demonstrating that restoration of SR improves major outcomes or hospital admissions for heart failure in unselected patients with AF, raising the possibility that the arrhythmia may not be the primary cause of LV dysfunction.

The majority of the remainder of this introductory Chapter reviews the prior literature identifying or investigating potential mechanisms that may underlie the association between AF and LV dysfunction (**Figure 1**).

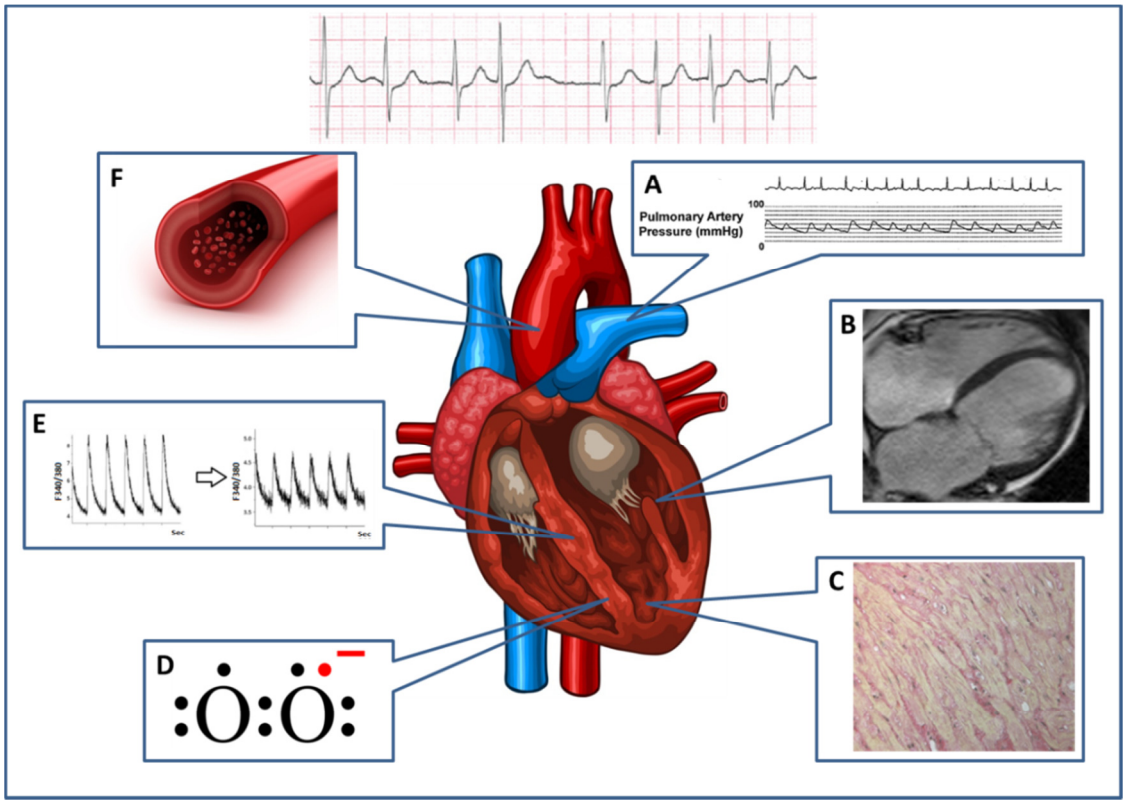


Figure 1: Systemic correlates of AF. *Clockwise from top right: (A) adverse haemodynamic effects; (B) ventricular remodelling; (C) myocardial fibrosis; (D) ventricular oxidative stress; (E) impaired ventricular calcium handling; (F) impaired endothelial function, myocardial perfusion and perfusion reserve. Top right image reproduced with permission from Clark et al[25]; bottom right image reproduced with permission from Iles et al[26]; middle left image reproduced with permission from Ling et al[27].*

1.2 Potential mechanisms underlying impaired left ventricular function in AF

While the association between AF and impaired left ventricular function is now clearly established, causation is much more challenging to ascertain. The possibilities are that AF may promote ventricular impairment by raising ventricular rate (the so-called tachycardia-induced cardiomyopathy[28]) or by other mechanisms (reviewed in more detail below). Alternatively, a pre-existing ventricular cardiomyopathy may lead to AF, via mechanical stretch and

structural remodelling of the atria, and altered myocardial intracellular calcium handling[29]. Finally, AF and LV dysfunction may be the culmination of common cardiovascular conditions such as hypertension or coronary artery disease, and could be considered tissue-specific manifestations of global myocardial damage[29].

The systematic evaluation of ventricular molecular and cellular abnormalities in AF is limited by poor access to human tissue samples. Atrial cardiomyocytes or trabeculae can be isolated from samples of the right atrial appendage excised at the time of cardiac surgery and cardiopulmonary bypass. Although the results of in vitro experiments on such preparations may not be fully reflective of in vivo conditions, these investigations have provided relevant insights into the changes in ion channel expression and function that accompany human AF[30]. The situation is even more challenging for investigations of the ventricular myocardium, as ventricular biopsy is rarely clinically indicated and is difficult to justify purely for research purposes due to the risk of complications[31]. Even when undertaken, biopsy carries the risk of sampling error, and patchy abnormalities may remain undetected[32]. The limited human data in the literature largely represent small case series of ventricular biopsy[33] or studies of tissue from explanted hearts following cardiac transplant[27]. Interpretation of these data is made more difficult by the lack of matched tissue from healthy control subjects.

1.2.1 Ventricular remodelling and dysfunction

It is well recognised that AF and other supraventricular tachycardias with an uncontrolled ventricular rate can cause a transient and reversible ventricular dysfunction that is termed "tachycardia-induced cardiomyopathy"[34, 35]. More recently, data from animal and human studies have suggested that, even in the absence of persistently elevated ventricular rates, AF can be associated with adverse atrial and ventricular remodelling and impairment of LV systolic and diastolic function[36-38]. The relationship between AF and LV dysfunction is complex and potentially bi-directional leading to a vicious electromechanical cycle[9]. Causality in individual cases cannot be determined at a single time-point, but a number of studies have undertaken serial evaluation around an intervention aimed at maintaining SR and these have provided important insight into causal relationships in the studied cohorts.

A recent multi-centre randomised clinical trial enrolled patients with persistent AF and idiopathic cardiomyopathy with LV ejection fraction (LVEF) <45% and randomised them to catheter ablation or medical rate control. The absolute improvement in LVEF at 6 months was 18±13% in the catheter ablation arm, compared to 4.4±13% in the rate control arm (p=0.0002)[39]. Late-breaking results from the as yet unpublished CASTLE-AF trial further suggest that improvements in LVEF following catheter ablation in patients with AF and LV dysfunction may also translate into a reduction in outcomes including all-cause mortality and unplanned hospitalisation for worsening heart failure.

These recent results are consistent with a prior randomised study of patients with persistent AF, symptomatic heart failure and LV ejection fraction <50%, which demonstrated significant improvement in LV ejection fraction by 1 month (and persisting at 6 months) in those randomised to catheter ablation (n=26) compared to those randomised to medical rate control (n=24)[38]. A similar improvement was seen in peak oxygen consumption and was mirrored by reductions in plasma B-type natriuretic peptide (BNP) concentrations and NYHA class. Importantly, all patients were assessed for adequate rate control at baseline by ambulatory monitoring and exercise testing thereby demonstrating that even rate-controlled AF has deleterious effects on LV function. The improvement in LV ejection fraction shown in this study is in keeping with the results of other (mainly observational) studies of patients with AF undergoing catheter ablation (summarised in a meta-analysis[40]).

A study involving serial echocardiographic studies prior to and at regular intervals up to 1 year after radiofrequency ablation demonstrated that ventricular function is not entirely normal, even in patients with apparent lone AF[13]. This carefully selected group demonstrated echocardiographic evidence of subtle LV systolic and diastolic dysfunction compared to age- and sex-matched controls, although LV ejection fraction remained largely within the normal range. The exclusion of other causes of LV dysfunction strongly suggests that AF may be causally associated with these abnormalities. Further evidence for this is provided by the post-ablation follow-up echocardiograms, which

demonstrated a progressive improvement in LV performance over time. Finally, there was a dose-response relationship between AF burden and adverse ventricular function with more marked baseline impairment and subsequent improvement noted in the chronic AF group than the paroxysmal AF group.

A subsequent study which used cardiac MRI to evaluate LV function before and after ablation for short-lasting paroxysmal AF confirmed impaired LV systolic function at baseline and improvement in LV ejection fraction following ablation in all but patients with a normal ejection fraction at baseline (**Figure 2**)[41].

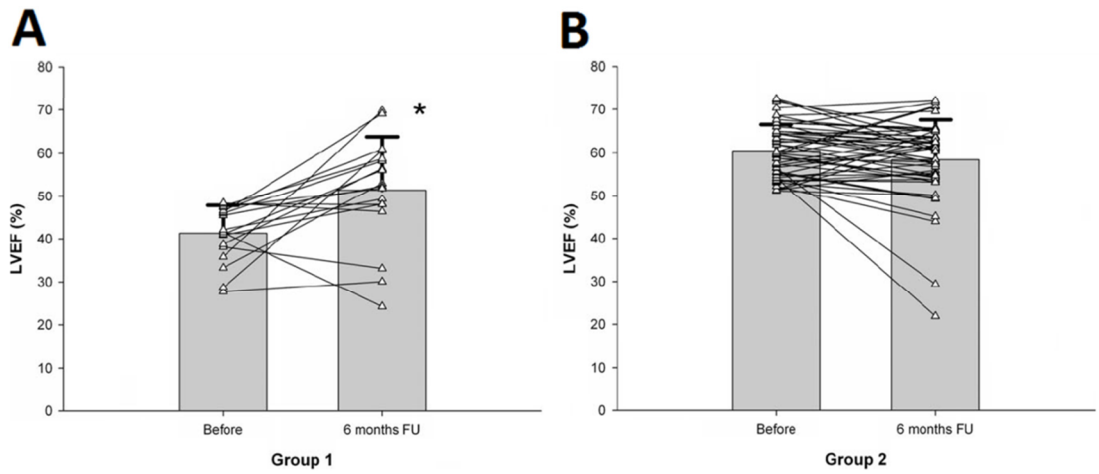


Figure 2: Effect of pulmonary vein isolation (PVI) ablation procedure on left ventricular ejection fraction (LVEF).*(**A**) Group 1 (LVEF<50% at baseline) demonstrate a significant increase in LVEF at 6 months post-procedure (*P=0.004). (**B**) There is no significant difference in LVEF between baseline and 6 months in Group 2 (LVEF≥50% at baseline). Of note, all six Group 2 patients with an LVEF reduction after the ablation and the only patient in Group 1 who experienced a significant decrease in LV function following PVI demonstrated AF recurrences. Reproduced with permission from Lutomsky et al[41].*

The findings in the group with normal ejection fraction may reflect the relatively low AF burden and the poor sensitivity of ejection fraction for

detecting subtle changes in LV systolic function. Support for the latter possibility comes from a study by Tops et al. who utilised speckle-tracking to investigate LV strain in selected patients undergoing ablation for AF[11]. Longitudinal and circumferential LV strain and strain rate were impaired at baseline compared with healthy controls. Intriguingly, maintenance of SR at follow-up was associated with improvement in these parameters whereas recurrence of AF was associated with further deterioration. These data support the presence of subtle LV dysfunction in patients with AF and maintained LV ejection fraction; its reversibility following AF ablation strongly implies that AF may be playing a causal role.

1.2.2 Adverse haemodynamics

AF is associated with impaired haemodynamic parameters such as reduced cardiac output and elevated pulmonary artery pressures. Multiple mechanisms may contribute to these findings, including: (i) loss of atrial systole and atrioventricular synchrony, (ii) elevated overall ventricular rate, (iii) irregularity in the pulse interval, (iv) valvular regurgitation and (v) neurohormonal effects. The role of some of these mechanisms has been directly assessed in human studies. In particular, in an invasive study involving ventricular pacing in patients with AF undergoing AV node ablation, AF and all forms of pacing were associated with reduced cardiac output compared to SR, emphasising the importance of atrioventricular synchrony[25]. Additionally, the effect of irregularity of the pulse interval was assessed by comparison of

haemodynamic parameters during irregular ventricular stimulation compared with regular stimulation. This assessment was undertaken after AV node ablation, with the rate of ventricular stimulation individualised to each patient based on the ventricular rate that had been observed in intrinsically conducted AF immediately prior to AV node ablation. Importantly, cardiac output was significantly reduced and pulmonary capillary wedge and right atrial pressures were significantly increased in the presence of an irregular pulse interval compared to regular pacing at the same rate. These results are in agreement with those of a prior similar study[42], and represent direct *in vivo* evidence of the adverse haemodynamic consequences of an irregular pulse interval *per se*.

A separate study showed that in patients with persistent AF and impaired LV function, improvement of atrial and ventricular function after successful cardioversion follows a different time course[43]. Whilst heart rate is slowed immediately and atrial contractility recovers by one week and remains unchanged thereafter, recovery of LV systolic function takes one month. Improvements in exercise tolerance and peak oxygen consumption mirrored the time course of recovery in LV function. These data suggest that the impairment in LV function seen in persistent AF may be due to a transient ventricular cardiomyopathy or stunning, due in part to an elevated ventricular rate but perhaps also to the irregular pulse interval.

1.2.3 Ventricular fibrosis

1.2.3.1 Histological studies

Although human data reporting ventricular changes in the presence of AF are sparse, one series that investigated 14 young patients with apparent "lone" AF refractory to initial medical therapy demonstrated abnormal histology in all cases[33]. Importantly, all patients had structurally normal hearts without atrial or ventricular dilatation and a normal LV ejection fraction. Three of fourteen had evidence of focal myocarditis (eosinophilic or lymphocytic), and initiation of corticosteroid therapy in addition to antiarrhythmic medications induced recovery of SR in all in this group. A further 3 patients had evidence of a diffuse cardiomyopathic process, whilst the remaining 8 patients had nonspecific diffuse fibrotic change with or without evidence of cardiomyocyte necrosis. However, such changes may not be specific to AF, as a separate study documented similar histological findings in the majority of patients with other forms of supraventricular tachycardia[44].

1.2.3.2 Cardiac magnetic resonance fibrosis assessment

More data are available from non-invasive studies using cardiac magnetic resonance (CMR) techniques, which have aimed to identify ventricular fibrosis in AF. Diffuse fibrosis cannot be visualised by the widely used method of late gadolinium enhancement (LGE) CMR, which relies on areas of presumed normal myocardium as a comparator to highlight discrete areas of high signal intensity in focal fibrosis, scarring or infarction.

Diffuse fibrosis can be detected by the recently developed method of quantitative CMR T1 mapping[45], usually requiring administration of a gadolinium-based contrast agent. T1 is the longitudinal (or spin-lattice) relaxation time of a tissue, and T1 mapping refers to the generation of pixel-wise parametric maps of T1 values[45]. Normal myocardium has a characteristic range of normal T1 values at a given field strength, and deviation from these values can be indicative of disease, including myocardial fibrosis.

Myocardial T1-mapping methods are used for native (i.e. without the use of gadolinium-based contrast agents) and also for post-contrast T1 measurement. Gadolinium-based contrast agents diffuse freely in the extracellular space and shorten T1 times; hence, low post-contrast T1 values can reflect diffuse fibrosis in the absence of other causes of expansion of the interstitial space. This method has been validated against histological assessment of fibrosis in right ventricular endomyocardial biopsy specimens taken from subjects who had undergone orthotopic heart transplantation[26]. However, post-contrast T1 values are influenced by native T1, the type and dose of contrast, haematocrit and glomerular filtration rate, and isolated post-contrast T1 values are not a preferred output in consensus guidelines[45]. The more robust technique of extracellular volume fraction (ECV) assessment (which relies on measurement of haematocrit, native T1 and post-contrast T1) is preferable, as it inherently accounts for these potential confounders.

1.2.3.3 CMR studies assessing fibrosis in patients with AF

A study of post-contrast T1 mapping in subjects with paroxysmal (n = 40) and persistent AF (n = 27) as well as healthy controls (n = 23) demonstrated significantly lower post-contrast T1 values in both sets of AF patients compared to age- and sex-matched controls[46]. Additionally, patients with persistent AF had lower post-contrast T1 values than the paroxysmal AF group. In keeping with established data showing that diffuse myocardial fibrosis increases with age, there was a negative correlation between increasing age and post-contrast T1 value in the healthy controls. In a multivariate model, only age, AF class and LV ejection fraction were independent correlates of post-contrast ventricular T1 values. These data suggest that increasing AF burden is associated with progressive diffuse LV fibrosis, and may play a role in adverse cardiac remodelling. A separate study demonstrated elevated ECV, consistent with diffuse myocardial fibrosis, in hypertensive patients with AF, and suggested that this was a powerful predictor of recurrent AF following catheter ablation[47].

1.2.3.4 Role of ventricular rate in development of LV fibrosis

Data from animal studies suggest that development of LV fibrosis is related to an elevated ventricular rate in the presence of AF. Induction of AF by rapid atrial pacing in dogs in the presence of AV node ablation and a paced ventricular rate of 80 bpm was sufficient to induce atrial but not ventricular fibrosis, whereas dogs without AV node ablation and a more rapid ventricular rate did develop significant ventricular fibrosis[48]. Heart failure and ventricular

fibrosis have been reported in a similar dog model despite the use of oral digoxin and metoprolol with the aim of achieving ventricular rate control[36]; however, the degree of ventricular fibrosis was less marked than the observed atrial fibrosis (**Figure 3**) and the ventricular rates of up to 180 beats per minute reported in this study may have contributed to a tachycardia-mediated cardiomyopathy[36].

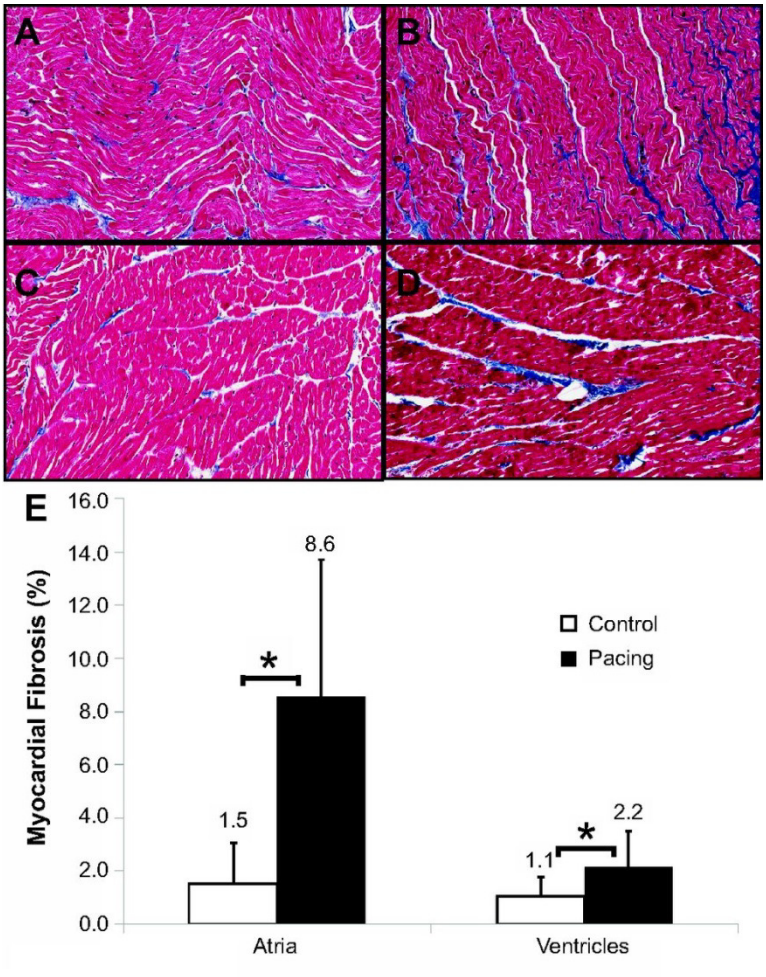


Figure 3: Fibrosis in the dog at baseline and at 6 months of AF. *(**A**) Left atrial (LA) histological sample from a control dog (2.0% fibrosis; shown in blue on Masson's trichrome stain). (**B**) LA sample from a 6-month AF dog (10.1% fibrosis). (**C**) LV sample from a control dog (1.0% fibrosis). (**D**) LV sample from a 6-month AF dog (2.4% fibrosis). (**E**) Fibrosis levels increased in both the atria and ventricles during chronic AF. Values above bars indicate SDs. *P < 0.01. Reproduced with permission from Dosdall et al.[36].*

Findings consistent with the paradigm of tachycardia-induced ventricular fibrosis have also been described in patients who had undergone previous ablation for incessant focal atrial tachycardia[49]. Focal atrial tachycardia provides a good model for study of human atrial arrhythmia as long-term "cure" and maintenance of SR is feasible following ablation. The subgroup with LV cardiomyopathy at baseline had lower post-contrast T1 values on CMR imaging at a mean of 5 years following ablation, consistent with a greater burden of diffuse ventricular fibrosis at baseline that was irreversible despite restoration of SR and improvement in LV ejection fraction. The lack of CMR imaging at baseline in this study means that development of fibrosis during the follow-up period, although less likely, cannot be excluded with certainty. Interestingly, there was also no significant difference in mean heart rate on 24 hour ECG monitoring prior to ablation between the patients with and without cardiomyopathy. Whilst this may reflect lack of statistical power to detect a true difference, it is also possible that the maximum ventricular rate tolerated before development of ventricular fibrosis and impaired LV function varies between individuals.

1.2.3.5 Mechanisms regulating myocardial fibrosis in AF

Atrial and ventricular fibrosis in response to AF may be regulated by different mechanisms. Study of cultured rat atrial and ventricular fibroblasts shows that nicotinamide adenine dinucleotide phosphate-oxidase 4 (NADPH

oxidase 4 / NOX-4) is more highly expressed in the atria than the ventricles, and this mediates the enhanced collagen and fibronectin production of atrial fibroblasts compared to ventricular fibroblasts in response to transforming growth factor beta (TGF-β)[50]. Thus, ventricular tissue appears inherently less susceptible to the development of fibrosis than atrial tissue, though prolonged exposure to an elevated ventricular rate can nevertheless still result in ventricular fibrosis. In summary, although it is currently not possible to definitively determine causality, there is strong circumstantial evidence that AF can induce diffuse ventricular fibrosis[51].

1.2.3.6 Prognostic importance of LV fibrosis in AF

A recent study highlighted the prevalence and prognostic significance of focal myocardial scar, as detected by late gadolinium enhancement (LGE). LV LGE was present in 13% of patients with AF and without known prior myocardial infarction (but with other cardiovascular comorbidities) undergoing a routine cardiac MRI study prior to pulmonary vein isolation[52]. Intriguingly, the presence of LGE was a powerful predictor of mortality with each 1% increase in LGE associated with a 15% increased risk of death. The patterns of LGE seen in this study were relatively equally divided between an ischaemic pattern, probably reflecting silent myocardial infarction, and a non-ischaemic pattern. The latter may have related to inclusion of patients with heart failure and/or reduced ejection fraction, or the presence of an AF-related ventricular cardiomyopathy in some of the studied cohort. This was the first study to

systematically assess the presence of focal ventricular fibrosis in patients with AF, and further studies are needed to identify whether these findings are more prevalent in this population than in a matched cohort of patients in SR.

There are also data defining the prognostic value of diffuse LV fibrosis in AF. ECV expansion (mainly due to diffuse fibrosis) is associated with increased mortality and heart failure in broadly unselected patients undergoing clinical cardiac MRI, independently of age, ejection fraction and previous infarct size[53] and also strongly predicts recurrence of AF following catheter ablation in hypertensive patients[47]. If AF caused diffuse LV fibrosis and adverse remodelling, targeting an aggressive rhythm control strategy to the subgroup of patients in whom AF is the primary pathology (rather than a consequence of another disease state) could clearly be important. The hypothesis that this strategy would improve clinical outcomes would need to be examined in an appropriately powered clinical trial.

1.2.4 Impaired ventricular perfusion / perfusion reserve in AF

Patients with AF and without obstructive epicardial coronary artery disease may still demonstrate clinical evidence of ischaemia, such as chest pain, ST depression or Troponin-release, often at the onset of arrhythmia[54, 55], implying the presence of microvascular coronary dysfunction, arrhythmia-induced coronary artery spasm, supply-demand mismatch, or a combination of these potential mechanisms. In a pig pacing model of AF, 6 hours of rapid atrial pacing (600 bpm) are sufficient to elicit a substantial reduction in coronary flow

reserve (CFR) in the absence of any significant change in fractional flow reserve (FFR), based on invasive measurements using a coronary pressure wire in the left anterior descending coronary artery[56]. CFR is influenced by abnormal flow in the epicardial coronary arteries as well as the microcirculation whereas FFR is specific to epicardial disease; hence these data support the hypothesis that AF can rapidly adversely affect microvascular coronary function. The investigators report that this reduction in CFR was abolished by pre-treatment with dronedarone (but not amiodarone) and suggest that this may reflect an attenuating effect of dronedarone on oxidative stress and consequent microvascular flow abnormalities[56]. However, as ventricular rates were not reported, it is not possible to identify the extent to which tachycardia (and reduced diastole duration) may have contributed to the reduction in CFR.

Myocardial perfusion and perfusion reserve have been evaluated using positron emission tomography and radioactively-labelled water in patients with persistent AF after exclusion of epicardial coronary artery disease[57], demonstrating derangements in AF. Myocardial blood flow at rest was markedly reduced in the AF group compared to age- and risk-matched controls as was adenosine-induced hyperaemic flow (**Figure 4**). Minimal coronary vascular resistance at rest and during hyperaemia was also significantly increased in AF patients compared to controls. Finally, in the subgroup of patients that maintained SR following cardioversion, myocardial blood flow at rest normalised, and hyperaemic flow and coronary vascular resistance were

significantly improved from baseline. These human findings are in accordance with the animal data and suggest that the presence of AF induces abnormalities in microvascular coronary function that are at least partially reversible with restoration of SR. However, the subgroup that maintained SR following cardioversion was small (10 patients) and confirmation of these findings in a larger cohort is awaited.

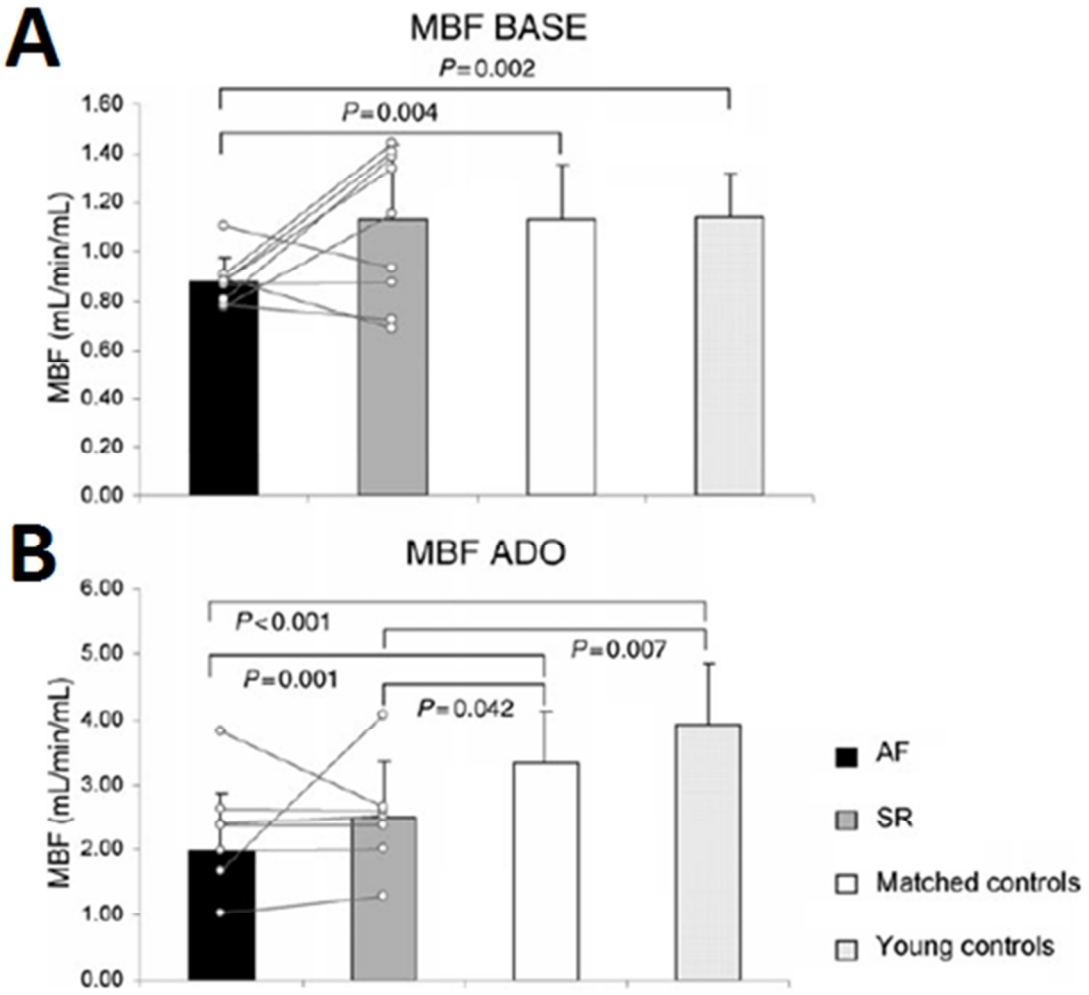


Figure 4: Myocardial perfusion and perfusion reserve. *Myocardial blood flow (MBF) in 10 patients (mean and individual trends) by positron emission tomography during AF and during sinus rhythm 4.1+/-2.3 months after cardioversion (SR) in comparison with age-/risk-matched and young controls as measured at baseline (**A**) and during adenosine infusion (**B**) for assessment of perfusion reserve. Reproduced with permission from Range et al[57].*

In a separate study, the effect of AF on coronary flow, flow reserve and vascular resistance were assessed invasively in patients in SR with no ventricular or valvular dysfunction and no significant epicardial coronary artery disease[58]. A coronary Doppler catheter was placed and measurements taken in SR, during AF induced by bursts of atrial pacing, and during regular atrial tachycardia with a rate of pacing equal to the overall ventricular rate observed during AF. The relative contribution of the irregularity of ventricular contraction in AF was also assessed by the inclusion of a second group of patients with complete AV block and dual chamber pacemakers in situ; in this group the ventricle was paced regularly at 115 bpm before and after induction of AF. In the first group of patients, acute induction of AF led to an increase in coronary flow which was lower than that seen in the presence of rapid atrial pacing and was associated with a reduction in coronary flow reserve and vascular resistance. By contrast, in the group with pacemakers in situ, only a small effect on coronary flow and an increase in coronary flow reserve were seen following induction of AF. The increase in coronary flow seen in both groups following induction of AF is likely to be explained by the elevated ventricular rate following acute induction of AF, as patients in this study were not receiving rate-control medications. However, this absolute rise in coronary flow appears insufficient relative to the increase in ventricular rate and consequent increase in myocardial metabolic demand., suggesting that

ventricular supply-demand ischaemic is an important pathophysiological mechanism in AF.

This concept is in keeping with a mechanistic study in pigs that demonstrated "supply-demand ischaemia" in the atria following acute induction of AF[59], evidenced by an increase in atrial lactate production despite compensatory rises in both atrial coronary conductance and oxygen extraction. Atrial supply-demand ischaemia has also been proposed as a potential trigger for atrial structural remodelling and has a molecular phenotype which resembles changes seen in hibernating ventricular myocardium[59]. Indeed, chronic ventricular ischaemia could underlie the impaired ventricular function commonly seen in AF.

1.2.5 Microvascular/endothelial dysfunction and inflammation in AF

The irregular pulse interval that is typical of AF seems to play a role in the impaired coronary flow observed in these patients, even when the overall ventricular rate is well controlled. Irregular pulse intervals can adversely affect blood pressure but no correlation has been demonstrated between blood pressure and coronary flow[58], leaving the possibility that irregular ventricular contraction might affect diastolic filling and coronary perfusion, or cause coronary vasoconstriction, possibly by increasing the release of vasoactive peptides such as angiotensin II or endothelin. Studies in a pig model of rapid atrial pacing have suggested that the angiotensin receptor blocker, irbesartan,

abolishes the impairment of microvascular flow otherwise seen with rapid atrial pacing (**Figure 5**), as well as preventing ventricular oxidative stress[60].

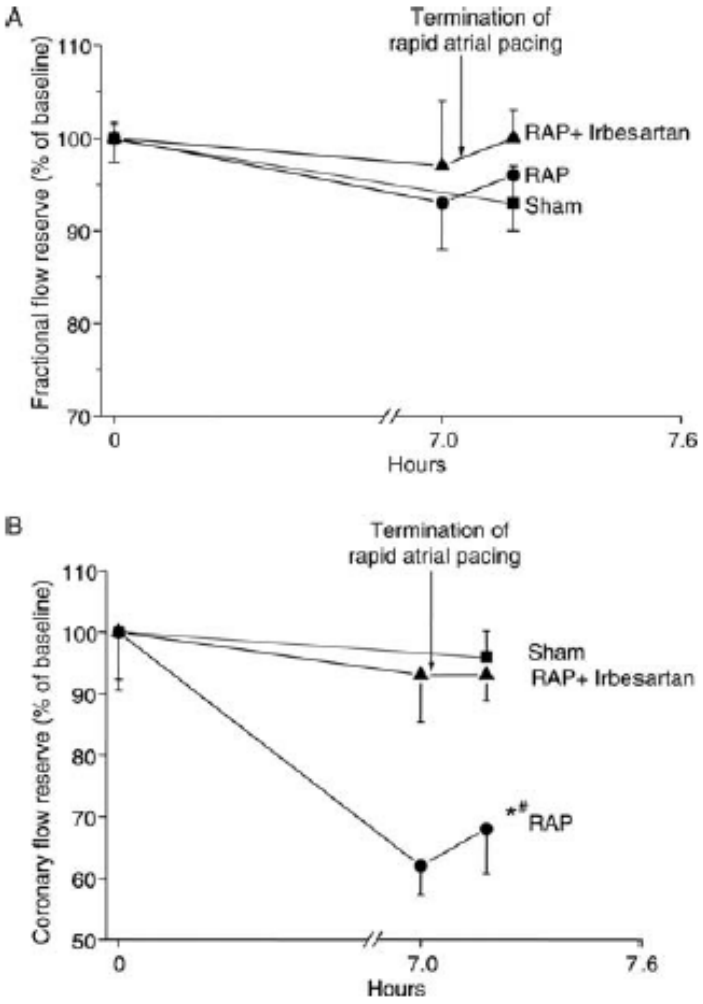


Figure 5: Flow reserve measurements during 7 hours of rapid atrial pacing (RAP) with and without administration of irbesartan.*(**A**) RAP has no significant effect on fractional flow reserve compared with sham animals, suggesting that RAP does not affect blood flow in the epicardial coronary arteries (mean+/-SEM). (**B**) RAP leads to a reduction in coronary flow reserve compared with sham (*P – 0.009, Tukey test) and RAP with irbesartan (#P – 0.022, Tukey test). Reproduced with permission from Goette et al[60].*

The link between AF and impaired vascular function is not limited to the coronary circulation, and there are numerous reports confirming an association between AF and systemic endothelial dysfunction. Non-invasive assessment of

endothelial function is most readily undertaken using flow-mediated dilatation (FMD), which assesses nitric oxide production in response to shear stress and by measurement of plasma levels of markers of endothelial damage or dysfunction, such as the von Willebrand factor and circulating endothelial cells. Endothelium-dependent FMD is abnormal in patients with AF[61] and a causative role for AF in endothelial dysfunction is suggested by the finding that cardioversion[62-64] and successful catheter ablation of AF[65] are associated with significant improvements in endothelial function.

Inflammation represents a potential link between AF, impaired endothelial function, and a reduction in myocardial perfusion and perfusion reserve. A recent study investigated the acute effects of AF induced by burst atrial pacing immediately prior to catheter ablation in patients with a history of paroxysmal AF but in SR at the time of the procedure[66]. This group was compared to patients who underwent regular atrial pacing at 150 bpm, a control group of patients with paroxysmal AF who were not paced and remained in SR, and a further control group of patients with no history of AF undergoing ablation of left-sided accessory pathways that were also not paced and in SR. The study showed that even at the very short time point of 15 minutes, rapid atrial rates (either through AF or rapid atrial pacing) were associated with increased local platelet activation and thrombin generation within the left atrium. Furthermore, AF (but not rapid atrial pacing) additionally led to local and systemic endothelial dysfunction (as assessed by

levels of asymmetric dimethylarginine) and inflammation (as assessed by levels of soluble CD40L). These data suggest that even a short duration of AF may cause inflammation and endothelial dysfunction, potentially mediated by atrial oxidative stress[67]. Further studies are needed to investigate whether inflammation and oxidative stress are an important mechanism underlying impaired myocardial perfusion and perfusion reserve and the thromboembolic risk of asymptomatic short-lasting episodes of AF[68].

1.2.6 Oxidative stress

Oxidative stress refers to the chronic disturbance of redox circuits and redox-responsive signal transduction pathways, and atrial oxidative stress is known to play an important pathophysiological role in the induction and maintenance of AF[67, 69-71]. Less is known regarding the potential importance of ventricular oxidative stress in AF. Limited data are available from a study by Cai *et al.* conducted in a pig model of rapid atrial pacing[72]. The protein level of endothelial nitric oxide synthase was significantly decreased in LV tissue from animals with pacing-induced AF compared to controls, although this difference was less pronounced than in the left atrium. Importantly, this finding could not be attributed to an elevated ventricular rate as both groups of animals underwent AV node ablation and the ventricles were paced at 100 bpm in both the AF and control groups.

A separate study, also conducted in a pig model of rapid atrial pacing, further demonstrated a significant increase in ventricular nicotinamide adenine

dinucleotide phosphate-oxidase 2 (NADPH oxidase 2 / NOX2) expression, a finding that was prevented by treatment with irbesartan[60]. Ventricular concentrations of F_2-isoprostanes and lectin-type oxidised LDL receptor 1 (LOX-1) protein, both markers of oxidative stress, were also elevated by rapid atrial pacing. These observations suggest that rapid atrial pacing induces oxidative stress in LV tissue by an angiotensin-mediated mechanism. Previous work demonstrated that plasma levels of angiotensin II are elevated within six hours of rapid atrial pacing, and angiotensin II appears to be an important mediator of oxidative stress in AF[73] by acting via the AT1 receptor to activate mitogen-activated protein kinases and stimulate proliferation of fibroblasts, cellular hypertrophy and apoptosis as well as inducing calcium release and PKC activation, which in turn promotes activation of NOX2 and NOX1 NADPH-oxidases[74]. A further study in the same model also reported a reduction in LV oxidative stress in the presence of dronedarone[56]. In contrast to Cai *et al.*, these studies cannot discriminate between the effect of AF and that of rapid ventricular rates induced by rapid atrial pacing with a competent AV node.

1.2.7 **Abnormal calcium handling**

Calcium handling abnormalities in the atrial myocardium have been implicated in the initiation and maintenance of AF, and have been recently reviewed[75]. Briefly, calcium handling abnormalities may be induced by oxidative stress[76] and can promote AF via *(i)* induction of delayed afterdepolarizations and triggered events, *(ii)* enhanced Ca^{2+} / calmodulin kinase type 2 activity and

associated hyperphosphorylation and increased open probability of the type 2 ryanodine receptor and *(iii)* up-regulation of the Na^+/Ca^{2+} exchanger, increasing the size of the inward current for a given amount of aberrant Ca^{2+} release[77].

In contrast, very sparse data are available on calcium handling in ventricular myocardium in AF. Some insight is provided by a small study which examined human LV myocardial tissue obtained from end-stage heart failure patients with or without AF (n = 6 in SR and n= 6 in AF) who underwent cardiac transplantation as well as neonatal rat ventricular cardiomyocytes subjected to regular or irregular electrical stimulation *ex-vivo*, to simulate SR and AF, respectively (**Figure 6**)[27]. To exclude effects of rate, all cardiomyocytes paced regularly or irregularly were stimulated the same number of times in total over a 24-hour period. The mRNA and protein levels of sarcoplasmic reticulum ATPase 2a pump (SERCA), an important determinant of intracellular calcium levels, were significantly lower in the ventricular myocardium of the heart failure patients with AF compared to those in SR. This finding was recapitulated in paced rat ventricular cardiomyocytes, suggesting that irregularity of ventricular contraction influences SERCA expression beyond any effect of heart failure or ventricular rate. Additionally, in both models AF was associated with a significant decrease in the phosphorylation of phospholamban (PLB), a key regulator of SERCA. Confirmation that these changes affect intracellular calcium handling was obtained from calcium imaging of rat cardiomyocytes, which demonstrated significantly reduced calcium transient amplitude and increased

time to peak calcium transient amplitude in cardiomyocytes exposed to irregular pacing compared with unpaced and regularly paced groups. Surprisingly, the rate of decay of the intracellular calcium transient was not significantly different between the groups.

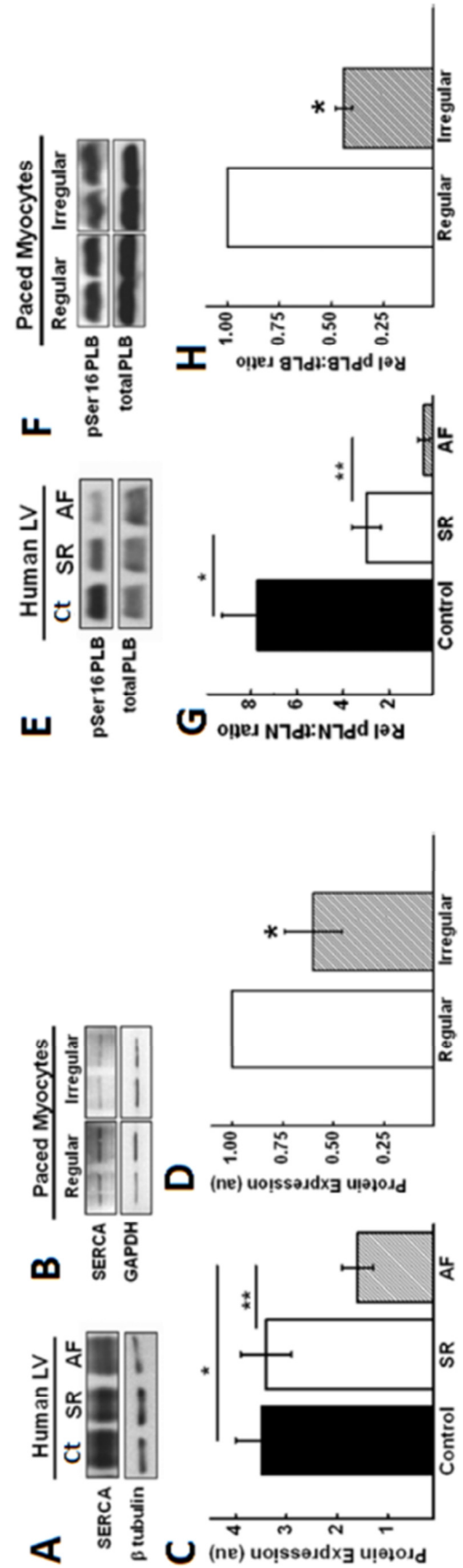


Figure 6: The effect of AF on sarcoplasmic reticulum Ca^{2+}ATPase (SERCA) and phospholamban. *Representative immunoblots showing SERCA expression in (A) human left ventricular (LV) myocardium from unused donor heart control (Ct), heart failure-sinus rhythm (SR) and heart failure-atrial fibrillation (AF) patients; (B) regularly paced vs irregularly paced cardiomyocytes. Quantitative analysis of SERCA expression in (C) human myocardial samples (P<0.05 control vs AF; P<0.01 SR vs AF) and (D) isolated paced cardiomyocytes (*P<0.05 regular vs irregular). GAPDH indicates glyceraldehyde-3-phosphate dehydrogenase. Representative immunoblots showing phospholamban and phosphorylated-phospholamban expression in (E) human left ventricular (LV) myocardium from unused donor heart control (Ct), heart failure-sinus rhythm (SR), and heart failure-atrial fibrillation (AF) patients; (F) regularly paced vs irregularly paced cardiomyocytes. Quantitative analysis of phosphorylated:total phospholamban (PLB) expression in (G) human myocardial samples (*P<0.05 control vs AF; **P<0.01 SR vs AF) and (H) isolated paced cardiomyocytes (*P<0.05 regular vs irregular). pSer, phosphoserine. Reproduced with permission from Ling et al[27].*

These findings suggest that impaired calcium handling may be partly responsible for the impaired LV contractile function that can be seen in AF, and that this may be influenced by the irregularity of ventricular contraction.

1.2.8 Unexplored potential mechanisms

Several other molecular and cellular changes have been demonstrated in the atria in AF, but further studies are required to assess if these may also extend to the ventricle. These include impaired myofibrillar energetics[78, 79], loss of myofibrils, accumulation of glycogen, changes in mitochondrial shape and size, fragmentation of the sarcoplasmic reticulum, dispersion of nuclear chromatin and increase in myocyte size[80].

Energetics in particular is worthy of further investigation. Altered cardiac energy metabolism is an early feature of cardiomyopathy[81] and is prognostically important[82, 83]. Energetic dysfunction is a prime candidate that could underlie LV dysfunction in AF.

1.3 Current knowledge gaps

The evidence summarised in this introductory Chapter demonstrates that AF is more than an atrial disease, being associated with systemic inflammation, endothelial dysfunction, and abnormalities in structure and function of the left ventricular myocardium that may be prognostically important.

Despite these observations, there is a paucity of previous studies that have prospectively assessed left ventricular structure and function in patients with AF using advanced imaging. In particular, whilst subtle LV dysfunction has been consistently demonstrated, the underlying mechanism or mechanisms have not been characterised in detail.

1.4 Questions addressed in this Thesis

This Thesis uses advanced CMR techniques to assess the following parameters:

- LV and left atrial (LA) structure and function
- LV energetics
- LV fibrosis (focal and diffuse)
- LV perfusion (at rest and at peak vasodilator stress)

1.5 Rationale for study design

CMR is an advanced imaging technique which offers excellent spatial resolution for evaluation of cardiac anatomy and global and regional function. High reproducibility[84] and absence of ionizing radiation make it well suited to longitudinal follow-up studies. Equally important in the current context, is the ability of CMR to non-invasively assess ventricular energetics[85], perfusion and perfusion reserve[86], and tissue characterisation (both regional and diffuse fibrosis)[87]. These unique characteristics render it ideally suited to the longitudinal study of AF patients before and after ablation, with the aim of

delivering insight into the relationships between AF and changes in ventricular structure, function and metabolism. Such insight would be novel: no previous published study has longitudinally investigated any of these parameters in AF patients undergoing ablation.

While CMR can assess a number of clinically-relevant parameters, tissue Doppler echocardiography remains the gold-standard approach for the non-invasive assessment of left ventricular diastolic function[88], including in atrial fibrillation[89]. Finally, collection of blood samples at each study timepoint means that biomarkers of interest can also be assayed.

1.6 Overview of Thesis

This Thesis is largely based on a prospective longitudinal multi-parametric study that was specifically designed to answer several distinct scientific questions (see Chapter 3, Chapter 5, and Chapter 6), as well as additional methodological work in healthy volunteers and patients with tachyarrhythmia (see Chapter 4). A comprehensive, overarching, and detailed description of methods is contained in Chapter 2.

The primary question that was explored was whether AF was associated with LV dysfunction in this cohort of patients with AF, and whether there was evidence of perturbation in LV energetics, since this is a characteristic and early feature of cardiomyopathy. The effect of reduction in AF burden and restoration

of SR after catheter ablation on these parameters was also examined. The results of these investigations are contained in Chapter 3.

T1 mapping has become established as an important MR technique allowing investigation of tissue characteristics, including diffuse myocardial fibrosis. However, there has historically been limited application of this technique in patients with AF due to technical limitations posed to conventional MR sequences by the often short and irregular RR interval. Therefore, a key goal of the present work was development of a T1 mapping technique that could function well in the presence of tachyarrhythmia. Chapter 4 describes the testing and validation of a novel approach of "systolic" T1-mapping in healthy volunteers and patients with tachyarrhythmia, including AF with a fast ventricular response. The methodological work described in this Chapter was essential groundwork allowing application of T1 mapping to the investigation of AF pathophysiology. Results of the application of T1 mapping techniques to investigation of the role of diffuse ventricular fibrosis in LV dysfunction in patients with AF are contained in Chapter 5.

Next, detailed and fully quantitative analysis of adenosine stress and rest perfusion MR images allowed comprehensive assessment of myocardial blood flow in patients with AF, and the relationship of these parameters to left ventricular dysfunction, as described in Chapter 6.

Finally, the overall conclusions of this Thesis and future research directions are briefly detailed in Chapter 7.

Chapter 2

Methods

2.1 **Ethical Considerations**

Research procedures received a favourable opinion from the South Central – Oxford B REC Committee (REC reference: 11/SC/0262) of the National Research Ethics Service (NRES) representing the NRES Directorate within the National Patient Safety Agency and Research Ethics Committees in England. The study also received approval from Oxford University Hospitals NHS Foundation Trust. All subjects gave written informed consent for all study procedures.

2.2 **Study Participants**

Patients undergoing first-time catheter ablation of AF in Oxford University Hospitals NHS Foundation Trust between November 2013 and August 2015 were screened for eligibility. Patients meeting inclusion criteria and without any exclusion criteria were provided with a patient information leaflet and invited to take part in the study. Patients who gave informed consented were then enrolled into the study.

Definitions of paroxysmal and persistent AF were based on contemporary clinical guidelines[23]. Clinical management of patients (including ablation strategy and choice of anticoagulant and antiarrhythmic drugs) was at the discretion of the responsible physician.

Matched control subjects in SR were recruited via local poster advertising. Interested individuals were provided with a participant information leaflet (PIL) and screened for eligibility. A subset of those meeting inclusion criteria and without any exclusion criteria who gave informed consent were then enrolled into the study; selection was based on achieving close age, gender and body mass index (BMI) matching to the included patient population.

2.2.1 Inclusion Criteria

All Subjects

- Male or female, at least 18 years of age
- Able and willing to give informed consent for participation in the study and able to comply with all study requirements

AF Patients

- Frequent (at least one episode per week) paroxysmal AF or persistent AF with adequate ventricular rate control (defined as a ventricular rate usually equal to or less than 90 beats per minute at rest) with an indication for catheter ablation

Matched Controls in SR

- Participants with no history of AF and no symptoms suggestive of arrhythmia (e.g. palpitations)
- These participants were selected to match the patients in the AF cohort for age, gender and BMI

2.2.2 Exclusion Criteria

Subjects with any of the following were not enrolled:

- Significant valvular disease (particularly moderate or severe mitral regurgitation, e.g. >grade II, and/or mitral stenosis & mitral annular calcification)
- Uncontrolled arterial hypertension (consistently >160/100 mm Hg)
- Known significant coronary artery disease or history of myocardial infarction, percutaneous coronary intervention or cardiac surgery
- Uncontrolled thyroid disease
- Systemic inflammatory diseases (e.g., rheumatoid arthritis, Crohn's, etc)
- Diabetes mellitus
- Inability to tolerate MRI scanning (claustrophobia, inability to lie flat)
- Contraindications to MRI (implantable devices or other metal implants, internal defibrillator, cranial aneurysm clips, metallic ocular foreign bodies, hypersensitivity to gadolinium)

- Contraindications to adenosine (asthma, 2nd or 3rd degree AV block)
- Inability to give informed consent
- Significantly impaired renal function (eGFR<30ml/min)
- Any other significant disease or disorder, which, in the opinion of the Investigator, may put the participants at risk because of participation in the study, or may influence the result of the study, or the participant's ability to participate in the study

2.3 **Study Timeline**

Patients were studied at three timepoints:

(i) up to 4 weeks prior to ablation

(ii) early post-ablation (up to 4 days from the procedure)

(iii) at later follow-up (between 6 and 9 months post-ablation)

The imaging and blood sampling procedures detailed below (sections 2.5 and 2.7) were undertaken at each visit, with the exception that ^{31}P-MRS assessment of myocardial energetics (section 2.5.1) and adenosine stress/rest perfusion (section 2.5.7), and were not undertaken at the early post-ablation timepoint. The complete CMR protocol and the abbreviated protocol used for the early post-ablation visit are outlined in **Figure 7** and **Figure 8**, respectively.

Controls were studied at a single timepoint (with a comprehensive protocol, identical to the pre-ablation and late post-ablation patient protocols).

2.4 Clinical Assessment

On the day of scanning, all subjects underwent a focused clinical assessment. This included history for:

- Inclusion and exclusion criteria as above
- Drug history including allergies

The following study procedures were also performed:

- Blood pressure measurement (x3 measurements in a recumbent position)
- 12 lead electrocardiogram (ECG)
- Height (cm) and weight (kg) using calibrated scales

2.5 CMR Scan Protocols

Subjects underwent CMR scanning which included the following:

(1) Phosphorus-31-MR spectroscopy (^{31}P-MRS) assessment of myocardial energetics
(2) Short axis cine stack to assess left ventricular volumes and systolic function
(3) Long axis cine imaging to assess left atrial volumes

(4) Native T1 mapping for tissue characterisation

(5) Tagging assessment of myocardial strain as a sensitive index of myocardial function

(6) Adenosine stress/rest perfusion imaging as a marker of perfusion reserve

(7) Stress T1 mapping as a novel marker of ischaemia and microvascular function

(8) Late gadolinium enhancement (LGE) to assess for focal areas of cellular necrosis/fibrosis

(9) Post-contrast T1 mapping and extracellular volume (ECV) estimation for detection of diffuse myocardial fibrosis

Examinations were performed mainly at 1.5 tesla (Siemens Avanto, Siemens Healthcare, Erlangen, Germany) using a 32-channel phased-array coil, whilst ^{31}P-MRS was undertaken at 3 tesla (TIM Trio, Siemens Healthcare).

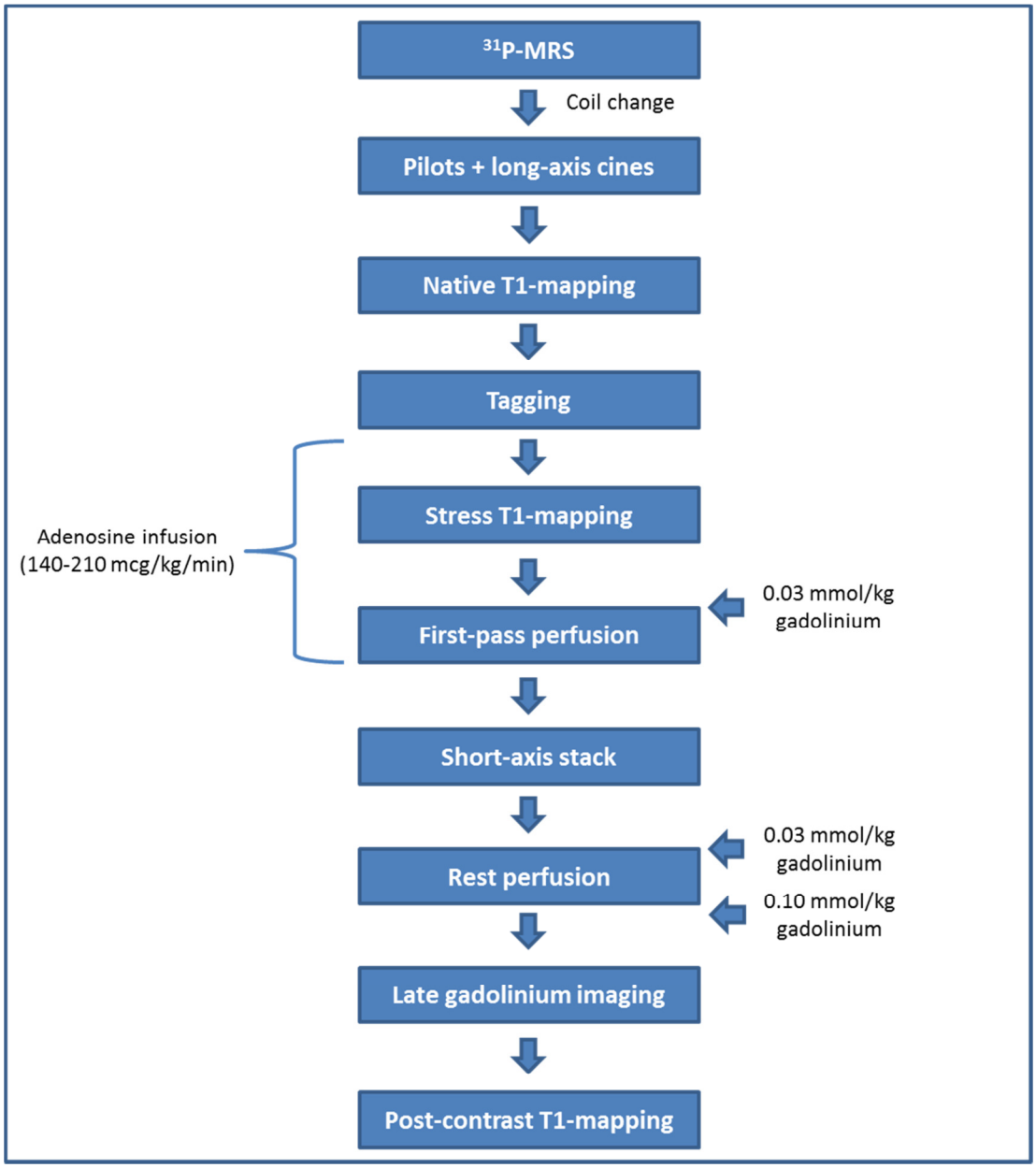


Figure 7: Complete CMR protocol. *This protocol was used for AF patients at the pre-ablation and late post-ablation time points, as well as for the control subjects in SR.* ^{31}*P-MRS was undertaken at 3T, the remaining parameters were acquired at 1.5T.*

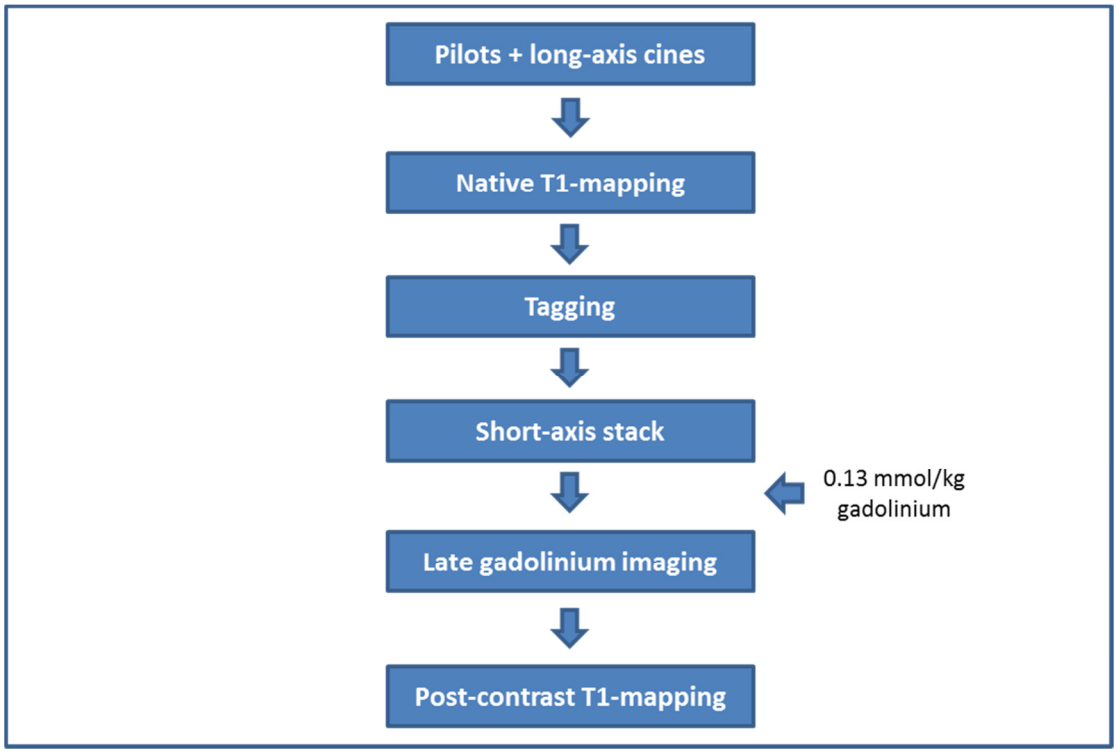


Figure 8: Abbreviated CMR protocol. *This protocol was used for AF patients at the early post-ablation visit and was acquired at 1.5T.*

Care was taken with positioning of ECG electrodes to ensure good ECG signal quality and a large R-wave to T-wave ratio, to reduce the risk of mis-triggering during acquisitions.

All images were acquired with the subject in the supine position and with a breath-hold at the end of normal expiration to minimise the effects of respiratory motion, except where indicated otherwise below. Three matching short-axis images (at basal, mid-ventricular and apical levels) were acquired for each imaging modality, allowing direct comparison of the data derived with each sequence. All image analysis was conducted offline using cmr42 post-

processing software (version 5.1.1, Circle Cardiovascular Imaging Inc., Calgary, Canada), except where indicated otherwise below.

2.5.1 Phosphorus-31 MR spectroscopy (^{31}P-MRS)

^{31}P-MRS studies were acquired on a 3 tesla Siemens Trio MR system (Erlangen, Germany) with the subject in the prone position, using a dedicated cardiac spectroscopy surface coil (modified from a standard Siemens 1.5 T Heart/Liver 31P coil[90]).

A 3-dimensional acquisition-weighted chemical shift imaging technique was used with 10 averages at the centre of K-space and ultrashort TE to minimise T2 effects and first-order phase artefacts. Acquisition time was ~9 minutes in a non-ECG gated and free-breathing acquisition. An optimised radiofrequency pulse centred between γ- and α-ATP resonance frequencies was used to ensure uniform excitation of all spectral peaks. Five Nuclear Overhauser Effect (NOE) pulses (2.5 ms, 222.2 V separated by 80.5 ms) were used to increase signal-to-noise. Acquisition matrix was 16 x 8 x 8 and field of view was 240 x 240 x 200 mm. Three 25-mm-thick saturation bands were used to minimise signal contamination in the heart, 2 placed over chest wall muscle and 1 placed over liver. The chemical shift imaging grid was placed with a central voxel in the mid-ventricular septum and rotated to maximize coverage of the septal myocardium.

The spectrum from the mid-ventricular septal voxel was fitted using a custom implementation of AMARES (the advanced method for accurate, robust,

and efficient spectral fitting) in a semi-automated spectroscopy post-processing pipeline[91] in Matlab (Mathworks Inc, Nattick, USA). Fitting used prior knowledge specifying 11 Lorentzian peaks (a,b,g-ATP multiplet components, PCr, PDE, and 2x2,3-DPG), fixed amplitude ratios, and scalar couplings for the multiplets. The fitted amplitudes were then corrected for blood contamination by subtracting 30% of the average of the two 2,3-DPG signals from each of the ATP amplitudes. The remaining PCr and ATP signals were corrected for the effects of partial saturation using the flip angle at the centre of the voxel, assuming no motion effects and with the T1 values shown in Table 1 in Rodgers et al.[92].

2.5.2 Cine imaging

Cardiac volumes were acquired using steady state free precession (SSFP) imaging. Scan parameters were typically: voxel size 2.0x2.0x8.0mm, FOV=380x380mm, TR/TE 39.6/1.12ms, flip angle 55°, matrix 192x192, GRAPPA=3, 24 reference lines, segments=15, concatenations=1. Pilot images were initially acquired and used to plan and acquire horizontal long axis (HLA), vertical long axis (VLA), left ventricular outflow tract (LVOT) long axis and short axis stack images.

Cines were acquired with retrospective gating for patients in SR at the time of the scan, and with arrhythmia-sorting as a first-choice method for patients in AF at the time of the scan. For patients in AF where acceptable images could not be obtained, prospectively-triggered cines were acquired

instead. Real-time acquisition sequences were also undertaken for all patients in AF during scanning, to allow visual assessment of ejection fraction and corroborate quantitative volumetric analysis. No cases were identified with discordance between visual assessment of ejection fraction on real-time acquisition and the results of blinded quantitative volumetric analysis.

Cine image analysis was conducted offline with cmr42 post-processing software (version 5.1.1, Circle Cardiovascular Imaging Inc., Calgary, ON, Canada). All data sets were anonymised and placed in a random order for contouring. Contours were placed by an operator not involved with data acquisition who was blinded to clinical status, study timepoint and rhythm at the time of scanning.

LV short axis epicardial and endocardial borders were manually contoured at end diastole and end systole (see Figure 9). LV end systolic (ESV) and end diastolic (EDV) volumes were used to calculate stroke volume (SV) as SV = EDV - ESV. Ejection fraction (EF) and cardiac output (CO) were calculated as EF = SV / EDV and CO = SV x HR, respectively. LV mass was calculated by subtracting the endocardial volume from the epicardial volume in end-diastole, based on prior knowledge of myocardial specific gravity (1.05 g/cm^3).

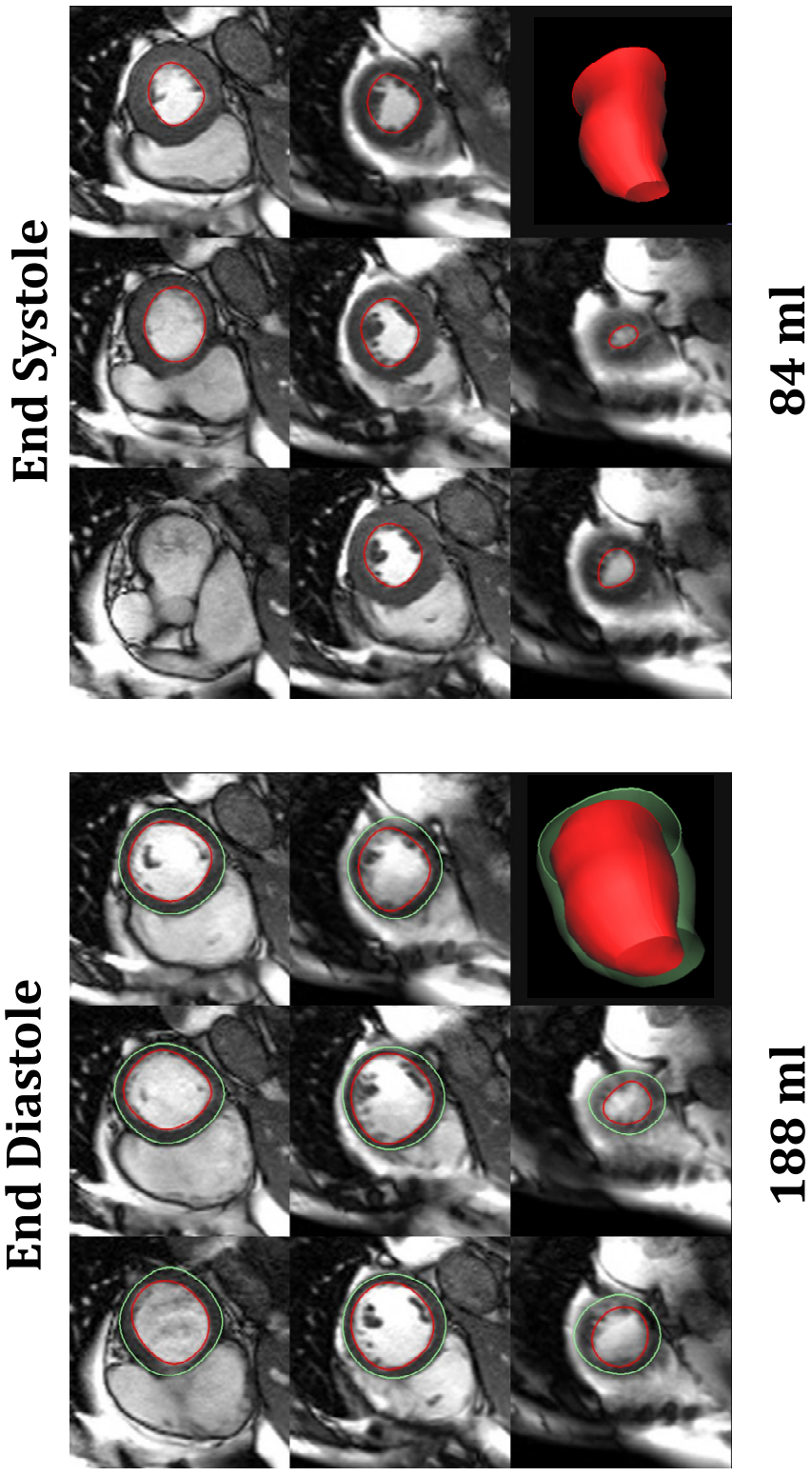


Figure 9: Representative myocardial contours in a patient in AF during CMR. *Manually drawn endocardial (red) and epicardial (green) contours are shown, as well as the derived 3D volume model and calculated end diastolic and end systolic volumes.*

Myocardial deformation was assessed using the established tissue-tracking method to obtain global myocardial values for peak systolic circumferential strain, peak systolic radial strain, and peak diastolic radial strain rate. All strain indices were derived on a segmental basis and then averaged to generate respective global values on a per-individual basis.

Left atrial maximal volume (LA_{max}) and minimal volume (LA_{min}) were determined with the biplane area-length method, as previously described[93] and used to calculate total left atrial emptying fraction: $LAEF = (LA_{max} - LA_{min}) / LA_{max}$.

2.5.3 Choice of short axis slice positions

Three short axis cine images (base, mid-ventricular and apical) were chosen for subsequent imaging. The basal slice was chosen carefully to avoid the LV outflow tract in systole using the LVOT view; the mid-ventricular slice was chosen to include the papillary muscles; care was taken to ensure that the apical slice contains sufficient myocardium to minimise partial volume effects[94]. These three short axis slice positions were subsequently copied and used for T1 mapping, tagging, perfusion imaging and LGE imaging to allow cross-modality comparisons.

2.5.4 T1 mapping (native)

Myocardial T1 mapping was performed using the Shortened Modified Look-Locker Inversion Recovery (ShMOLLI) sequence, as previously described[95].

Briefly, T1 maps are based on 5-7 images with specific TI = 100-5000 ms, collected using SSFP readouts in a single breath-hold, typically for a patient in sinus rhythm: TR/TE = 201.32/1.07 ms, flip angle = 35º, FOV = 340x255 mm, matrix = 192x144, 107 phase encoding steps, interpolated voxel size = 0.9 x 0.9 x 8 mm, GRAPPA = 2, 24 reference lines, cardiac delay time TD = 500 ms; 206 ms acquisition time for single image, phase partial Fourier 6/8, segments = 79, measurements = 1, bandwidth = 898 Hz/Px.

Specific modifications to the ShMOLLI sequence were undertaken to permit application in the presence of tachyarrhythmia (including AF), and these modifications were validated in patients. This novel methodological work is described in detail in Chapter 4: Systolic ShMOLLI myocardial T1 mapping for application in tachyarrhythmia and improved robustness to partial-volume effects. Briefly, the approach taken was to reduce the trigger delay to permit readout in systole, thereby avoiding the mistriggering that is often encountered when applying the standard diastolic readout sequence in the presence of tachyarrhythmia.

To assess the quality of T1 model fitting for each T1 map, parametric maps of the goodness of fit (R^2 maps) were used. R^2 maps provide an additional means to identify areas with potentially compromised T1 accuracy and allow critical assessment of the quality of T1 maps generated[96].

Offline post-processing was conducted using dedicated in-house software “MC-ROI” written in IDL by Professor Stefan K Piechnik (Interactive

Data Language, Ver. 6.1, Exelis Visual Information Solutions, Inc., Boulder, USA). Endo- and epicardial contours were manually traced on each T1 map, taking care to avoid partial-volume effects of neighbouring tissues. Manually drawn endo- and epicardial contours were both then "eroded" by 1 pixel towards the centreline of the myocardium, again to further minimise contamination of the myocardium sample by partial volume effects, as previously published[97]. Each slice was then divided into 6 segments, using the anterior right-ventricular-left-ventricular insertion point as reference. All voxels in each myocardial segment were analysed, and segmental data extracted for further analysis included mean T1 value, standard deviation of T1 value and median R^2 value between the manually drawn outlines. A manually drawn contour was also placed in the LV blood pool, away from the papillary muscles if present, to obtain an estimate of the blood T1 value. No motion correction techniques were employed.

2.5.5 Post-contrast T1 mapping and ECV estimation

T1 maps were re-acquired at 15 minutes after a top-up of intravenous MR contrast agent, at identical slice positions and using the same sequence parameters as for native T1 mapping (see 2.5.4). This time interval has previously been shown to allow dynamic equilibration between contrast agent distribution in the blood and myocardium[45, 98].

Offline post-processing of T1 maps acquired post-contrast was conducted using the same methods as outlined for native T1 maps (see 2.5.4). R1 of blood and myocardium was calculated as R1=1/T1 on both native and

post-contrast maps. Haematocrit was measured on a blood sample drawn on the same day, immediately prior to the CMR scan. ECV was then estimated using the following equation as previously described[98]:

$$\text{ECV} = (1 - \text{haematocrit}) \times \left(\frac{\Delta R1_{myocardium}}{\Delta R1_{blood}}\right)$$

2.5.6 Tagging assessment of myocardial strain

Tagged cine MRIs were acquired with an ECG-triggered segmented k-space gradient echo sequence with spatial modulation of magnetization in orthogonal planes. The scan parameters were typically: voxel size 2.1 x 1.4 x 8.0 mm, FOV = 360 x 292 mm, matrix 141 x 256, TR/TE = 40.45/3.89 ms, flip angle 14°, segments = 9, phases = 16, concatenations = 1, grid tag distance = 7mm, bandwidth = 184 Hz/Px.

Post-processing of tagging images was performed using CIM-Tag software (Auckland, New Zealand). Semiautomated analysis was performed by aligning a grid to the myocardial tagging planes in end-diastole. End-systole was determined visually, and tags adjusted at each frame through the cardiac cycle to derive peak systolic circumferential strain (PSCS) for the mid-ventricular slice, which is expressed as a percentage change from end-diastole. Normal PSCS has been described as −19±2%[99]; impaired myocardial contractility is shown by a more positive value.

2.5.7 Adenosine stress/rest perfusion

Participants were asked to abstain from caffeine and other adenosine antagonists for 24 hours prior to imaging. Two intravenous cannulae were placed (ideally one in each antecubital fossa), to allow independent and simultaneous administration of both an infusion of adenosine and a subsequent rapidly-delivered bolus of gadolinium-based contrast agent.

Perfusion imaging was performed every cardiac cycle during the first pass of intravenous MR contrast agent using a T1-weighted fast (spoiled) gradient echo sequence. Scan parameters were typically: voxel size 2.8 x 2.3 x 10.0 mm, FOV = 360 x 270 mm, matrix 96 x 160, TR/TE = 160.76/1.05 ms, flip angle 12^{o}, TI 100 ms, GRAPPA = 2, 18 reference lines, measurements = 50, segments = 57, concatenations = 1, phases = 1, 1 shot per slice, bandwidth 651 Hz/Px. A test scan was acquired first without contrast agent to allow any problems (e.g. artefacts, breath-holding or ECG-mistriggering) to be identified and addressed.

For stress perfusion, adenosine was infused initially at 140 μg/kg/min. In the absence of a satisfactory haemodynamic response (defined as a heart rate increase of at least 10 beats per min from the baseline heart rate and/or a drop in systolic blood pressure drop of at least 10mmHg from the baseline systolic blood pressure) and development of typical symptoms (e.g. chest tightness, dyspnea, flushing), the rate of infusion was sequentially increased to 180 μg/kg/min and then to a maximum of 210 μg/kg/min. Heart rate and blood

pressure were measured before, at one minute intervals during, and after adenosine stress.

Image acquisition commenced at peak stress, at least 3 minutes after commencement of adenosine. Subjects were asked to hold their breath for as long as possible at the end of normal expiration. A bolus of intravenous MR contrast agent (0.03mmol/kg body weight of Gd-DTPA [Dotarem®; Guerbet, France] delivered at 6 ml/s) and an immediate 15ml bolus flush of 0.9% sodium chloride also delivered at 6ml/s were administered via a power injector; this injection was manually triggered after an interval of 3 heart beats from the initiation of image acquisition. The adenosine infusion was discontinued when contrast was seen in the LV cavity. Rest perfusion imaging was performed in an identical fashion (but without adenosine administration) after a gap of at least 15 minutes from cessation of the adenosine infusion.

Offline perfusion analysis was undertaken as previously described[86, 100]. Endo- and epicardial contours were manually placed with careful frame-by-frame manual correction for respiratory motion. A region of interest was also placed in the LV blood pool, taking care to avoid the papillary muscles. In order determine adequacy of adenosine stress, splenic switch-off was also assessed visually in addition to conventional haemodynamic parameters described above – this technique has recently been described as method of identifying inadequate stress response in adenosine perfusion CMR[101].

Quantitative perfusion analysis of absolute myocardial blood flow (MBF) was performed as previously described[102, 103]; in brief, MBF was determined by model-independent deconvolution of signal intensity curves with an arterial input function measured in the LV blood pool, with explicit accounting for any delay in the arrival of the tracer.

Endocardial , epicardial and LV blood pool contours were exported in an anonymised format from cmr[42] and imported into an analysis tool written by Professor Michael Jerosch-Herold (Brigham and Womens' Hospital, Boston, MA, USA) and running in MatLab (version R2008a, The Mathworks, Natick, MA). Baseline and stress MBF were each independently calculated on a segmental basis, with blinded manual assessment of fitting quality in every myocardial segment. Segments where the tissue signal intensity curve did not fit well were rejected from further analysis. All segments that passed this quality check were averaged to derive global baseline and stress MBF values on a per-individual basis.

Absolute baseline MBF is known to be closely related to baseline RPP[104], and baseline MBF was therefore corrected for baseline RPP using the following formula, to account for differences in cardiac work as previously described[57, 105]: baseline $MBF_{corrected}$ = baseline MBF / (baseline RPP / 10,000). Adenosine-stress induced MBF was not corrected, as this parameter is grossly independent of RPP[106].

2.5.8 Late gadolinium enhancement (LGE) imaging

Late gadolinium enhancement imaging was acquired using a T1-weighted phase-sensitive inversion recovery sequence at ~8-10 minutes after the administration of top-up intravenous MR contrast agent (0.1 mmol/kg body weight of Gd-DTPA [Dotarem®; Guerbet, France]). The inversion time was adjusted for optimal nulling of remote normal myocardium.

The scan parameters were typically: voxel size 2.0 x 1.5 x 8.0 mm, matrix 144x256, FOV=380x285mm, TR/TE=800.20/3.36ms, flip angle 25^{o}, GRAPPA=2, 24 reference lines, segments=25, phases=1, concatenations=1, measurements=1, bandwidth=130Hz/Px.

Images were assessed by 2 experienced operators at the time of acquisition, and LGE suspected on short-axis imaging was confirmed with additional imaging in long-axis or perpendicular to the lesion. Semi-quantitative analysis was undertaken with cmr42 postprocessing software (version 5.1.1, Circle Cardiovascular Imaging Inc., Calgary, ON, Canada), by setting a signal intensity threshold at 5 SD above the mean intensity of a reference region of interest placed in a remote area of myocardium with no visual evidence of enhancement, as previously described[107].

2.6 Echocardiography

Transthoracic echocardiography was undertaken in the left lateral position to determine the ratio of peak early diastolic mitral inflow velocity to spectral

tissue Doppler-derived peak early diastolic velocity at the mitral annulus (E/E'), as a marker of LV diastolic function[108]. These measures were averaged over at least 10 cardiac cycles for patients in AF during imaging[108]. E/E' values reported are the average of lateral and septal measurements.

2.7 Blood Collection, Handling, Storage and Analysis

Venous blood (20 ml) was drawn prior to each CMR scan and collected into 2x citrate, 2x EDTA, and 2x serum sample tubes. Samples were centrifuged at 2500 rpm, at 4°C for 10 minutes and the plasma/serum was divided into 3 aliquots for each sample type. These were stored at -80°C pending batch analysis at study completion.

NT-proBNP was measured in plasma using an automated immunoassay (Roche Diagnostics, Basel, Switzerland). Uncertainty measurements were 9% at a level of 63 pg/ml and 4% at a level of 457 pg/ml.

2.8 Rhythm Monitoring

2.8.1 Assessment of change in AF burden by Holter monitoring

AF burden in paroxysmal AF patients was estimated pre-ablation using a 7-day Holter monitor. All patients were requested to undertake similar 7-day Holter monitoring after the last follow-up visit (at 6-9 months post-ablation). As the purpose of these investigations was to investigate asymptomatic recurrence of AF and AF burden, they were not performed in patients with ECG-documented

persistent AF either pre- or post-ablation (in whom AF burden was assumed to be 100%). Patients with a history of persistent AF who had undergone cardioversion to SR pre-ablation (n=3) were excluded from the calculation of change in AF burden post-ablation.

2.8.2 Event monitoring

All patients were issued with a validated leadless ECG event monitor (Omron HCG-801, Omron Healthcare, UK)[109, 110] and requested to undertake intermittent ECG event monitoring for approximately 3 months following an initial 3-month post-ablation blanking period. Patients were asked to make at least 2 recordings per day (even in the absence of symptoms), with further recordings at the time of symptoms. Event monitoring was not requested in patients with ECG-documented recurrence of persistent AF.

2.8.3 Classification of patients post-ablation

Patients were classified based on both (*i*) rhythm during each study assessment and (*ii*) presence or absence of recurrent AF post-procedure. For the former, patients were categorised by rhythm at the pre-ablation visit and at both follow-up visits. For example, a patient in AF pre-ablation who had recovered SR early after ablation but relapsed to AF by the last follow-up visit, was classified as 'AF-SR' at the early timepoint and 'AF-AF' at the last follow-up. Patients with at least one of the following were classified as having recurrent AF post-procedure: (*i*) ECG-documented clinical recurrence after the blanking period, (*ii*) ≥30s[111] of AF or other atrial arrhythmia (such as atrial flutter or atrial tachycardia) on post-

ablation Holter monitoring or (*iii*) ≥1 rhythm strip (30s) showing AF or other atrial arrhythmia on intermittent ECG monitoring.

2.9 Data Blinding for Analysis

Whilst interim analyses were conducted in an unblinded fashion, results reported in this Thesis are the result of blinded re-analysis that was undertaken for all potentially subjective analysis techniques (e.g. cine imaging, strain, T1-mapping, perfusion).

The Excel randomisation function was used to generate anonymous codes for all scans. The alphabetical order of the anonymised codes was thus randomised with respect to patient versus control status, and study timepoint for patients. Studies were then anonymised using cmr[42], and operators not involved with data collection placed contours on the anonymised datasets. Relevant data were extracted using automated Excel macros that parsed scientific reports saved directly from cmr[42]. In the case of T1-mapping, the anonymised studies were exported in DICOM format from cmr[42] and imported into MC-ROI for analysis.

Chapter 3

Left ventricular function and energetics in atrial fibrillation

3.1 Abstract

3.1.1 Background

"Lone" atrial fibrillation (AF) may reflect a subclinical cardiomyopathy that persists after sinus rhythm (SR) restoration, providing a substrate for AF recurrence. To test this hypothesis, this study investigated the effect of restoring SR by catheter ablation on left ventricular (LV) function and energetics in patients with AF but no significant comorbidities.

3.1.2 Methods

Fifty-three patients with symptomatic paroxysmal or persistent AF and without significant valvular disease, uncontrolled hypertension, coronary artery disease, uncontrolled thyroid disease, systemic inflammatory disease, diabetes mellitus, or obstructive sleep apnoea (i.e. "lone" AF) undergoing ablation and 25 matched controls in SR were investigated. Magnetic resonance imaging quantified LV ejection fraction (LVEF), peak systolic circumferential strain (PSCS), and left atrial volumes and function, whereas Phosphorus-31 MR spectroscopy

evaluated ventricular energetics (ratio of phosphocreatine-to-ATP). AF burden was determined before and after ablation by 7-day Holter monitoring; intermittent ECG event monitoring was also undertaken after ablation to investigate for asymptomatic AF recurrence.

3.1.3 Results

Before ablation, LV function and energetics were significantly impaired in patients compared with control subjects (LVEF, 61% [interquartile range (IQR) 52–65%] versus 71% [IQR 69–73%], p<0.001; PSCS, -15% [IQR -11 to -18%] versus -18% [-17 to -19%], p=0.002; ratio of phosphocreatine to ATP, 1.81±0.35 versus 2.05±0.29, p=0.004). As expected, patients also had dilated and impaired left atria compared with control subjects (all p<0.001). Early after ablation (1-4 days), LVEF and PSCS improved in patients recovering SR from AF (LVEF, +7.0±10%, p=0.005; PSCS, -3.5±4.3%, p=0.001) but were unchanged in those in SR during both assessments (both p=ns).

At 6 to 9 months after ablation, AF burden reduced significantly (from 54% [IQR 1.5%-100%] to 0% [IQR 0%-0.1%], p<0.001). However, LVEF and PSCS did not improve further (both p=ns) and remained impaired compared with control subjects (p<0.001 and p=0.003, respectively). Similarly, there was no significant improvement in atrial function from before ablation (p=ns), and this remained lower than in control subjects (p<0.001). The ratio of phosphocreatine to ATP was unaffected by heart rhythm during assessment and AF burden before ablation (both p=ns). It was unchanged after ablation

(p=0.57), remaining lower than in control subjects regardless of both recovery of SR and freedom from recurrent AF (p=0.006 and p=0.002, respectively).

3.1.4 Conclusions

Patients with "lone" AF have impaired myocardial energetics and subtle LV dysfunction, which do not normalise after ablation. These findings suggest that AF may be the consequence (rather than the cause) of occult cardiomyopathy, which persists despite a significant reduction in AF burden after ablation.

3.2 Introduction

Atrial fibrillation (AF) is the most common sustained clinical arrhythmia, and is associated with an increased risk of severe stroke[5], myocardial infarction[6], and premature death[7]. The worldwide incidence, prevalence and age-adjusted mortality from AF are increasing, presenting a rapidly-growing public health and economic burden[112].

Mechanistic studies in animal models of pacing-induced AF indicate that atrial remodelling[113], oxidative stress[114] and impaired coronary reserve[60] induced by AF are important in arrhythmia maintenance. However, direct translation of these findings is challenging because human AF often reflects multiple interacting causative factors. Indeed, no unique mechanisms for AF have been identified in patients[115], even in the up to one third of cases in which AF occurs in the absence of identifiable underlying cardiovascular disease or

other specific cause[116] (conventionally referred to as "lone" AF, although the use of this term has recently been questioned[117]).

Subtle left ventricular (LV) dysfunction has been observed in patients with AF[11], with several studies showing that adverse LV structural remodelling and dysfunction are at least partially reversible after restoration of sinus rhythm (SR) with catheter ablation[40]. Even when the ventricular rate is well controlled, AF may lead to LV dysfunction by reducing myocardial perfusion reserve, impairing calcium handling, and increasing myocardial oxidative stress and fibrosis[10]. However, large-scale clinical trials of pharmacological strategies designed to restore SR have failed to show prognostic benefit (e.g. reduction in death, stroke or heart failure hospitalisations) compared with ventricular rate control[19-21], whereas the effect of catheter ablation remains to be investigated. These results could reflect limited efficacy and potential toxicity of antiarrhythmic medications; nevertheless, it remains the case that at present there are no published large-scale randomized clinical data demonstrating that restoration of SR improves major outcomes in patients with AF, raising the possibility that, at least in patients with "lone" AF and controlled ventricular rate, the arrhythmia may not be the primary cause of LV dysfunction. Instead, a subclinical cardiomyopathy that persists after restoration of SR may provide a substrate for AF initiation and recurrence and have an effect on patient prognosis.

Here, cardiac magnetic resonance (MR) was used to serially assess atrial and LV volumes and function in patients with AF before and after catheter ablation. Both early and late post-ablation MR assessments were included, to quantify the proportion of any improvement in LV function resulting from short-term changes in haemodynamics versus longer-term beneficial cardiac remodelling. Phosphorus-31 MR spectroscopy (^{31}P-MRS) was also used to determine myocardial energetics before and after ablation because altered cardiac energy metabolism has been identified as an early marker of cardiomyopathy[118].

3.3 Methods

This prospective study was undertaken in a single tertiary centre. The study protocol was approved by a local Research Ethics Committee, and all subjects gave written informed consent.

3.3.1 Patient population

Detailed inclusion and exclusion criteria are provided in Chapter 2. Briefly, patients undergoing first-time catheter ablation of symptomatic paroxysmal or persistent AF were screened for eligibility. Individuals with significant valvular disease, uncontrolled arterial hypertension, known coronary artery disease, uncontrolled thyroid disease, systemic inflammatory disease, asthma, diabetes mellitus, or obstructive sleep apnoea were not enrolled.

Clinical management of patients (including ablation strategy and choice of anticoagulant and antiarrhythmic drugs) was at the discretion of the responsible physician.

3.3.2 Control group

Control subjects in SR were recruited via poster advertising. Exclusion criteria were identical to those for patients, except that volunteers with a history of palpitations or arrhythmia were not enrolled. Control subjects were selected to match patients for age and gender.

3.3.3 Study protocol

Full details of the study protocol are contained in Chapter 2: General Methods. Briefly, patients were studied at three timepoints: up to 4 weeks prior to ablation, early after ablation (up to 4 days from the procedure), and at later follow-up (between 6 and 9 months after ablation). Myocardial energetics was not assessed at the early post-ablation timepoint. Controls were studied at a single timepoint.

3.3.4 Cardiac magnetic resonance and echocardiography

Full details of the cardiac MR imaging, ^{31}P-MRS and echocardiography protocols, including pulse sequence parameters and detailed description of analysis methods are contained in Chapter 2: General Methods.

3.3.5 Statistical analysis

A priori sample size calculation was performed to detect a change in the primary outcome of LVEF after ablation. On the basis of the assumption that patients with AF have an LVEF of 55±10%, it was calculated that paired analysis of 45 patients before and after ablation would give >90% power to detect a change in LVEF of at least 5 percentage points (2-sided $\alpha = 0.05$). This number of patients would also allow detection of a change in PCr/ATP ratio after ablation of ≥10% with >90% power (2-sided $\alpha=0.05$). Recruitment was extended to ~60 patients to allow for incomplete follow-up, claustrophobia, and other obstacles to completing the protocol. On the basis of pilot data indicating that the PCr/ATP ratio was 1.84±0.41 in AF patients (n=10) and 2.12±0.26 in normal subjects (n=8), it was calculated that recruitment of ≥20 controls and ≥40 AF patients (1:2 allocation) would give >90% power to detect a 13% reduction in PCr/ATP ratio in patients compared with control subjects.

Statistical analyses were performed with IBM SPSS Statistics for Windows, version 20.0 (IBM Corp., Armonk, NY, USA), GraphPad Prism version 6 (GraphPad Software, San Diego, California, USA) and G*Power version 3.1.9.2[119]. Normality of data was assessed with Kolmogorov-Smirnov tests. Normally-distributed data were compared by use of *t* tests (paired when appropriate) and 1-way ANOVA. Non-normally distributed unpaired data were compared by use of the Mann-Whitney *U* test or the Kruskal-Wallis test, and non-normally distributed paired data were compared with the Wilcoxon signed-

rank test or the related-samples Friedman 2-way ANOVA by ranks. The χ^2 test was used to compare proportions. All tests were 2 tailed, values of $p < 0.05$ (after Bonferroni or equivalent adjustment for multiple comparisons when appropriate) were considered significant. Data are shown as mean ± SD or median and interquartile range (IQR).

3.4 Results

A total of 58 patients with AF consented to the study, 53 provided at least 1 set of imaging data and 45 completed all 3 study visits (**Figure 10**).

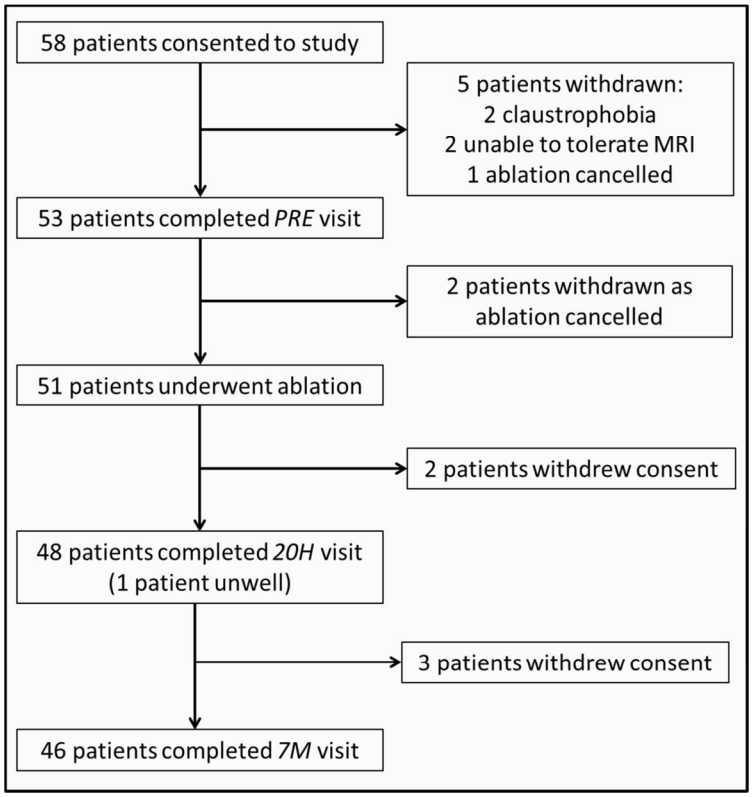


Figure 10: Flowchart of patients with atrial fibrillation through the study. *The number of patients consenting to the study, completing the pre-ablation (PRE) visit, undergoing ablation, and completing the early (20H) and late (7M) visits are shown. The number of patients not completing each stage is also indicated, with reasons given. MRI indicates magnetic resonance imaging.*

The early follow-up visit was conducted at a median of 20 hours after ablation (IQR 19-23 hours) and the late follow-up visit at a median of 7 months (IQR 7-9 months).

Baseline characteristics of patients and control subjects are detailed in **Table 1**.

Table 1: Baseline characteristics of the study groups.

	AF Patients (n=53)	SR Controls (n=25)	p value
Age (years)	63 ± 8	61 ± 6	0.294
Male (%)	75	72	0.743
BMI (kg/m^2)	27 (24 – 31)	26 (24 – 29)	0.277
Pulse (bpm)	64 (54 – 80)	60 (60 – 66)	0.620
SBP (mmHg)	130 (124 – 145)	126 (119 – 139)	0.124
DBP (mmHg)	81 ± 11	78 ± 10	0.257
Ever smoked (%)	38	20	0.117
Alcohol (units/week)	9 (1 – 20)	6 (0 – 19)	0.690

Medications and procedural details of ablation categorised by AF type are summarised in **Table 2**. Of 26 persistent AF patients, 3 (12%) underwent cardioversion to SR prior to the pre-ablation CMR scan.

Table 2: Baseline characteristics and ablation details for patients, categorised by AF type.

	Paroxysmal AF (n=27)	Persistent AF (n=26)	p value
Male (%)	78	73	0.691
BMI (kg/m^2)	25 (24 – 29)	29 (25 – 35)	**0.033**
Pulse (bpm)	56 (48 – 64)	72 (65 – 90)	**0.001**
CHA_2DS_2-VASc	1 (0 – 2)	2 (1 – 2)	**0.046**
In AF at *PRE* (%)	22	88	**<0.001**
Ablation type (%)			
Radiofrequency	48	85	**0.005**
Cryoballoon	48	4	**<0.001**
Laser balloon	4	4	0.978
Medications at PRE (%)			
ACEI / ARB	26	62	**0.009**
Beta-blocker	19	73	**<0.001**
Flecainide	37	8	**0.011**
Sotalol	33	8	**0.021**
Digoxin	4	27	**0.018**
Dronedarone	7	0	0.157
Amiodarone	4	12	0.280
Warfarin	48	69	0.119
NOAC	33	31	0.842
Medications at 7M (%)			
ACEI / ARB	30	54	0.074
Beta-blocker	15	42	**0.026**
Flecainide	19	0	**0.021**
Sotalol	11	0	0.080
Digoxin	0	4	0.314
Dronedarone	7	0	0.157
Amiodarone	4	8	0.530
Warfarin	41	46	0.691
NOAC	19	19	0.947

ACEI indicates angiotensin converting enzyme inhibitor; ARB, angiotensin receptor blocker; NOAC, non-vitamin K oral anticoagulant

Median time from the first diagnosis of AF was 3.7 years (IQR 2.0 – 7.3 years). Patients with persistent AF had slightly higher body mass index and pulse than patients with paroxysmal AF, but exclusion of patients with uncontrolled ventricular rate meant that the pulse rate was well-controlled in the persistent AF group (median 72 bpm, IQR 65-90 bpm). Median AF burden in patients with paroxysmal AF before ablation was 2.6% (~4.5 hours per week), whereas median AF burden in all patients was 54% (~91 hours per week).

3.4.1 Results in control subjects and patients with AF before ablation

LV volume, function and mass indices and left atrial volumes and function in control subjects and pre-ablation patients are summarised in **Table 3**. There were no significant differences in LV end-diastolic volumes between the groups, but patients with AF had significantly larger end-systolic volumes and hence lower LVEF than matched control subjects (both $p<0.001$). However, the impairment in LVEF was subtle, and the median LVEF in patients (61%) fell at the lower end of the normal range by MR imaging (57-81%)[120]. PSCS was more clearly abnormal in patients with AF (median, -15% [IQR, -11% to -18%]; normal, -19±2%[99]) and was significantly impaired compared with control subjects (**Table 3**). As expected, patients with AF had dilated and impaired left atria compared with control subjects (all $p<0.001$; **Table 3**).

Table 3: Left ventricular and left atrial indices in the study groups.

	AF Patients (n=53)	SR Controls (n=25)	p value
LV end-diastolic volume (mL)	149 ± 39	137 ± 30	0.189
LV end-systolic volume (mL)	58 (43 – 75)	41 (33 – 51)	**<0.001**
LV stroke volume (mL)	81 (71 – 94)	93 (83 – 109)	**0.035**
LVEF (%)	61 (52 – 65)	71 (69 – 73)	**<0.001**
Cardiac output (L/min)	5.6 ± 1.5	6.0 ± 1.4	0.326
LV mass index (g/m^2)	61 ± 12	56 ± 13	0.112
LV mass/end-diastolic volume (g/mL)	0.85 (0.73 – 0.96)	0.77 (0.73 – 0.86)	0.181
Peak systolic circumferential strain (%)	-15 (-11 – -18)	-18 (-17 – -19)	**0.002**
LV E/E' ratio	7.0 (5.8 – 8.7)	7.6 (6.3 – 8.6)	0.304
LV LGE area, %	0.2 (0 – 0.5)	0.1 (0 – 0.3)	0.190
LA_{max}, ml	102 ± 35	77 ± 22	**<0.001**
LA_{min}, ml	71 ± 36	35 ± 11	**<0.001**
LAEF, %	30 (16 – 49)	53 (49 – 61)	**<0.001**

AF indicates atrial fibrillation; E/E' ratio, ratio of peak early diastolic mitral inflow velocity to spectral tissue Doppler-derived peak early diastolic velocity at the mitral annulus; LAEF, left atrial total emptying fraction; LA_{max}, left atrial maximal volume; LA_{min}, left atrial minimal volume; LGE, late gadolinium enhancement; LV, left ventricular; LVEF, left ventricular ejection fraction; and SR, sinus rhythm.

Consistent with the exclusion of patients with uncontrolled hypertension, LV mass index (by MR) and LV diastolic function (by echocardiography) were within the normal range in both patients and control subjects (**Table 3**). The ratio of LV mass to LV end-diastolic volume (which identifies the presence of concentric LV remodelling in the absence of an absolute increase in LV mass[121]) was also similar between patients and control subjects, and was consistent with data reported from healthy control subjects of a similar age in a previous MR study[122].

The quality of ^{31}P-MRS data was equally good in patients and control subjects (median Cramér-Rao lower bounds[123] coefficient of variation of PCr/ATP, 15% for patients and 14% for controls, p=0.52; representative spectra are shown in **Figure 11A**). Myocardial energetics were significantly impaired in patients with AF compared with control subjects (PCr/ATP 1.81±0.35 versus 2.05±0.29, p=0.004; **Figure 11B**).

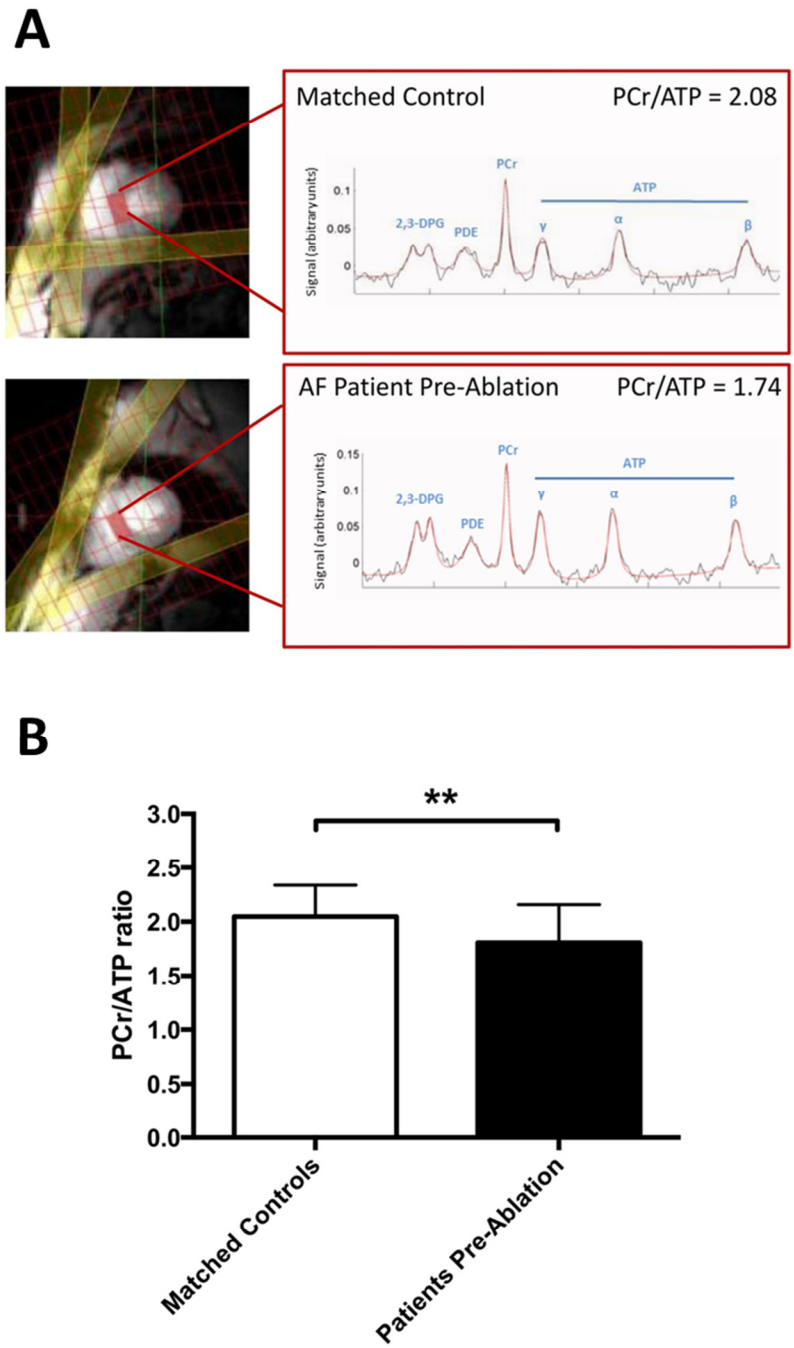


Figure 11: Representative ^{31}P-MR spectra and myocardial energetics in the study groups.*(A) Images (left) show a mid-ventricular short axis slice, with the selected voxel positioned on the septum and highlighted (red rectangle). Saturation band positions are also shown (yellow). Spectra show both raw data (black) and fitted line (red); peaks are labelled corresponding to 2,3-diphosphoglycerate (2,3-DPG), phosphodiester (PDE), phosphocreatine (PCr) and gamma (γ), alpha (α) and beta (β) peaks of adenosine triphosphate (ATP). Representative ^{31}P-MR spectra (right) from a control subject in SR with PCr/ATP = 2.08 and a patient with AF pre-ablation with PCr/ATP ratio = 1.74. (**B**) PCr/ATP ratio in patients and controls (n=52 and n=25, respectively; p=0.004 by unpaired t-test).*

Energetics were similarly impaired regardless of the preablation intrascan rhythm and regardless of Holter-determined AF burden for those in SR (PCr/ATP 1.80±0.39 for pre-ablation AF, 1.86±0.35 for pre-ablation SR with higher-than-median AF burden, and 1.77±0.32 for pre-ablation SR with lower-than-median AF burden; p=0.84; **Figure 12A**). By contrast, presence of AF (rather than SR) during the pre-ablation scan was associated with a significantly lower LVEF (median, 54% [IQR, 48% - 60%] versus 64% [IQR, 63% - 69%]; p<0.001), but there was no difference in LVEF between patients in SR with higher or lower AF burden (p=0.34; **Figure 12B**).

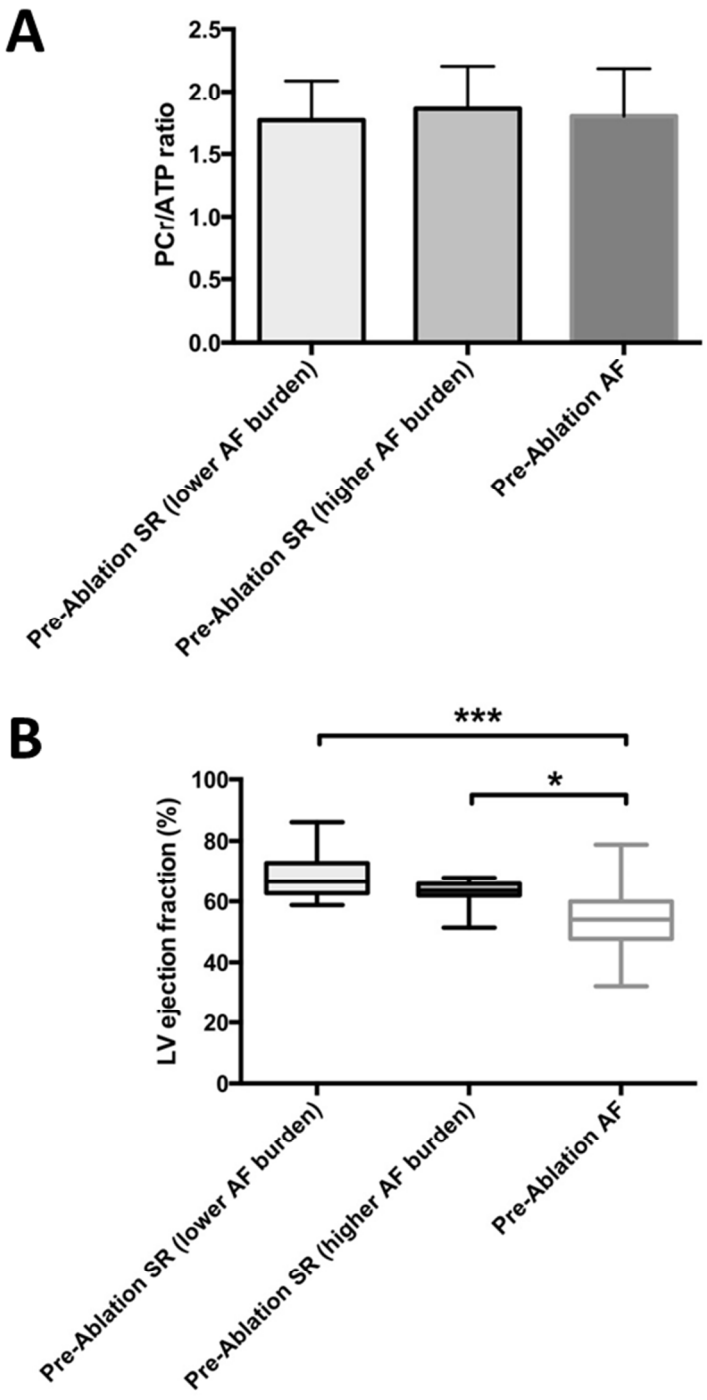


Figure 12: Effect of intra-scan rhythm on LVEF and myocardial energetics in AF patients before ablation.*(A) Myocardial energetics determined by PCr/ATP ratio categorised by rhythm during scan and, for patients in SR, by Holter-determined AF burden (higher or lower than median). There is no difference between the groups (n=10 for SR with lower AF burden, n=11 for SR with higher AF burden and n=28 for AF, p=0.84 by one-way ANOVA). (B) LVEF in AF patients pre-ablation, similarly categorised. Note significantly lower ejection fraction in those in AF compared to those in SR at the time of the scan, irrespective of AF burden (Kruskal-Wallis p=0.0002).*

LGE, indicating LV fibrosis or scar, was an infrequent finding that was detected in 8 patients (15%) and 2 control subjects (8%). In 5 patients, LGE had a localised subendocardial or transmural pattern consistent with a small infarct (which had not been identified on echocardiography); 4 of these patients had no obstructive coronary artery disease at angiography, and the cause of infarction was presumed to be embolic. The other 3 patients and both control subjects had a non-ischaemic pattern of diffuse or patchy fibrosis. No subject had LGE affecting the midventricular septum (i.e., the site of sampling for ^{31}P-MRS). When the subjects with LGE were removed from the analysis, PCr/ATP and LVEF in patients with AF remained significantly impaired compared with control subjects in SR (PCr/ATP, 1.81±0.37 in the 45 remaining patients versus 2.01±0.26 in the 23 remaining control subjects, P=0.02; median LVEF, 61% [IQR, 52%–65%] in the 45 remaining patients versus median 71% [IQR, 69%–73%] in the 23 remaining control subjects, P<0.001). Quantitative analysis of LGE demonstrated no difference in the area of enhancement between patients and control subjects (median, 0.2% [IQR, 0%–0.5%] in patients versus 0.1% [IQR, 0%–0.3%] in control subjects; P=0.19). No new areas of LGE were noted at the postablation scans.

3.4.2 Outcomes following ablation

Ablation was undertaken in 51 patients, with no significant early procedural complications. Radiofrequency ablation was used in 35 patients (69%), cryoballoon ablation in 14 patients (27%) and laser balloon ablation in 2

patients (4%). In the time-span between the end of the 3-month blanking period and the 7-month visit, 9 patients (18%) underwent an attempt at electrical cardioversion and 3 patients (6%) underwent a second ablation procedure as a result of recurrence of AF or a left atrial tachycardia.

At 20 hours, the classification of patients by rhythm groups was as follows: SR-SR, 24; AF-SR, 21; AF-AF, 3. At 7 months, the numbers were the following: SR-SR, 21; AF-SR, 19; AF-AF, 4; SR-AF, 2. Of 46 patients scanned at 7 months, 25 (54%) had evidence of ≥1 episodes of recurrent AF after ablation. However, Holter-determined AF burden at 7 months was significantly lower than before ablation (median, 0% [IQR, 0% to 0.1%] versus median 54% [IQR, 1.5% to 100%]; $p<0.001$).

3.4.3 Early effect of ablation on LV function

Early after ablation, there was no significant overall change in LVEF (median, 61% [IQR, 51-65%] ≤4 weeks before ablation versus 61% [IQR, 57-66%] at 20 hours; n=48; p=0.07). However, there was a significant increase in LVEF (+7.0±10%) in the AF-SR sub-group, unlike the SR-SR and AF-AF sub-groups, in which LVEF was unchanged (**Figure 13A**). A similar pattern was seen for PSCS, with a significant change of -3.5±4.3% (indicating improvement) in the AF-SR sub-group but no change in the other sub-groups (**Figure 13B**).

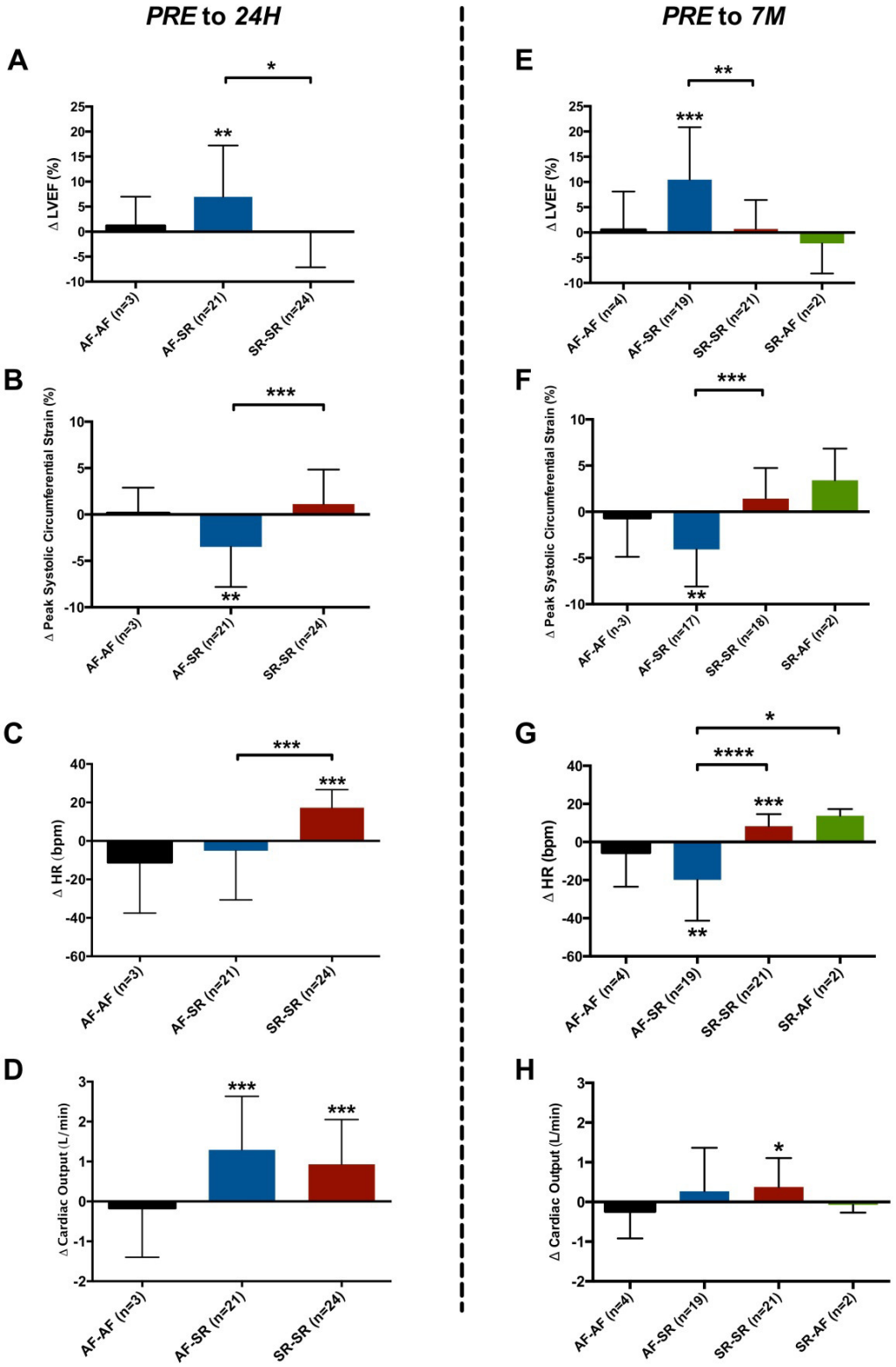


Figure 13: Change in LVEF, PSCS, heart rate and cardiac output early and late after ablation, categorised by the intra-scan rhythm at each timepoint. *One-sample t-tests assessed*

if changes in each sub-group are significantly different to zero. Changes between sub-groups were compared using one-way ANOVA; p values for sub-group comparisons are Bonferroni-corrected for multiple comparisons. (A) At 20H, LVEF improves only in the AF-SR sub-group (p=0.005). (B) Similarly, PSCS also improves only in the AF-SR sub-group (denoted by a more negative change; p=0.001). (C) Only the SR-SR sub-group show a significant increase in heart rate early post-ablation (p<0.001), and both the AF-SR and SR-SR sub-groups show a significant increase in cardiac output, without differences between sub-groups (D).

At 7M, the pattern of change in LV function from PRE in sub-groups is similar to that at 20H – only the AF-SR sub-group show significant improvement in LVEF (E, p<0.001) and PSCS (denoted by a more negative change; F, p=0.001). (G) The heart rate changes from PRE in the AF-SR and SR-SR groups are significantly different (p<0.0001), and there is also a significant difference between the AF-SR and SR-AF groups (p=0.03). (H) Similarly to 20H, there are no significant differences between sub-groups in the change in cardiac output, with only the SR-SR sub-group demonstrating a small increase (p=0.03).

The SR-SR sub-group showed a significant increase in heart rate from ≤4 weeks before ablation to 20 hours (**Figure 13C**), consistent with the expected inflammation[124] and increase in sympathetic activity[125] induced by the procedure; this effect was entirely counteracted in the AF-SR sub-group by the reduction in ventricular rate associated with recovery of SR.

Overall, cardiac output increased significantly after ablation (6.6±1.6 L/min at 20 hours compared with 5.6±1.5 L/min at ≤4 weeks before ablation; p<0.001), driven by both the AF-SR and SR-SR sub-groups (**Figure 13D**).

3.4.4 Late effect of ablation on LV function and myocardial energetics

Late after ablation, there was a modest but statistically significant increase in LVEF from before ablation (median, 62% [IQR, 52% - 65%] <4 weeks before ablation versus 65% [IQR, 59-68%] at 7 months; n=46; p=0.004). However, there was no significant change in LVEF from 20 hours to 7 months (p=0.24),

and LVEF at 7 months remained lower than in matched controls ($p<0.001$), including when analysis was restricted to patients in SR at 7 months (median, 66% [IQR, 61% - 69%] versus 71% [IQR, 69% - 73%], $p=0.002$). Similarly, PSCS in patients in SR at 7 months was impaired compared with matched control subjects (median, -16% versus -18%; $p=0.035$) with no significant overall improvement compared with ≤4 weeks before ablation ($p=0.375$).

The AF-SR subgroup again showed significant improvements in both LVEF and PSCS at 7 months, with no changes seen in the other subgroups (**Figure 13E** and **Figure 13F**, respectively). In the 16 patients who were in AF ≤4 weeks before ablation, recovered SR at 20 hours, and remained in SR at 7 months, there was a significant improvement in LVEF across the 3 visits (median, 55% [IQR, 47% - 61%] ≤4 weeks before ablation, 60% [IQR, 55% - 62%] at 20 hours, and 64% [IQR, 60 – 69%] at 7 months; overall trend $p=0.002$; $p=0.001$ for comparison between ≤4 weeks before ablation and 7 months; $p=0.07$ for comparison between 20 hours and 7 months).

At 7 months, the AF-SR subgroup showed a significant reduction in heart rate, whereas the SR-SR subgroup showed a significant increase in heart rate, likely due to withdrawal of rate-controlling medications (**Figure 13G**). There was a trend toward an overall increase in cardiac output from before ablation (5.9±1.4 L/min at 7 months compared with 5.6±1.5 at ≤4 weeks before ablation, $p=0.054$); with no significant differences between sub-groups (**Figure 13H**).

When patients were grouped by the presence or absence of AF after ablation (rather than by intrascan rhythm), the changes in both LVEF and PSCS from ≤4 weeks before ablation to 7 months were similar between groups (median, 2.7% [IQR, -2.3% to +9.7%] in those with recurrent AF [n=25] versus 3.3% [IQR, -1.4% to +8.3%] in those without recurrent AF [n=21], p=0.83 for LVEF; mean -0.2±4% in those with recurrent AF (n=23) versus -2.0±5% in those without recurrent AF (n=17), p=0.21 for PSCS).

Myocardial energetics, as determined by PCr/ATP ratio, was unchanged from ≤4 weeks before ablation to 7 months (**Figure 14A**). There were no significant changes in PCr/ATP ratio from ≤4 weeks before ablation to 7 months in any of the intrascan rhythm subgroups (**Figure 14B**) or between patients with and without AF recurrence after ablation (**Figure 14C**). Overall, energetics remained impaired at 7 months compared with matched control subjects (1.78±0.33 versus 2.04±0.29, p=0.001).

Ablation led to a significant reduction in atrial volume (LA_{max}, 86±30 mL at 7 months from 102±37 mL at ≤4 weeks before ablation; n=46 in paired analysis; p<0.001), driven by both the AF-SR and SR-SR subgroups (p=0.007 and p<0.001, respectively, **Figure 15**). Indeed, at 7 months after ablation, atrial volume in patients with AF was not different from that in control subjects (LA_{max}, 86±30 mL in patients versus 77±22 mL in control subjects; p=0.202). Although LAEF at 7 months improved as expected in the AF-SR subgroup, (p<0.001; **Figure 15**), there was no significant overall improvement in atrial

function after ablation (median LAEF, 40% [IQR, 27% - 47%] at 7 months from 35% [IQR, 17% - 49%] ≤4 weeks before ablation; n=46 in paired analysis; p=0.373), and it remained impaired at 7 months compared with control subjects (p<0.001). Similarly, LAEF failed to improve even in patients with no recurrent AF (median LAEF, 40% [IQR, 32% - 48%] at 7 months from 42% [IQR, 16% - 49%] ≤4 weeks before ablation; n=21 in paired analysis; p=0.230), again remaining impaired at 7 months compared with control subjects (p<0.001).

3.4.5 Effect of Medications

There were no associations between β-blocker or angiotensin-converting enzyme inhibitor/angiotensin II receptor blocker use (**Table 2**) and myocardial energetics, LVEF, or PSCS, either pre-ablation or at 7 months (all p=ns).

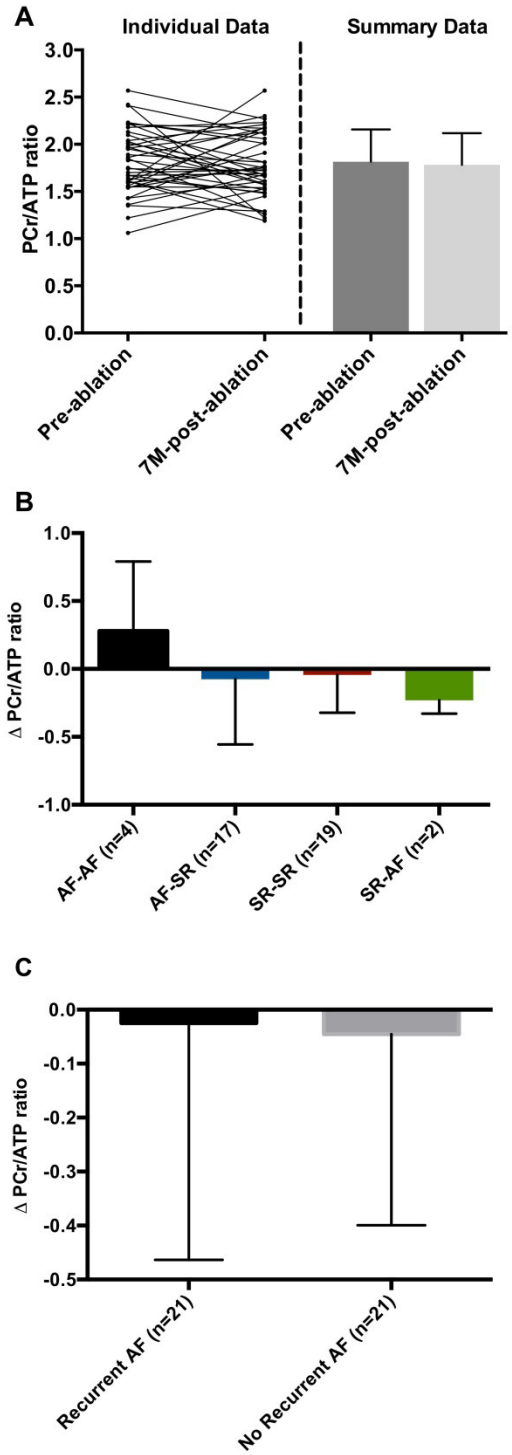


Figure 14: Myocardial energetics before ablation and late post-ablation. *(**A**) In all patients, there was no change in PCr/ATP from pre-ablation to 7 months (7M) post-ablation (n=42, p=0.57 by paired t-test). There were also no significant differences in the change in PCr/ATP ratio post-ablation in any sub-groups based on either intra-scan rhythm combinations (p=0.37 by one-way ANOVA; **B**) or presence or absence of recurrent AF post-ablation (p=0.87 by unpaired t-test; **C**).*

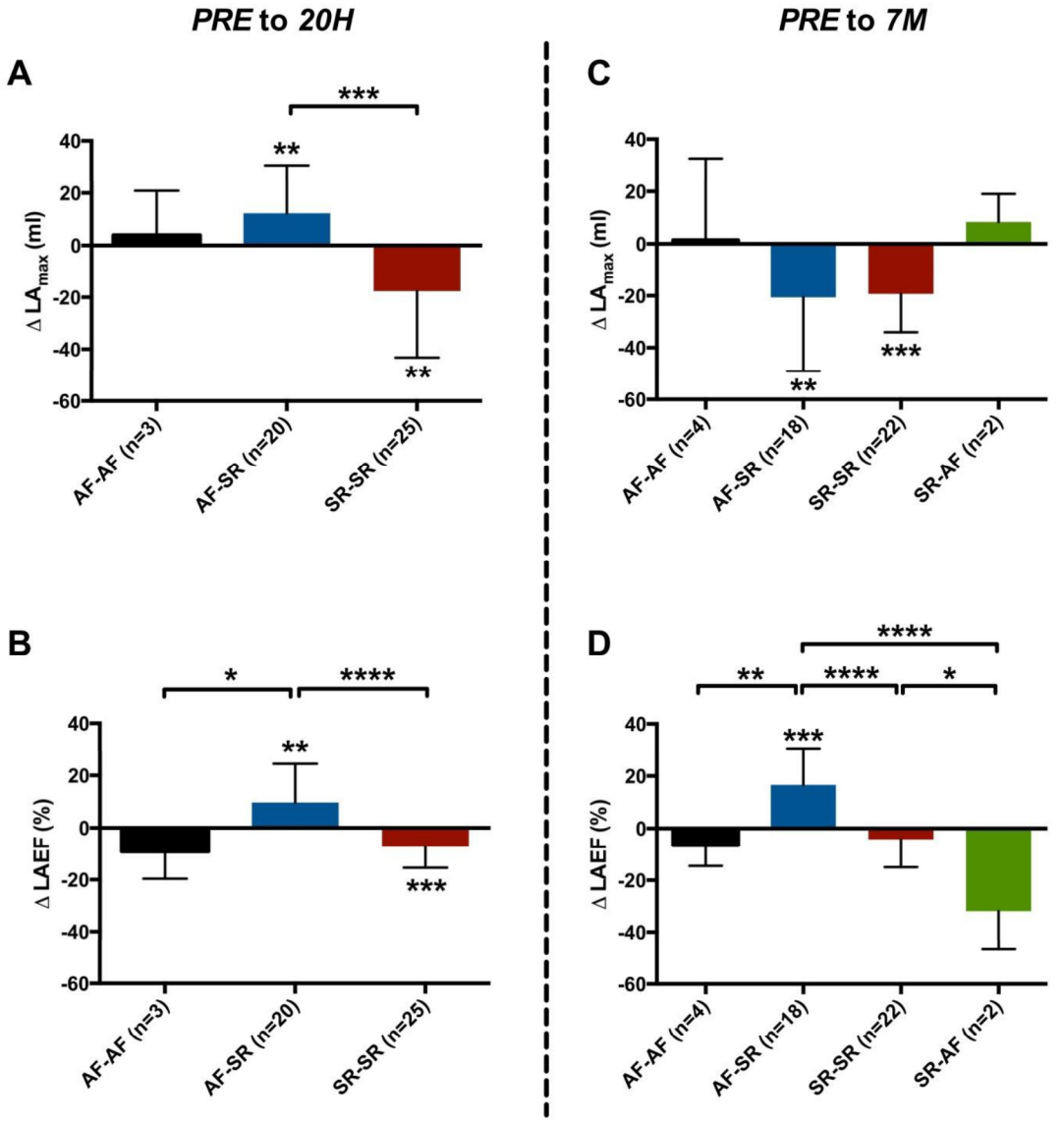


Figure 15: Change in left atrial maximal volume and emptying fraction early and late after ablation, categorised by the intrascan rhythm at each timepoint. *One-sample t-tests assessed if changes within each sub-group are significantly different to zero. Changes between sub-groups were compared using one-way ANOVA; p values for sub-group comparisons are Bonferroni-corrected for multiple comparisons. LAmax denotes maximal left atrial volume and LAEF denotes left atrial emptying fraction. (A) 20 hours after ablation (20H), maximal left atrial volume increases from ≤4 weeks before ablation (PRE) in the AF-SR sub-group (p=0.008) and decreases in the SR-SR sub-group (p=0.002). (B) Similarly, left atrial emptying fraction improves in the AF-SR sub-group (p=0.009) and worsens in the SR-SR sub-group at 20 hours (p<0.001). (C) At 7 months (7M), both the AF-SR and SR-SR sub-groups show decreases in maximal left atrial volume from ≤4 weeks before ablation (PRE; p=0.007 and p<0.001, respectively). (D) Only the AF-SR sub-group show a significant improvement in left atrial emptying fraction from ≤4 weeks before ablation to 7 months (p<0.001).*

3.5 Discussion

This prospective study enrolled patients undergoing first-time ablation of AF, using MR methods to investigate the effect of reducing AF burden on LV function and energetics. For the first time, this work demonstrates evidence of significantly impaired myocardial energetics in the ventricular myocardium of patients with "lone" AF compared with matched control subjects in SR. It further documents a subtle reduction in LV systolic function in AF patients compared with control subjects, with modest improvement (but not normalisation) after ablation. Much of the improvement in LV function occurs early after the procedure, is limited to patients with AF who recover SR at the time of the assessment, and thus likely reflects changes in haemodynamics at the time of the scan rather than true beneficial cardiac remodelling resulting from the reduction in AF burden. Indeed, despite a significant reduction in AF burden at 7 to 9 months after ablation, myocardial energetics does not change and LV function does not improve further, remaining impaired compared with control subjects in SR. Taken together, these data imply that "lone" AF may be the consequence (rather than the cause) of an occult cardiomyopathic process.

3.5.1 Left ventricular function in AF

AF has been implicated as a cause of LV dysfunction because previous studies have shown an improvement in LV function after catheter ablation[40] (including reversal of subtle systolic[11] and diastolic dysfunction[13]). The patient population

in the present study had normal LV diastolic function overall, but LVEF by CMR was subtly reduced with the group median falling at the lower end of the normal range (**Table 3**), even after successful ablation. There was no evidence of LV dilatation, hypertrophy or concentric remodelling in these AF patients compared with matched control subjects in SR, and LGE (indicating LV fibrosis/scar) was an infrequent finding in both groups. These results are consistent with the intention to focus on patients with "lone" AF, and the decision to exclude patients with significant cardiovascular comorbidity or uncontrolled ventricular rate. Nevertheless, there was clear evidence of reduced LV systolic function by both LVEF and PSCS in preablation patients compared with matched control subjects, in keeping with the results of a previous study with similar inclusion criteria[13].

The effect of AF ablation on LV function has been investigated previously, with a recent meta-analysis showing an overall improvement in LVEF of ~6% (95% CI, 4%-9%), with the largest improvements seen in patients with persistent AF (compared with patients with paroxysmal AF) and those with low LVEF (compared with those with normal LVEF)[40]. By using cardiac MR imaging both early and late after ablation the present study adds significant further insight into the effect of AF on LV function. The results indicate that approximately half the overall improvement in LVEF observed at 7 months occurs by 20 hours and that improvement is restricted to patients who were in AF at the scan done ≤4 weeks before ablation and in SR at scans after ablation

(rather than those in whom ablation caused a significant reduction in AF burden on ECG monitoring but who happened to be in SR at the time of both scans). Equally important is the finding that LV function remains impaired in patients with AF after ablation compared with matched control subjects, even when considering only those in SR at 7 months and who had experienced a significant reduction in AF burden after the procedure. The modest improvement in LVEF in patients recovering SR from AF may reflect the increase in LAEF, consistent with recovery of coordinated atrial mechanical activity. However, when considering the entire patient cohort, LAEF was unaffected by ablation and remained abnormal despite a significant reduction in AF burden. This finding is consistent with atrial structural and functional remodelling being driven by a process independent of the arrhythmia itself (e.g., fibrotic atrial cardiomyopathy[126, 127]).

Taken together, these data suggest that LV dysfunction in patients with paroxysmal or persistent AF reflects the combination of adverse haemodynamic effects induced acutely by the arrhythmia itself and an underlying cardiomyopathy. Catheter ablation and restoration of SR can improve LV haemodynamics, resulting in modest improvement in LVEF; however, the underlying cardiomyopathy persists and LV function does not completely normalise (**Figure 16**).

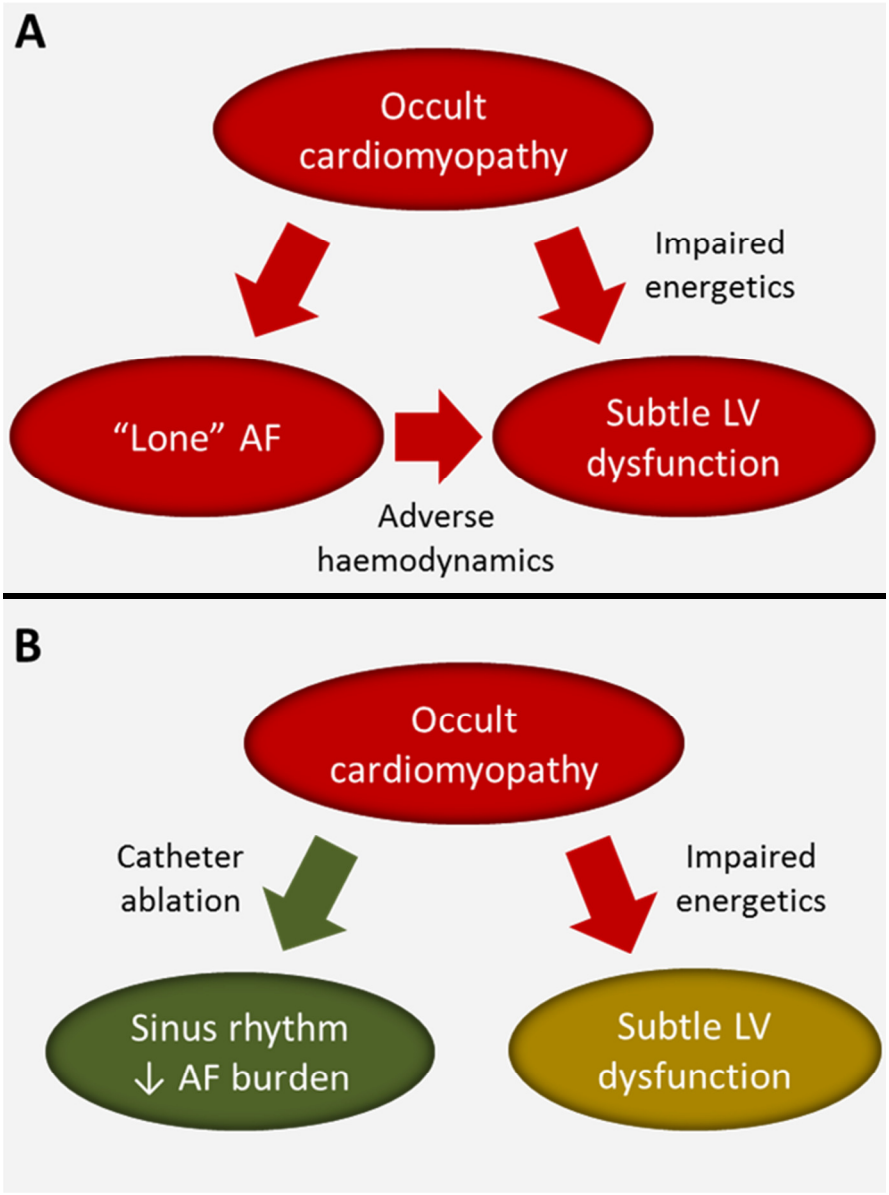


Figure 16: Proposed schematic representation of the relationships between "lone" AF, subtle LV dysfunction and "upstream" cardiomyopathy, and the effect of ablation. *(**A**) "Lone" AF and subtle LV dysfunction may be tissue-specific manifestations of an "upstream" occult cardiomyopathy, characterised by impaired energetics. AF further contributes to LV dysfunction via adverse haemodynamics. (B) Successful catheter ablation restores sinus rhythm and/or reduces AF burden, and leads to a modest increase in LV function via improvement in haemodynamics. However, the underlying cardiomyopathy remains and myocardial energetics and LV function do not normalise.*

3.5.2 Myocardial energetics in AF

Altered cardiac energy metabolism is an early feature of cardiomyopathy[81] and is prognostically important[82, 83]. Very few studies have investigated myocardial energetics in AF. Ex vivo investigations have shown a selective reduction in myofibrillar creatine kinase in atrial tissue from patients with AF compared with control subjects in the absence of changes in total creatine kinase or myosin ATPase activity[78]. In goats with pacing-induced AF, impaired atrial energetics was detected ex vivo shortly after the arrhythmia induction[79]. No previous in vivo study has investigated energetics in the LV myocardium in human AF. Use of ^{31}P-MRS allowed non-invasive assessment of myocardial energetics in patients with AF both before and after ablation. The PCr/ATP ratio measured by this method is reduced when demand for ATP outweighs ATP synthesis (as in ischaemia) or with reduction in the total creatine pool (as occurs in heart failure)[118]. The finding of a significantly lower LV PCr/ATP ratio in patients with AF than in control subjects supports the notion of an underlying cardiomyopathy, particularly in the context of the demonstrated subtle LV dysfunction. It is important to note that the findings that energetics is not affected by heart rhythm at the time of assessment and does not improve after successful AF ablation suggest that the cardiomyopathic process may be "upstream" of AF (**Figure 16**). This is befitting the idea that underlying atrial disease may actually precede and promote "lone" AF, as suggested by a number of recent studies[128-130].

The reduction in PCr/ATP ratio in patients with AF compared with matched control subjects is relatively subtle, which may reflect the relative insensitivity of this measure to the true degree of underlying energetic dysfunction compared with other ^{31}P-MRS parameters such as the rate of ATP production (the creatine kinase flux) or the creatine kinase forward rate constant k_f[131]. Future studies should determine the rate of creatine kinase flux in patients with AF because this parameter reflect both the underlying cardiomyopathy and the response to treatment more accurately than the PCr/ATP ratio[82, 132].

3.5.3 Clinical implications and future directions

These results support the notion that "lone" AF is the consequence of an occult cardiomyopathy that persists despite restoration of SR. This raises the intriguing possibility that such a process (which may develop with ageing and exposure to risk factors) may also contribute to recurrence of AF after ablation. However, future studies are needed to examine whether therapeutic strategies that target the adverse cardiometabolic phenotype reduce AF recurrence and improve outcomes. In line with this paradigm, the present findings may add mechanistic insight to recent clinical trial data showing that weight loss and intensive risk factor management can dramatically reduce AF burden, symptoms, and adverse cardiac remodelling[133] and improve AF-free survival after ablation[134].

This study also shows that the improvement in LVEF after ablation may not reflect beneficial LV remodelling induced by SR. The results of studies appropriately powered to determine the effects of ablation on hard end points are awaited, and the present data suggest that, at least in "lone" AF, caution is needed when interpreting improvement in LVEF as a biomarker of possible prognostic benefit from ablation. Further studies are needed to determine whether ^{31}P-MRS assessment of myocardial energetics (PCr/ATP or creatine kinase flux) could play an important role in this regard.

3.5.4 Limitations

AF presents technical challenges to quantitative cardiac MR imaging because of the irregularity of the RR interval. As described in Methods, a number of techniques were used to counter these issues. In addition, images were analysed in a blinded fashion and in randomised order to reduce risk of systematic bias. Although the quantitative assessments in this study were not corroborated using invasive measures, previous work has shown that MR assessment of volumes and EF is accurate in AF and correlates well with catheterisation measurements[135].

This study design cannot exclude that 6 to 9 months is too soon for full recovery of ventricular function or energetics after successful ablation; nevertheless, this is a reasonable time point for medium-term follow-up and failure of normalisation by this time is clinically relevant. It is also possible (but perhaps less likely) that a short duration of "lone" AF can cause irreversible

damage to the ventricular myocardium, with the extent of damage unrelated to cumulative AF burden. This hypothesis could be tested in future population-based large-scale imaging studies that include rhythm-monitoring investigations.

3.6 **Conclusion**

Patients with "lone AF" show impaired LV function and myocardial energetics compared with matched control subjects in SR, and these parameters do not normalise despite a significant reduction in AF burden after successful ablation.

These findings imply that AF may be the consequence (rather than the cause) of an underlying cardiomyopathy. Comprehensive therapeutic strategies to target and reverse the adverse cardiometabolic phenotype may be needed to reduce AF recurrence and to improve outcomes.

Chapter 4

Systolic T1 mapping for application in tachyarrhythmia

4.1 Abstract

4.1.1 Background

T1 mapping using the Shortened Modified Look-Locker Inversion Recovery (ShMOLLI) technique enables non-invasive assessment of important myocardial tissue characteristics. However, tachyarrhythmia may cause mistriggering and inaccurate T1 estimation. This study was designed to test whether systolic T1 mapping might overcome this, and whether T1 values or data quality would be significantly different compared to conventional diastolic T1 mapping.

4.1.2 Methods

Native T1 maps were acquired using ShMOLLI at 1.5T (Magnetom Avanto, Siemens Healthcare) in 10 healthy volunteers (5 male) in sinus rhythm, at varying prescribed trigger delay (TD) times: 0ms, 50ms, 100ms and 150ms (all "systolic"), 340ms (MOLLI TD 500ms, the conventional TD for ShMOLLI) and also "end diastolic". T1 maps were also acquired using a shorter readout, to

explore the effect of reducing image readout time and sensitivity to systolic motion. The feasibility and image quality of systolic T1 mapping was tested in 15 patients with tachyarrhythmia (n=13 atrial fibrillation, n=2 sinus tachycardia; mean HR range 93-121 bpm).

4.1.3 Results

In healthy volunteers, systolic readout increased the thickness of myocardium compared to the diastolic readout. There was a small overall effect of TD on T1 values (p=0.04), with slightly shorter T1 values in systole compared to diastole (maximum difference 10ms). While there were apparent gender differences (with no effect of TD on T1 values in males and more marked differences in females, and that this effect was exaggerated in thinner myocardial segments in females), dilatation and erosion of contours suggested that the effect of TD on T1 in females was almost entirely due to more partial-volume effects in diastole. All T1 maps were of excellent quality, but systolic TD and shorter readout were associated with less variability in segmental T1 values. In tachycardic patients, systolic acquisitions produced consistently excellent T1 maps (median R^2 = 0.993).

4.1.4 Conclusions

In healthy volunteers, systolic ShMOLLI T1 mapping reduces T1 variability and reports clinically equivalent T1 values to conventional diastolic readout; slightly shorter T1 values in systole are mostly explained by reduced partial-volume effects due to the increase in functional myocardial thickness. In patients with

tachyarrhythmia, systolic ShMOLLI T1 mapping is feasible, circumvents mistriggering and produces excellent quality T1 maps. This extends its clinical applicability to challenging rhythms (such as rapid atrial fibrillation) and aids the investigation of thinner myocardial segments. With further validation, systolic T1 mapping may become a new and convenient standard for myocardial T1 mapping.

4.2 Introduction

Myocardial T1 mapping is a quantitative technique that permits non-invasive assessment of biologically important properties of regional and global myocardium, independent of cardiac function[45]. It relies on alterations of the longitudinal relaxation time constant (T1) of the myocardium due to increased water content or other changes to the local molecular environment[96, 136-140]. Various T1 mapping sequences are available, and these can be broadly divided into inversion recovery methods, saturation recovery methods and mixed inversion and saturation recovery methods[141].

The recently described Shortened Modified Look-Locker Inversion Recovery (ShMOLLI) method uses sequential inversion recovery measurements, permitting a T1 map to be acquired within a short 9-heartbeat single breath-hold[95]. It is a stable and reproducible method for T1 mapping[97], which has already been used in the characterisation of many important cardiac diseases, including acute myocardial infarction[107], acute myocarditis[142], hypertrophic

cardiomyopathy[143], dilated cardiomyopathy[143], cardiac amyloidosis[137] and aortic stenosis[144].

The ShMOLLI sequence uses a fixed post-R-wave trigger delay of 340 ms and the resultant trigger time of ~600 ms equates to readout in mid-diastole for typical heart rates (e.g. 60-80 bpm). However, many cardiac diseases are associated with tachyarrhythmia (e.g. atrial fibrillation with fast ventricular response, sinus tachycardia), which can lead to mistriggering and inaccurate T1 estimations. Consequently, the application of inversion recovery T1 mapping methods in cardiac patients with tachyarrhythmias is severely limited.

Attempts to address this problem during daily clinical imaging led to the hypothesis that reduction in ShMOLLI trigger delay (i.e. "systolic" T1 mapping) may circumvent this issue without significantly affecting estimated T1 values or data quality compared to a conventional diastolic readout. In this study, ShMOLLI sequence parameters were systematically altered to investigate the effects of systolic T1 mapping on T1 values and data quality in healthy volunteers. Initial experience with systolic T1 mapping in patients with tachyarrhythmia is also reported.

4.3 **Methods**

Ethical approval was granted for all study procedures and all subjects gave written informed consent.

4.3.1 Volunteer experiments

Ten healthy volunteers (50% male, age 36±7 years) in normal sinus rhythm (HR 61±9 bpm), without symptoms or history of cardiac disease, not on cardiovascular medications and with normal left ventricular function on CMR were included.

4.3.1.1 MR acquisition parameters

All data were collected using a 1.5 tesla MR system (Magnetom Avanto, Siemens Healthcare, Erlangen, Germany) using a 32-channel cardiac coil array. T1 maps were acquired without administration of any contrast agents based on a prototype ShMOLLI implementation (based on WIP 561, syngo MR B17A version) [95].

The goal was to alter the image sampling within the cardiac cycle using the permissible range of physiological trigger delay (TD), which, in this WIP implementation, is defined as the time from the R-wave to the start of the inversion preparation in the sequence. **Figure 17** illustrates the relation between TD, "MOLLI TD" specific to WIP 561, and the trigger time (TT, time to acquisition of the centre of k-space), such as in cine.

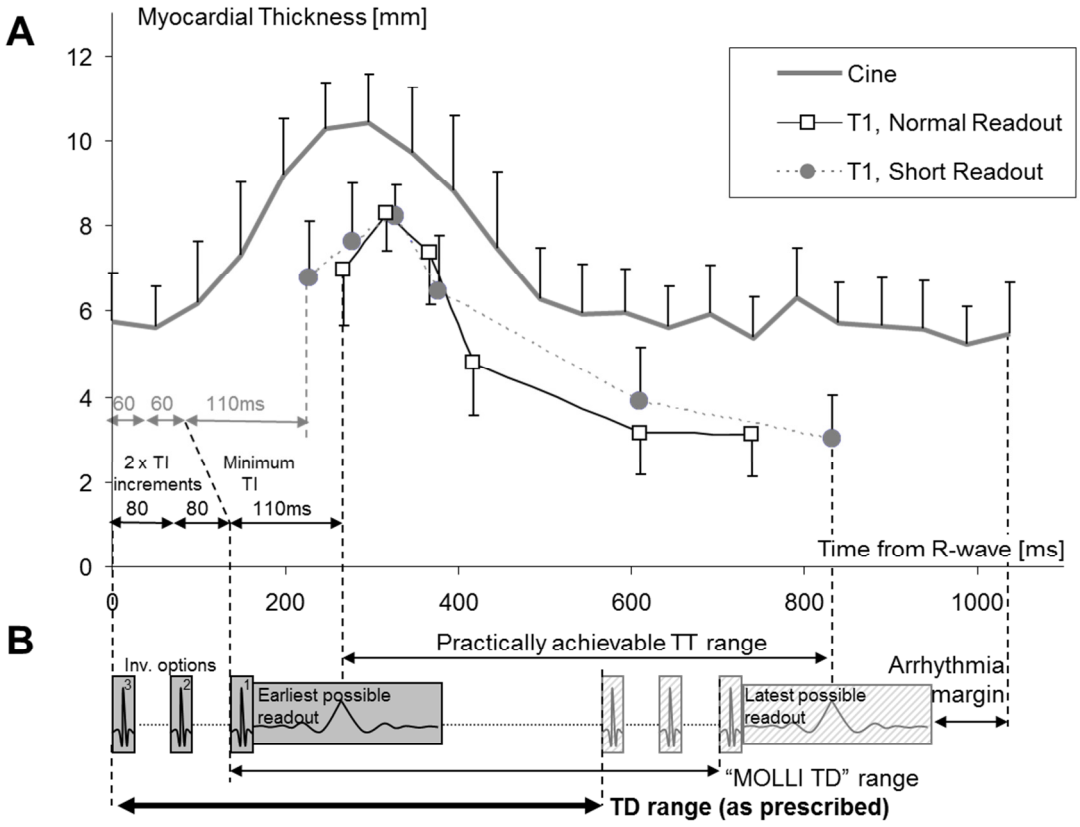


Figure 17: Elements of the ShMOLLI pulse sequence that affect the practically achievable range of trigger times within the cardiac cycle, with associated changes in myocardial thickness. *(**A**) Evolution of myocardial thickness over the cardiac cycle based on cine outlines. Shaded circles and open squares respectively indicate the acquired positions from the R-wave and the estimates of myocardial thickness from the short and normal readout variants of ShMOLLI studied in this work. Note that myocardial thickness from T1 maps is less by ~1 pixel on each outline (2mm altogether) to avoid partial-volume impact on T1. (**B**) Elements of pulse sequence that limit the TD range: the duration of inversion pulse, required delays to achieve the range of inversion times (TI) and readout duration outside of the k-space centre. Short readout ShMOLLI achieved earlier TT by reducing TI increments from 80 to 60 ms. The relationship between prescribed TD range, resulting MOLLI TD range and practically achievable TT range is also illustrated.*

The duration of required preparations limits the shortest MOLLI TD to 270 ms. In order to achieve sampling earlier in the cardiac cycle, the MOLLI TI increment was reduced from 80 to 60 ms[145], which shortened the minimum limit of MOLLI TD to ~230 ms. In order to allow acquisition during higher heart rates (and shorter RR intervals), additional shortening was achieved by using a

smaller matrix size of 176 (compared to conventional 192). This reduced the total readout time by approximately ~10 ms. These latter techniques were combined and are henceforth referred to as "*short readout*" (compared to "*normal readout*"). Conversely, the latest readout is limited by the subsequent R-wave. Based on earlier experience, the automatic end-diastolic TD was shortened by 50 ms to reduce the occurrence of mistriggering.

4.3.1.2 Pilot Experiments

A subset of two volunteers underwent a pre-study pilot scan to inform experimental design. Serial T1 maps were acquired with systematic alteration of physiological TD in 50 ms increments from 0 ms to 500 ms. Based on these data, four "systolic" TDs leading to imaging earlier in the cardiac cycle were chosen for further evaluation: 0 ms, 50 ms, 100 ms and 150 ms.

4.3.1.3 CMR Scan Protocol

Following standard planning, end-expiration basal, mid-ventricular and apical short-axis slice positions were selected and used for all T1 maps.

Serial native (or pre-contrast) T1 maps were acquired in a semi-automated fashion using recorded breathing instructions. This minimised variability and ensured that at least 20 seconds passed between any two T1 maps, to allow sufficient time for full T1 relaxation between experiments.

At each slice position, six different TDs were investigated: the four "systolic" TDs chosen from the pilot experiments (0 ms, 50 ms, 100 ms and 150

ms), conventional ShMOLLI (340 ms, "MOLLI TD" 500 ms; readout in mid-diastole for typical heart rates of 60-80 bpm) and imaging in "end-diastole" (defined as the captured cycle TD minus 50 ms). For each of these six TDs, two separate T1 maps were acquired: one with the *short readout* parameters for matrix size and TI increment as described above and another with the *normal readout*. In five volunteers, the order of acquisition of the T1 maps was randomised to exclude systematic intra-scan effects (such as change in heart rate or compliance with breathing instructions).

As T1 maps were acquired at 3 slice positions, 6 TDs and with both the *normal* and *short readout*, a total of 36 T1 maps were provided from each volunteer. R^2 maps (of goodness-of-fit for how well T1 model fitting was achieved for each T1 map) were visually assessed in real time during the scan; acquisitions were repeated if quality was deemed insufficient (as previously described[96]).

4.3.1.4 Image post-processing

Offline post-processing was conducted using dedicated in-house software "MC-ROI" written in IDL by Professor Stefan K Piechnik (Interactive Data Language, Ver. 6.1, Exelis Visual Information Solutions, Inc., Boulder, USA). Endo- and epicardial contours were manually traced on each T1 map, taking care to avoid partial-volume effects of neighbouring tissues. Each slice was then divided into 6 segments, using the anterior right-ventricular-left-ventricular insertion point as reference. All voxels in each myocardial segment were analysed, and

segmental data extracted for further analysis included mean T1 value, standard deviation of T1 value and median R^2 value between the manually drawn outlines. No motion correction techniques were employed.

Quality assessment of T1 maps was performed as previously described[96]. The presence of off-resonance artefacts and diaphragmatic movement was assessed by examination of the raw T1-weighted bSSFP images and R^2 maps by an assessor blinded to TD and *normal*/*short readout*. Segments with suspected artefacts were rejected. Further assessment of quality of T1 maps was provided by analysis of the standard deviation of segmental T1 values; this is a surrogate for T1 map quality in healthy volunteers without known myocardial pathology (which can lead to biological variation in T1 values within segments in patients).

The thickness of myocardium was the average distance between epi- and endocardial outlines towards the centre of the left ventricle. The impact of partial-volume was studied by inflating and eroding the myocardial outlines as previously described[97]. Myocardial midline values (i.e. a single line of pixels equidistant to endo- and epicardial outlines) were also evaluated.

4.3.2 Validation in patients

In order to examine the feasibility and image quality of systolic ShMOLLI T1 mapping, systolic acquisitions (TD 0 ms – TD 150 ms) were tested in 15 patients with tachyarrhythmia. All patients underwent CMR examinations at 1.5 tesla (Magnetom Avanto, Siemens Healthcare, Germany) for clinical indications and had a mean HR range between 93 and 121 bpm (n=13 atrial fibrillation, n=2

sinus tachycardia). The degree of tachycardia (resulting in an average shortest RR interval of 488 ms) meant that acquisition using the conventional ShMOLLI sequence parameters would result in mistriggering and it was therefore not possible to directly compare the systolic readout against the conventional sequence in this population without compromising T1 values.

Data are also presented from a single patient with atrial fibrillation and a slow ventricular response (mean heart rate 40-50 bpm), to demonstrate the occasional need to adjust the TD to optimise T1 fit and improve T1 estimation.

4.3.3 Statistical analysis

Statistical analyses were performed using IBM SPSS Statistics for Windows, Version 20.0 (IBM Corp., Armonk, NY, USA) and GraphPad Prism version 6 (GraphPad Software, San Diego, California, USA). Normality of data was assessed using the Kolmogorov-Smirnov test. Most variables including T1 and T1 SD did not follow a strictly Gaussian distribution; hence, all statistical tests used were non-parametric. For consistency with other literature reports, T1 values are presented as mean ± SD; non-parametric data are presented as median and range/IQR. The Kruskal-Wallis test was used to assess the effect of TD (6 groups); pairwise comparisons were made using the Bonferroni-Dunn approach for variables where the Kruskal-Wallis test was significant. The Kolmogorov-Smirnov test was used to assess effect of *short* versus *normal readout* (2 groups). P values < 0.05 (after adjustment for multiple comparisons)

were considered significant (*) with smaller P values stratified by size (< 0.01 = **, < 0.001 = ***).

4.4 Results

4.4.1 Volunteer experiments

For each of the 12 combinations of TD and *normal*/*short readout*, the respective maps yielded estimates of 180 myocardial segments (10 volunteers x 3 slices x 6 segments), making a total of 2160 segments collected in the experiment. 54 (2.5%) segments were excluded due to the presence of suspected image artefacts, leaving 2106 (97.5%) segments in the final analysis. The variants with short TD (0-50 ms) had the lowest rejection rates (median 1.1%, range 0.6%-1.7%) and the end-diastolic readout the largest (median 5%, range 3.9%-6.1%; mostly due to mistriggering). Using the *short readout* resulted in a minor (0.7%) improvement in segment rejection rates compared to the *normal readout*.

All included T1 maps were of excellent quality, with median R^2 values of at least 0.996. Sample mid-ventricular T1 and R^2 maps for two systolic TDs and TD 340 ms (standard ShMOLLI) with both *short* and *normal readout* are shown in **Figure 18**. The increased myocardial thickness in the systolic TDs compared to the diastolic TD is readily appreciated, but T1 and R^2 maps have an otherwise similar visual appearance irrespective of the combination of sequence parameters.

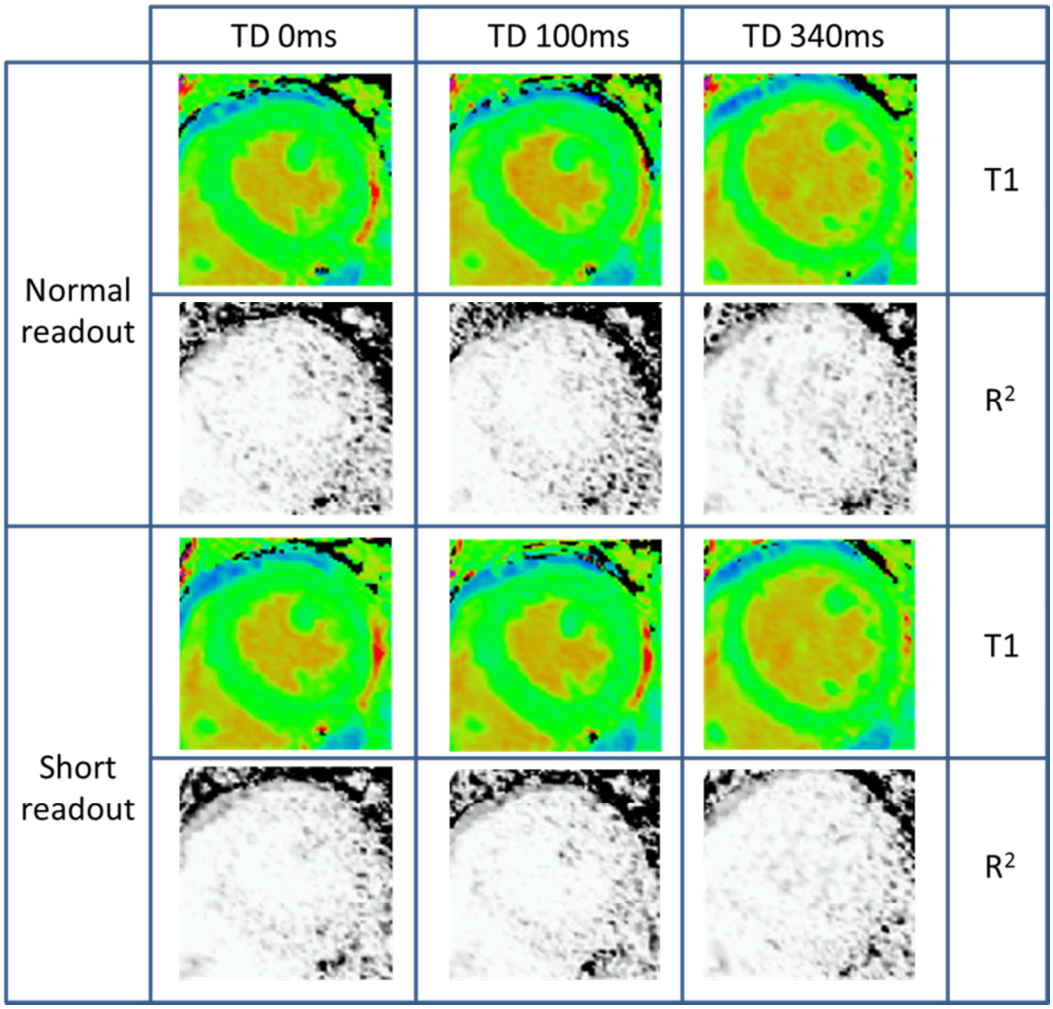


Figure 18: Representative T1 and R^2 maps acquired from a single volunteer with different combinations of TD and readout. *TD 0 ms, 100 ms and 340 ms (MOLLI TD 500 ms; conventional ShMOLLI) are shown, using both the normal and short readout. Note the clearly increased myocardial thickness in both systolic acquisitions compared to the conventional diastolic acquisition. T1 values and quality of R^2 maps are visually similar irrespective of TD and normal/short readout.*

4.4.1.1 Effect of TD and normal/short readout on trigger time and myocardial thickness

Across all subjects, the maximal thickness on T1 maps was achieved at TT ~ 320 ms (prescribed TD = 50-100 ms) at 7.5±2.5 mm compared to the standard or end-diastolic acquisitions at 4.7±2mm (all $p<0.001$). The variation in trigger

time (TT) led to acquisition of T1 maps at different points in the cardiac cycle, with resultant increased myocardial thickness in the systolic acquisitions compared to conventional ShMOLLI or the end-diastolic acquisition.

An example of the evolution of myocardial thickness in representative cine measurements in a single healthy volunteer is shown in **Figure 17**, together with the myocardial thickness calculated from the T1 maps. As described in Methods, myocardial outlines on T1 maps were placed away from areas of partial-volume effects; hence the thickness is lower than on corresponding cine images where they are drawn directly on the tissue interfaces. The overlay in **Figure 17** demonstrates the achievable range of cardiac delay times for the MOLLI technique, which is limited by the combined preparation ranges and the arrhythmia range.

4.4.1.2 Effect of TD and normal/short readout on fit quality, T1 values and variability

4.4.1.2.1 Fit quality

TD had no effect on fit quality, as assessed by R^2 values ($p=0.36$; **Figure 19A**). *Short readout* improved R^2 values compared to *normal readout* (median 0.997 versus 0.996, $p<0.001$). This improvement was possibly due to increased voxel volume (~19%) and thus higher SNR, and was independent of TD.

4.4.1.2.2 T1 values

While shorter TD was associated with slightly lower T1 values, with an overall statistical significance (p=0.04), none of the pairwise comparisons of TD reached statistical significance (all $p \geq 0.12$). Overall significance was lost with minimisation of the partial-volume effects by erosion of myocardial contours (see 4.4.1.3 below). T1 values were not affected by *normal*/*short readout* (p=0.41; **Figure 19B**).

4.4.1.2.3 T1 variability

The TD and *normal*/*short readout* had an impact on segmental T1 variability, as measured by standard deviation of segmental T1 values (**Figure 19C**). TD < 150 ms was associated with a lower standard deviation of segmental T1 values than TD ≥ 150 ms (mean 43.4 ms versus 50.5 ms, p<0.001). *Short readout* was associated with a lower standard deviation of segmental T1 values than *normal readout* (mean 45.6 ms versus 48.0 ms, p=0.001).

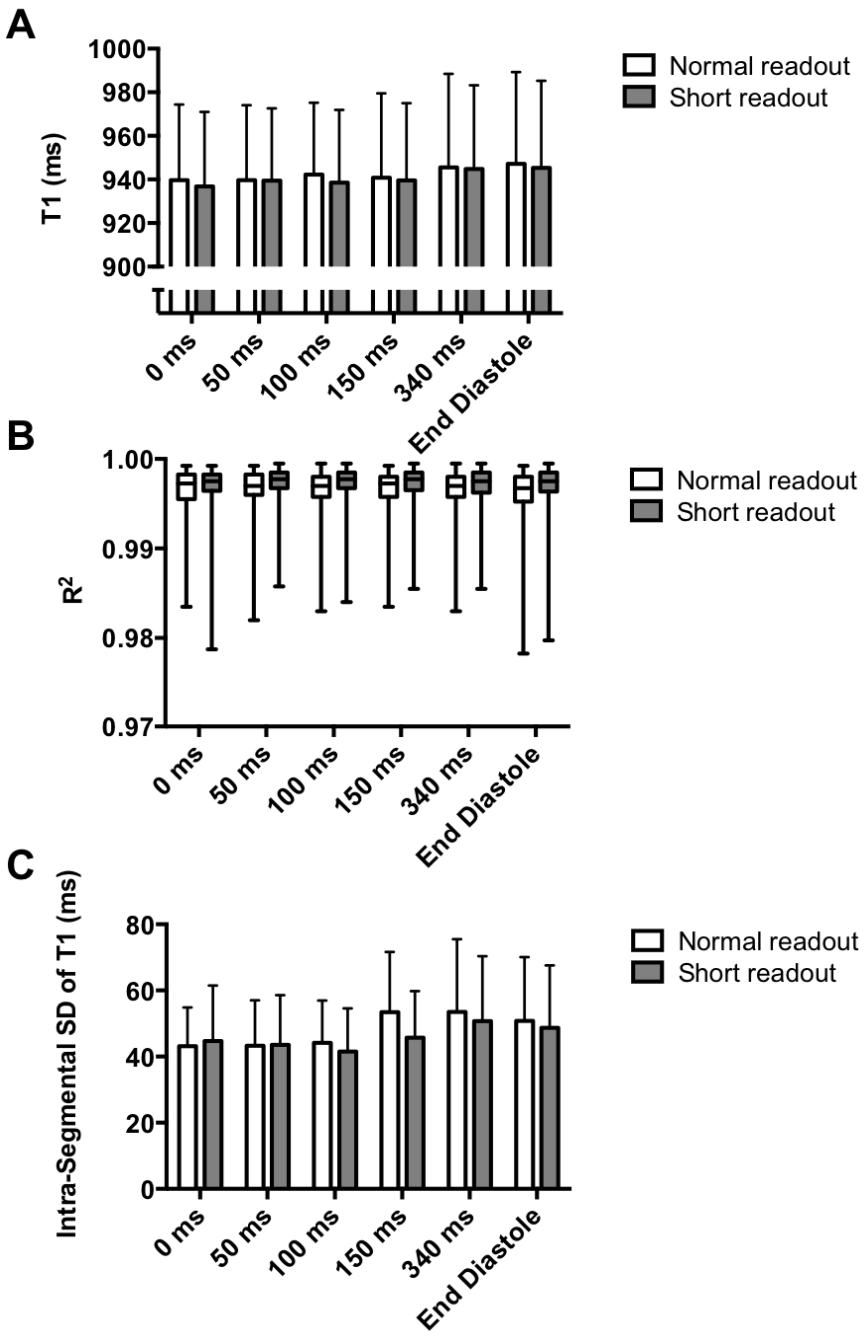


Figure 19: Effect of TD and normal/short readout on segmental myocardial T1, R^2 and T1 SD.*(**A**) Note slightly shorter T1 values in systole compared to diastole (mean ± SD). The apparent effect of short readout leading to lower T1 values compared to normal readout relates to the slightly shorter TT achieved with the short readout. P=0.04 for overall effect of TD on T1 values. (**B**) Effect of TD and normal/short readout on median segmental R2 values (median ± range). Note equivalent values irrespective of TD and normal/short readout (p=ns for both). (**C**) Effect of TD and normal/short readout on standard deviation of T1 values within each myocardial segment (mean ± SD). Note lower standard deviation in systolic acquisitions (TD < 150 ms) compared to diastolic readout (p<0.001).*

4.4.1.3 Partial-volume effects

Partial-volume effects appear to underlie most of the significant dependencies of T1 values identified above, as revealed by inflation and deflation of the myocardial contours.

The identified degree of dependence of T1 on TD (~10 ms, ~1% of the mean normal T1 value with drawn contours) became smaller with any degree of myocardial erosion or centreline T1 estimates, with no statistical significance (p=ns for all). Conversely, the dependence became stronger with any degree of myocardial outline dilatation, and reached statistical significance ($p \leq 0.001$) for 2 or 3 pixel dilatation when comparing TD 50 ms to conventional diastolic ShMOLLI (TD 340 ms) (**Figure 20A**).

Partial-volume effects also appear to underlie most of the effect of TD on intra-segmental pixel T1 variability. Even when the difference is at its strongest comparing the T1 maps acquired with TD = 50 ms versus standard ShMOLLI (smaller pixels, lower SNR and thinner myocardium), the statistical significance is amplified by myocardial contour dilatation but lost for any degree of erosion and for the centreline myocardial T1 estimates (**Figure 20B**).

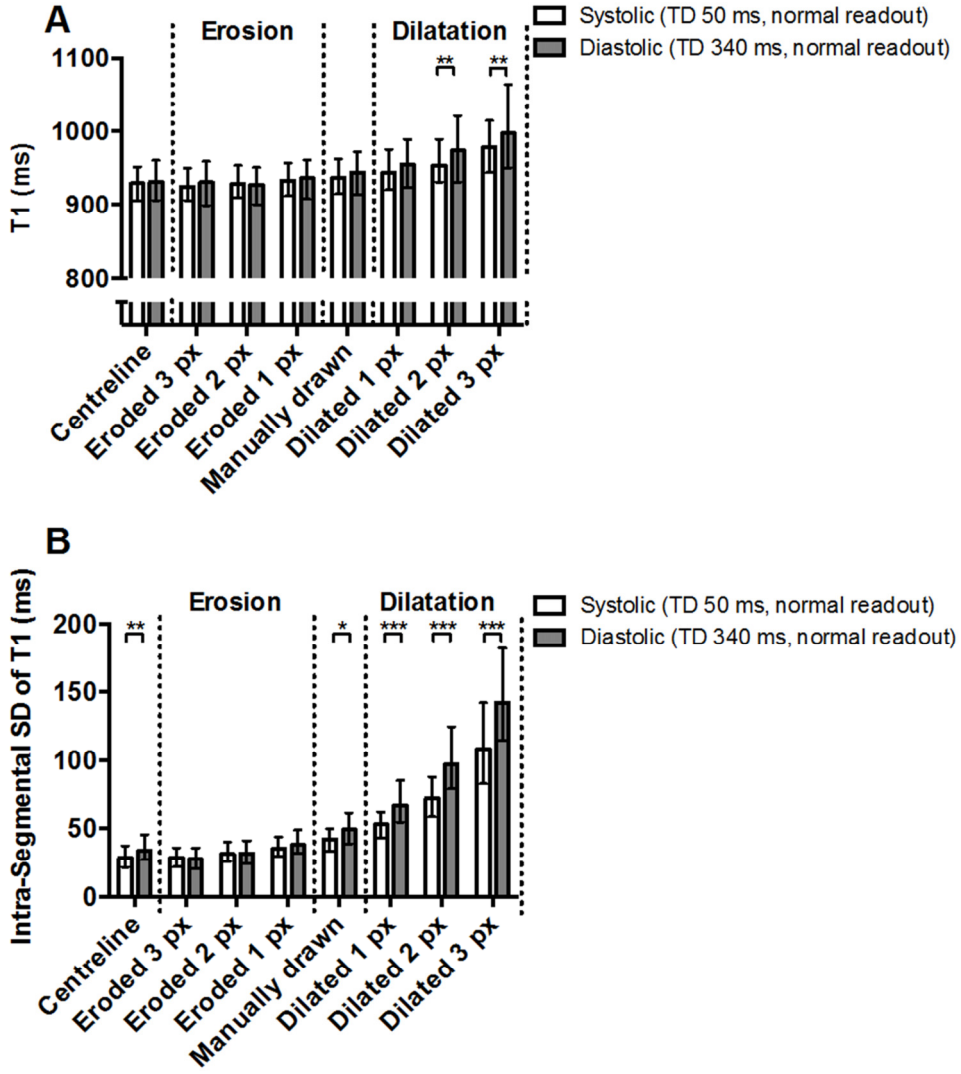


Figure 20: Effect of dilating and eroding manually drawn contours. *Effects of dilation and erosion of contours by 1-3 pixels (px) on myocardial T1 (**A**) and intrasegmental T1 SD (**B**) in representative diastolic (TD 340 ms, normal readout) and systolic (TD 50 ms, normal readout) acquisitions (median +/- IQR). Note that dependencies generally decrease with any degree of myocardial volume erosion or with centreline estimates but become amplified when the myocardial outline is inflated, which most affects the thinner myocardium in the diastolic phases. This suggests that partial-volume effects in thinner myocardial segments are responsible for the relationship between TD and myocardial T1 and T1 SD.*

4.4.1.4 Effects of gender

A much stronger dependency of T1 values on TD was noted in females than in males, and appears to relate to greater partial-volume effects in females due to thinner myocardium.

In females, diastolic T1 values were a maximum of 20 ms longer than systolic ones (972 ms in diastole versus 952 ms in systole, $p<0.001$; **Figure 21A**). However in males, there was no significant effect of TD on T1 values, with a maximum difference of 5 ms (924 ms in diastole versus 919 ms in systole, $p=0.84$; **Figure 21B**).

To ascertain if this was driven by partial-volume effects, the female data were re-analysed for myocardial segments with a thickness in the lowest and highest tertiles of thickness for the female participants (<2.97 mm and >3.87 mm, respectively, when acquired using the conventional 340 ms prescribed TD; **Figure 21C**). In the thicker segments, there was no significant difference in T1 values between diastolic and systolic readouts (966 ms versus 962 ms, respectively, $p=0.06$). In contrast, T1 values were significantly higher with the diastolic compared to the systolic readout in the thinner segments (976 ms versus 959 ms, $p<0.001$). It can be inferred that the differences seen in T1 values between systolic and diastolic readout in females were driven by greater partial-volume effects in diastole (from adjacent high T1 values in the blood-pool), with thinner myocardium much more susceptible to this phenomenon.

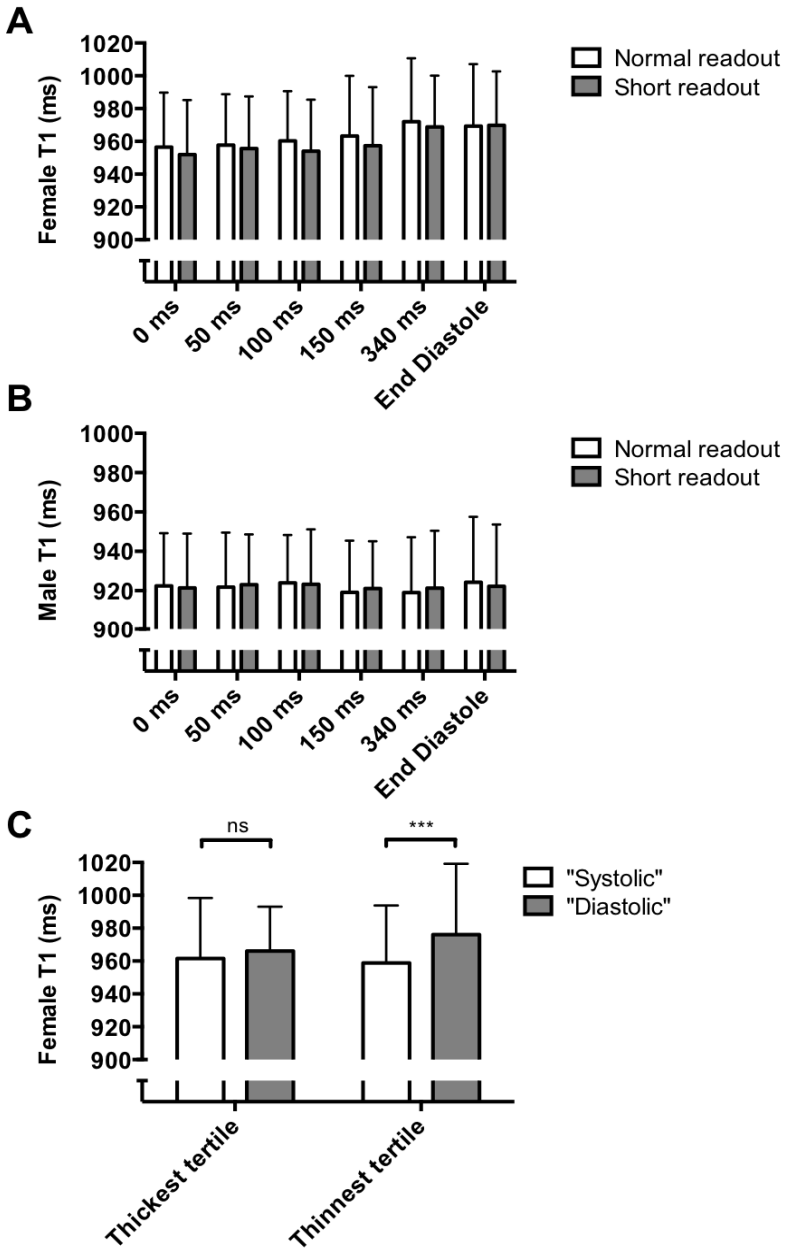


Figure 21: Effect of TD and normal/short readout on segmental myocardial values in females and males. *Note the stronger effect of TD on T1 values in females (**A**) than in the unselected population (see Figure 3A), and lack of any relationship between TD and T1 values in males (**B**). Repeat analysis of segments from females by thickness showed that there was no significant difference in T1 values between diastolic and systolic readout in the thickest tertile (p=0.06), but there was an exaggerated difference for the thinnest tertile (p<0.001) (**C**). This suggests that increased partial-volume effects in diastole (particularly in thinner myocardial segments) are responsible for the gender effect and the relationship between TD and T1 values. Systolic readout was defined as TD 0 ms to TD 150 ms, and diastolic readout as TD 340 ms and "end diastole". The cut-offs for tertiles of female myocardial segmental thickness were defined based on the conventional ShMOLLI sequence thickness in the included female volunteers (<2.97 mm for lowest tertile and > 3.87 mm for highest tertile). T1 values are shown as mean±SD.*

4.4.2 Validation in patients

In 15 patients with tachyarrhythmia (mean HR range 93 – 121 bpm), systolic ShMOLLI acquisition parameters produced consistently excellent T1 maps (median $R^2 = 0.993$). A summary of patient characteristics and T1 and R^2 results is presented in **Table 4**. In contrast, initial attempts to acquire T1 maps using the conventional sequence parameters (MOLLI TD 500 ms / *normal readout*) resulted in mistriggering in such patients, leading to poor estimation of T1 values. A representative example of this effect is shown in **Figure 22**.

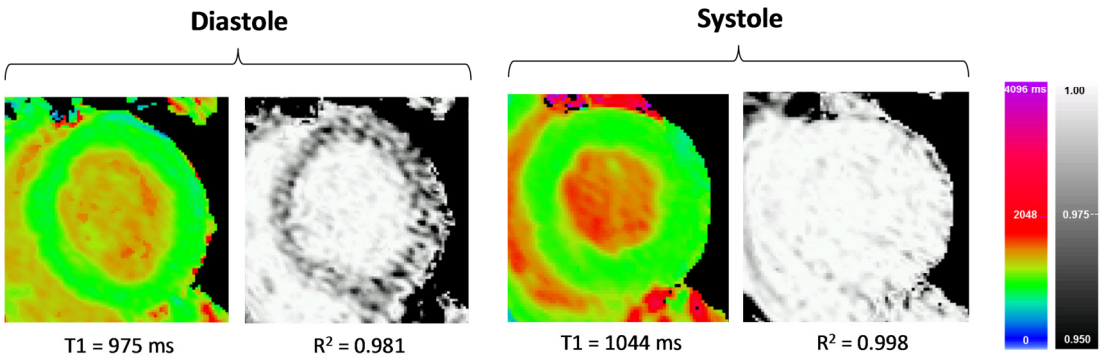


Figure 22: Representative T1 and R^2 maps acquired using diastolic and systolic T1 mapping. *Conventional diastolic ShMOLLI T1 mapping was acquired with TD 340 ms and normal readout, whereas systolic T1 mapping was acquired with TD 0 ms and short readout at 1.5 T. In this patient with sinus tachycardia (mean HR range 120 – 130 bpm) and myocardial oedema post cardiac arrest, mistriggering of the diastolic T1 map resulted in underestimation of T1 values and distinctively darker appearance of myocardial tissue on the R^2 map. In contrast, systolic T1 mapping circumvented mistriggering with excellent T1 fit on the R^2 map. Normal myocardial T1 by ShMOLLI at 1.5 T is 962±25 ms[97].*

Table 4: Results of Systolic ShMOLLI Acquisitions in Patients with Tachyarrhythmia

#	Diagnosis	Rhythm	HR range (bpm)	Number of T1 maps	Mean TT (ms)	Mean T1 (ms)	Median R^2	Mean RR (ms)	RR range (ms)
1	Rate-related cardiomyopathy	AF	90 - 140	2	343	943	0.992	683	435 - 1117
2	Post cardiac arrest	ST	120 - 130	4	213	1025	0.999	484	462 – 507
3	Cardiomyopathy	AF	80 - 120	4	218	975	0.992	645	457 – 953
4	Takotsubo cardiomyopathy	AF	130 - 150	2	213	1092	0.995	423	393 – 520
5	Cardiac amyloidosis	AF	80 - 100	3	213	1112	0.995	712	570 - 815
6	Rate-related cardiomyopathy	AF	100 - 130	1	223	1022	0.994	525	442 - 600
7	Rate-related cardiomyopathy	AF	90 – 120	1	263	938	0.993	836	477 – 1127
8	Rate-related cardiomyopathy	AF	100 - 120	3	223	984	0.990	668	382 – 1097
9	Rate-related cardiomyopathy	AF	70 – 110	2	308	960	0.986	906	567 – 1495
10	Cardiomyopathy	AF	80 – 120	7	354	1037	0.990	667	470 - 1102
11	Post cardiac arrest	AF	90 - 120	2	223	1035	0.991	762	570 – 1008
12	Cardiac amyloidosis	AF	70 – 100	6	218	1142	0.998	742	605 - 1135
13	Myocarditis	AF	90 - 120	6	218	981	0.993	732	543 – 1020
14	Rate-related cardiomyopathy	AF	90 - 110	2	213	954	0.991	723	472 - 1025
15	Cardiomyopathy	ST	120 - 130	3	332	1035	0.997	472	468 – 475
Average			**93 - 121**	**3.2**	**252**	**1016**	**0.993**	**665**	**488 - 933**

4.5 Discussion

This work demonstrates that alteration of ShMOLLI sequence parameters to permit readout in end-systole ("systolic ShMOLLI T1 mapping") yields T1 values that are clinically equivalent to those derived by the conventional sequence in healthy volunteers, with the benefit of a slight improvement in data quality. Furthermore, these data suggest that, in healthy volunteers, the T1 differences between diastolic and systolic readout are driven by reduced partial-volume effects in systole due to functionally increased myocardial thickness, implying that the systolic readout may provide a more robust sample of myocardial T1. Finally, this study demonstrates that this technique is feasible and produces consistently excellent T1 maps in patients with tachyarrhythmia. This is the first evaluation and application of a systolic readout inversion recovery method for T1 mapping in tachyarrhythmia, which is highly relevant for real-world clinical applications.

4.5.1 Variation of T1 values within the cardiac cycle

The findings of slightly lower T1 values in systole compared to diastole concur in general with some previous reports on the effects of systolic readout using other MOLLI-based sequences[146, 147]. Kawel *et al.* compared a single systolic trigger delay time of 150 ms ("early systole") with conventional mid- to end-diastolic readout in healthy volunteers, and found diastolic T1 values higher than systolic values, with mean differences of 5 ms and 15 ms in native T1

values on separate examinations at 3 Tesla (absolute T1 values not reported)[146]. Reiter *et al.* reported an even larger mean difference of 25 ms (984 ms in diastole and 959 ms in systole)[147].

The mechanism for these differences has been attributed to myocardial contraction, which is known to compress the myocardial vascular bed[148]. Reduced intra-myocardial blood volume partition in systole can explain both lower native T1 values (less of longer T1 of blood) and higher systolic myocardial T1 post-contrast (less lower T1 species in blood volume)[146]. While this mechanism is conceptually attractive, ShMOLLI or MOLLI techniques fit T1 values over several heartbeat cycles and would be expected to produce a complex average of their systolic and diastolic blood volume fractions, potentially combined with inflow effects. Theoretical approaches are yet to address the relative impact of these underlying effects on myocardial T1.

However, the initial findings[149] in this study have been recently and independently supported by Tessa *et al.* [150], who compare MOLLI T1 maps acquired with a single systolic trigger delay (MOLLI TD 330 ms, shortest possible in Siemens WIP448, which corresponds to TD=0 ms in this study) against conventional diastolic MOLLI. Tessa et al. similarly found no significant differences between systolic and diastolic T1 values derived from small (4-9 pixels), manually drawn segmental ROIs after extensive removal of segments judged ineligible for analysis. The authors also speculate that the discrepancy between their results (based on a method of analysis that will inherently reduce

partial-volume effects) and those of Kawel *et al* [146] and Reiter *et al* [147] may emphasise the importance of partial-volume effects in diastole as a factor in the apparent variability of T1 values within the cardiac cycle.

In line with the discussion of future research in Tessa *et al.*[150], the present study systematically evaluated a number of different systolic and diastolic trigger delays in healthy volunteers with no evidence of cardiac pathology whilst also demonstrating consistently excellent systolic T1 maps in patients with tachyarrhythmia. These data extend confidence in systolic T1 mapping beyond the findings of Tessa *et al.* who studied a heterogeneous group of patients with a variety of myocardial pathologies, including previous myocardial infarction, cardiomyopathy, valve disease, and athletes with echocardiographic or ECG abnormalities. This patient population may have contributed to high rejection rates of myocardial segments in their study, either because they were pathologic on visual evaluation (~7%) or because they were judged ineligible for analysis (~21% for diastolic T1 maps)[150]. With the use of inline R^2 and coloured T1 maps, the segmental exclusion rate in the present study was as low as 2.5%, offering clear diagnostic benefit when assessing pathological T1 changes.

The current work also extends the initial investigations of Tessa *et al.*[150] into the importance of partial-volume effects by systematic manipulation of myocardial contours, examination of differences in T1 between male and female healthy volunteers and exploration of thicker and thinner myocardial segments

in females. These investigations demonstrate that the systole-diastole differences in the presented ShMOLLI experiments can be attributed nearly completely to partial-volume effects in healthy volunteers without known cardiac pathology.

4.5.2 Potential advantages of systolic T1 mapping and future directions

End systole has a shorter quiescent period than end diastole [151], but is less sensitive to RR variability and arrhythmia. Systolic readout has been advocated for other CMR applications including first-pass myocardial perfusion imaging[152], and has drawn a lot of interest for application in T1 mapping[146, 147, 149, 150, 153]. The aim of this work was to develop and test a systolic readout ShMOLLI sequence in order to allow reliable T1 mapping in tachyarrhythmia, and the results indicate that this is a valid method for such purposes. The systolic readout naturally increases the myocardial wall thickness and is thus less sensitive to partial-volume effects, which is a certain advantage for a number of additional applications. These data support the use of systolic T1 mapping in female patients (who have thinner myocardium than males) and the advantages may extend to other situations where partial-volume effects in thin myocardium are a particular issue, such as investigations of apical myocardium or patients with dilated cardiomyopathy, although specific systematic comparative studies may be warranted.

Together with findings reported above by other investigators, these data confirm that systolic readout offers an important advantage in that data can be acquired almost irrespective of heart rate and rhythm – i.e. as the method requires little scanner operator experience in handling arrhythmias, it can be readily applied in many clinical situations. The patient data reported support this, as the sequence consistently provided T1 maps of excellent quality without need for further adjustment of acquisition parameters despite the presence of tachyarrhythmia. The shortest possible imaging (TD 0 ms) was chosen for simplicity in the majority of these patients, minimising TT and thus maximising heart rate tolerated before mistriggering occurs. The presented healthy volunteer data suggest that a choice of TD 50 ms (corresponding to a TT of 250-300 ms) might serve better to maximise the myocardial thickness. In practice, the only situation in which the choice of TD 0 ms was found to be suboptimal was in atrial fibrillation with a slow ventricular response. In a patient with such a rhythm (mean HR 40-50 bpm), cardiac motion artefact was noted on raw images, indicating data acquisition during mid-systolic ventricular contraction (rather than the relative lack of cardiac motion characteristic of end-systole). Following rapid identification of the artefact on R^2 maps and determination of the correct timing from cine images, repeat acquisition with TD 100 ms resulted in an excellent quality T1 map (**Figure 23**).

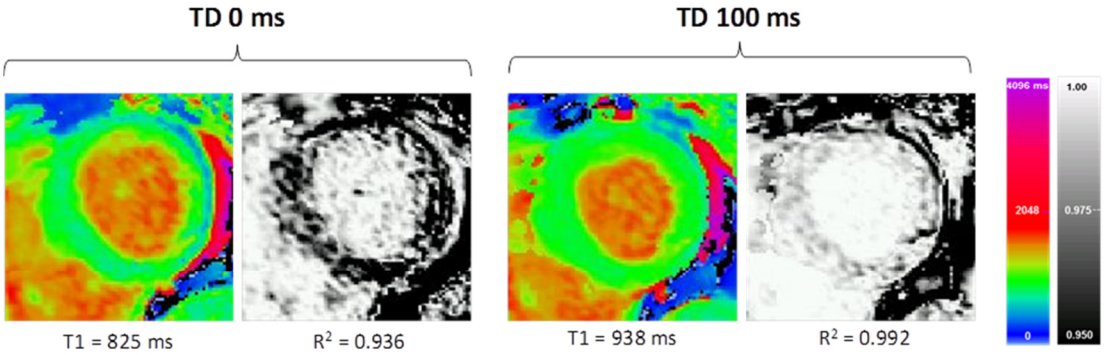


Figure 23: Example of adjustment of TD to optimise T1 fit and improve T1 estimation. *In this patient with atrial fibrillation and slow ventricular response (mean HR 40-50 bpm), TD 0 ms (short readout) was associated with underestimation of T1 values and distinctively darker appearance of myocardial tissue on the R2 map. Examination of cine images led to the recognition that the longer RR interval was associated with delayed peak systolic contraction, and thus TD 0 ms acquired data during the peak of myocardial contraction in mid-systole with associated cardiac motion. Subsequent repeat acquisition with a "tailored" TD of 100 ms (short readout) led to data acquisition at end-systole, avoiding myocardial motion and leading to much improved T1 fit on the R2 map.*

4.5.3 Limitations

The number of volunteers included in this study is relatively small, but effects of inter-individual differences are reduced as all combinations of sequence parameters were undertaken in all volunteers. While a specific implementation of ShMOLLI with its corresponding conditional reconstruction was tested, the primary hypothesis has been independently confirmed by another research group using the classic 17-heart-beat MOLLI variant [150]. This work focused on validation of systolic ShMOLLI for the determination of native myocardial T1 values. Further studies are needed to identify the implications of the use of this technique for post-contrast T1 mapping and ECV quantification. ShMOLLI acquisitions in this implementation are not motion corrected; while in-plane motion components can be corrected in post-processing, very low segmental

rejection rates were achieved in this study without needing to employ this technique. The focus was instead placed on ensuring the best possible breath-holds at time of data acquisition, as this has the added advantage of also reducing the impact of *through-plane* motion. Subjects who have difficulty breath-holding (particularly those with thin myocardial walls) would likely benefit from a combination of both approaches, but this was not specifically tested in this study.

The main limitation for the current evidence in the field is that it is only observational - much further work is needed on simulating the underlying biophysical mechanisms. In particular, it would be hard to extrapolate the current findings to saturation-recovery based techniques, in which end-diastolic readout is usually preferred in order to enable robust saturation time sampling within a single heartbeat. These techniques also do not average T1 recovery over several heartbeats and thus may have different sensitivity to the myocardial blood volumes during the sequence evolution.

4.6 **Conclusions**

In healthy volunteers, systolic ShMOLLI T1 mapping reduces T1 variability and reports clinically equivalent T1 values to conventional diastolic readout; slightly shorter T1 values in systole are mostly explained by reduced partial-volume effects due to the increase in functional myocardial thickness. In patients with tachyarrhythmia, systolic ShMOLLI T1 mapping is feasible, circumvents

mistriggering and produces excellent quality T1 maps. This extends its applicability to challenging rhythms (including atrial fibrillation with a rapid ventricular response) and aids the investigation of thinner myocardial segments. With further validation, systolic T1 mapping could even become a new and convenient standard for myocardial T1 mapping.

Chapter 5

Diffuse myocardial fibrosis in atrial fibrillation

5.1 Abstract

5.1.1 Introduction

Atrial fibrillation (AF) is associated with reduced left ventricular (LV) function and diffuse myocardial fibrosis (DMF), but it is unclear whether DMF is: (1) due to comorbidities or to AF itself, or; (2) responsible for the LV dysfunction. This work aimed to characterize the cardiac phenotype in "lone" AF without significant comorbidities, determine whether there is significant DMF, and investigate whether DMF is a determinant of LV function before and after restoration of sinus rhythm (SR).

5.1.2 Methods

Patients with lone paroxysmal/persistent AF underwent cardiac magnetic resonance (1.5 Tesla) including cine, T1-mapping and ECV quantification (ShMOLLI), and plasma NT-proBNP assessment, before (n=52) and 6-9 months after (n=45) catheter ablation. Analyses were blinded, and results compared with those from matched controls in SR (n=19).

5.1.3 Results

Compared to controls, pre-ablation patients had significantly lower LV ejection fraction (median LVEF 62%, IQR 52-66%, versus 69%, IQR 65-73%; p<0.001) and higher NT-proBNP (median 349pg/mL versus 50pg/mL, p<0.001). However, there were no significant differences in native myocardial T1 (median 946ms versus 933ms, p=0.22) and ECV (27±2% versus 26±3%, p=0.20). Post-ablation, T1 markers of DMF were unchanged (both p=ns), including in the sub-group of patients in AF pre-ablation and SR post-ablation (rhythm at time of CMR, n=18), despite significant improvement in LVEF (p=0.008) and NT-proBNP (p<0.001).

5.1.4 Conclusion

In lone AF, LV dysfunction is independent of diffuse myocardial fibrosis, and may be fully reversible with appropriate treatments. These novel data strongly argue against a causal relationship between AF and DMF; underlying comorbidities may instead predispose to both LV fibrosis and AF.

5.2 Introduction

Atrial fibrillation (AF) presents a rapidly-growing public health and economic burden[112], and is frequently complicated by heart failure symptoms and hospitalisations[154]. Subtle left ventricular (LV) dysfunction is increasingly recognised in AF, even when ventricular rate is well-controlled[10]. In order to improve therapeutic strategies, a more advanced insight into the

pathophysiology of heart failure in AF is necessary. This includes understanding whether progressive LV diffuse myocardial fibrosis (DMF) is an important and necessary contributor to LV dysfunction in AF, since DMF is not fully reversible once established and plays a significant role in the progression of heart failure[155].

Cardiac magnetic resonance (CMR) mapping methods allow non-invasive and quantitative assessment of myocardial tissue characteristics. T1-mapping has been most widely applied in this context[45]. The T1 relaxation time is a magnetic property measured in milliseconds[95], which is very sensitive to changes in tissue free water content. Different tissue types have specific normal ranges for a given T1-mapping method and magnetic field strength. The extracellular volume (ECV) may be estimated by undertaking T1-mapping before and after gadolinium-contrast administration, and adjusting for the haematocrit[45]. ECV may serve as a surrogate for DMF, which may not be detected by late gadolinium enhancement (LGE) imaging[156], when confounders (such as oedema or amyloidosis) have been excluded[45].

Previous studies suggested that AF is associated with higher native (pre-contrast) T1 values[157], lower LV post-contrast T1 values[46, 158] and elevated ECV[47], which can be consistent with the presence of DMF. However, cardiovascular comorbidities as well as the single-timepoint and cross-sectional nature of these investigations may have confounded the results, and thus did

not allow assessment of the precise role of AF in the development of DMF, and the relationship between DMF and LV dysfunction.

To address these knowledge gaps, this work investigated whether DMF contributes to LV dysfunction and recovery in patients with AF. The LV phenotype of patients with lone AF without significant comorbidities was examined using advanced CMR techniques pre- and post-catheter ablation. This allowed determination of the effect of reduction in AF burden and restoration of SR on T1 markers of DMF, and the relationship with change in LV function.

5.3 Methods

5.3.1 Study population

Detailed inclusion and exclusion criteria are provided in Chapter 2: General Methods. Briefly, patients undergoing first-time catheter ablation of symptomatic paroxysmal or persistent AF were screened for eligibility. Individuals with significant valvular disease, uncontrolled arterial hypertension (≥160/90 mmHg), known coronary artery disease, amyloidosis, uncontrolled thyroid disease, systemic inflammatory disease, asthma, diabetes mellitus or obstructive sleep apnoea were not enrolled. Further exclusion criteria were contraindications to CMR (including implanted metallic devices and claustrophobia) or gadolinium administration (including allergy or estimated glomerular filtration rate <30 ml/min).

Control subjects in SR were recruited via poster advertising. Exclusion included those for patients, and a history of palpitations or arrhythmia. Controls were selected to match patients for age, gender, and other baseline characteristics.

5.3.2 Study protocol

Patients underwent pre-ablation assessment at up to 4 weeks prior to the procedure, and were then invited for an identical follow-up visit at between 6 and 9 months post-ablation. Controls were studied on a single occasion.

5.3.3 Cardiac magnetic resonance protocol and analysis

Full details of the cardiac MR imaging protocol, including pulse sequence parameters and detailed description of analysis methods are contained in Chapter 2.

As patients with tachyarrhythmia were included, a variant of the ShMOLLI sequence investigated in Chapter 4 was used for all subjects (including controls in SR and patients in SR at the time of imaging). The previous experiments (see Chapter 4) demonstrated that this variant (TD=0ms, *short readout*) is feasible in tachyarrhythmia (including AF with a fast ventricular response), circumventing mistriggering and producing excellent quality T1 maps, with clinically equivalent T1 values to a conventional diastolic readout[159].

5.3.4 Statistical analysis

Based on the assumption that AF patients have an ECV of 34±3%[47], we calculated that paired analysis of 45 patients before and after ablation would give >90% power to detect a change in ECV of at least 2 percentage points (2-sided $\alpha = 0.05$, correlation between groups 0.2).

Statistical analyses were performed using IBM SPSS Statistics for Windows, version 24.0.0.1 (IBM Corp., Armonk, NY, USA) and GraphPad Prism version 6 (GraphPad Software, San Diego, California, USA). Normality of data was assessed using Kolmogorov-Smirnov tests. Normally-distributed data were compared using t-tests (paired when appropriate). Non-normally-distributed unpaired data were compared using the Mann-Whitney U-test, and non-normally-distributed paired data were compared using the Wilcoxon signed-rank test. The Chi-square test was used to compare proportions. All tests were two-tailed, and p values < 0.05 were considered significant. Data are shown as mean ± SD or median and interquartile range (IQR), as appropriate.

5.4 Results

A total of 52 patients with AF (27 paroxysmal, 25 persistent), and 19 matched controls in SR were included. Patients and controls were well matched for all baseline characteristics, including age, gender, body mass index, heart rate, and arterial blood pressure (**Table 5**). In paroxysmal AF patients, median AF burden was 2.6% (equivalent to ~4 hours per week). In persistent AF patients, median

duration of uninterrupted AF at the time of ablation was approximately 11 months.

Table 5: Baseline characteristics of the study groups.

	AF Patients (n=52)	SR Controls (n=19)	p value
Age (years)	65 (56 – 68)	65 (57 – 70)	0.938
Male (%)	75	79	0.730
BMI (kg/m^2)	28 ± 5	28 ± 3	0.590
Pulse (bpm)	62 (54 – 83)	66 (60 – 72)	0.789
SBP (mmHg)	130 (124 – 146)	141 (124 – 158)	0.132
DBP (mmHg)	81 ± 11	81 ± 12	0.991

5.4.1 Pre-ablation left ventricular indices

Compared to matched controls, LV ejection fraction (LVEF) was significantly lower in patients with AF (median 62% versus 69%, p<0.001; **Table 6**). In keeping with subtle LV dysfunction in patients with AF, peak systolic circumferential strain was impaired (median -15% versus median -17% in controls, p=0.008; Table 2) and plasma NT-proBNP concentration was significantly higher (median 349 pg/ml versus median 50 pg/ml in controls, p<0.001; **Table 6**). In contrast, there were no differences between the groups in LV mass index or the ratio of LV mass to LV end-diastolic volume (a marker of concentric LV remodelling[121]). Similarly, LGE was an infrequent finding, being present in 8 (15%) patients with AF and 3 (16%) controls in SR, with no

difference in the area of LGE between the groups. The pattern of LGE was non-ischaemic in all but one subject. These results are summarised in **Table 6**.

Table 6: Left ventricular indices in the study groups

	Patients with AF (n=52)	**Controls in SR (n=19)**	**p value**
LV end-diastolic volume (mL)	148 ± 39	133 ± 30	0.119
LV end-systolic volume (mL)	61 ± 24	43 ± 15	**0.002**
LVEF (%)	62 (52 – 66)	69 (65 – 73)	**<0.001**
Peak systolic circumferential strain (%)	-15 (-11 to -18)	-17 (-16 to -19)	**0.008**
LV mass index (g/m^2)	61 ± 12	55 ± 11	0.084
LV mass/end-diastolic volume (g/mL)	0.86 ± 0.18	0.85 ± 0.13	0.896
LV LGE area, %	0.2 (0.0 – 0.5)	0.1 (0.1 – 0.9)	0.549
Plasma NT-proBNP (pg/ml)	349 (129 – 946)	50 (30 – 126)	**<0.001**

As expected, the majority of patients with persistent AF were in AF during pre-ablation CMR imaging (22 of 25, 88%), whilst the majority of patients with paroxysmal AF were in SR during pre-ablation CMR imaging (21 of 27, 78%).

Patients with persistent AF had significantly lower LVEF compared to patients with paroxysmal AF (median 55%, IQR 49–63% versus median 64%, IQR 59–67%; p=0.009). Similarly, plasma NT-proBNP concentrations were higher in patients with persistent AF (median 748 pg/ml, IQR 537–1149 pg/ml versus median 141 pg/ml, IQR 62–237 pg/ml; p<0.001).

5.4.2 Pre-ablation LV tissue characterisation

Native and post-contrast T1-maps were generally of high quality, including in patients in AF at the time of imaging (see **Figure 24**). To maximise the accuracy of reported T1 values, each segment was strictly assessed for image quality before inclusion, as previously described[96], and only good-to-excellent quality segments were included. In total, 249 of 1392 (17.8%) segments were excluded due to off-resonance artefacts, poor T1 fit as evidenced by the R^2 maps, patient movement or low signal-to-noise ratio. In keeping with this stringent quality control process, R^2 values in included segments were excellent (median native R^2 = 0.996, IQR 0.994–0.997; median post-contrast R^2 = 0.997, IQR 0.995–0.998). Native and post-contrast R^2 values were statistically slightly lower in patients with AF compared to controls in SR (**Table 7**); and in patients in AF during CMR compared to patients in SR during CMR (**Table 8**); however, absolute differences were very small and unlikely to affect T1 values, given the excellent R^2 values observed in all groups.

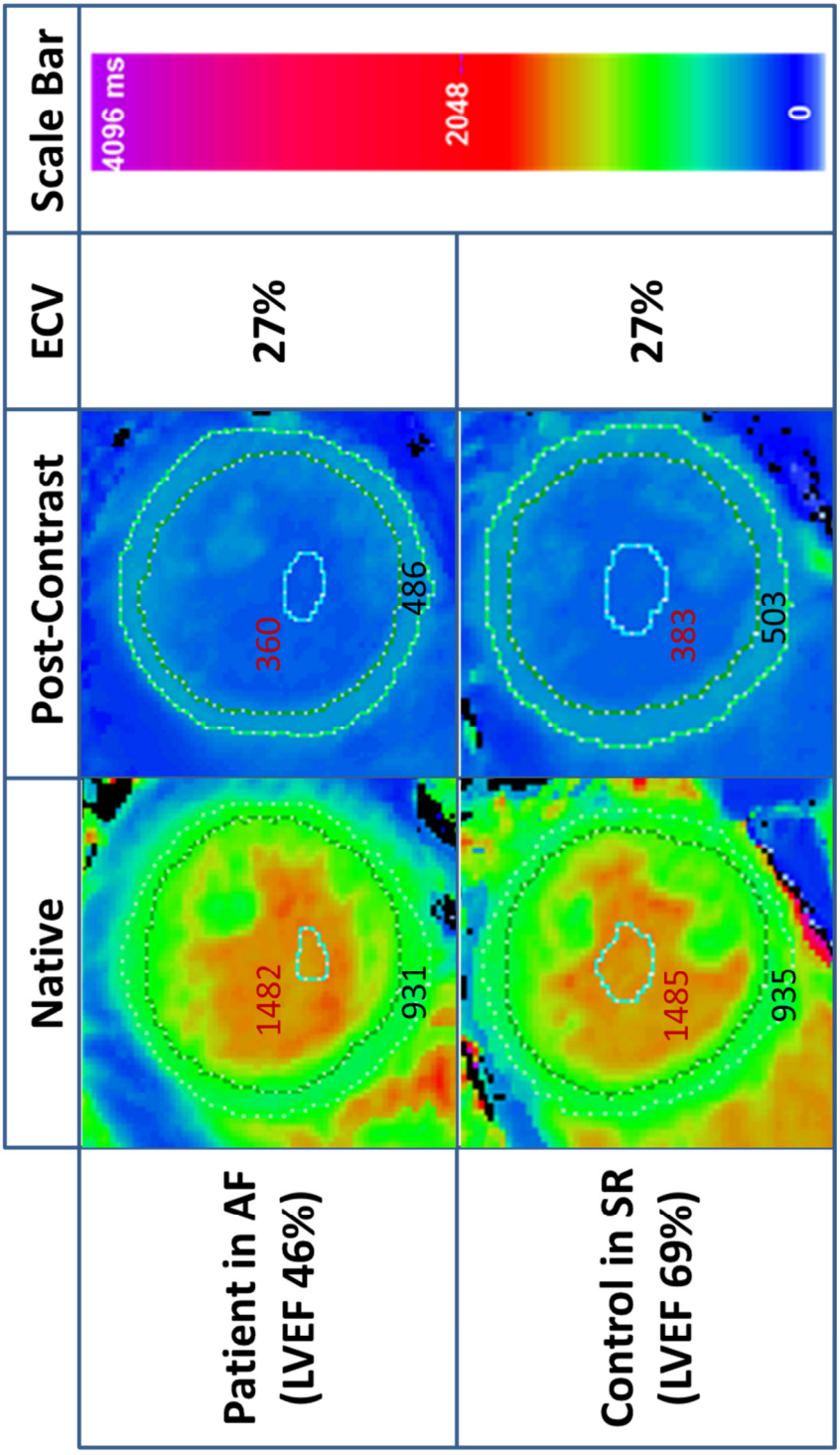


Figure 24: Representative native and post-contrast T1-maps from a patient in AF during CMR and a control in SR. *Myocardial (black) and blood pool (red) T1 times and manually drawn endocardial, epicardial and blood pool contours are shown on native and post-contrast T1-maps from a patient in AF during CMR and a control subject in SR. Despite the patient having a LVEF of 46%, the T1 times and ECV are very similar to the control subject with a LVEF of 69%.*

Table 7: Pre- and post-ablation T1, R^2, haematocrit and ECV values

	1 Controls in SR (n=19)	2 AF Patients pre-ablation (n=45)	p value (1 vs 2)	3 AF Patients post-ablation (n=45)	p value (1 vs 3)	p value (2 vs 3)
Native myocardial T1 (ms)	933 (917 – 972)	945 (926 – 971)	0.249	944 (926 – 964)	0.406	0.266
Native myocardial R^2	0.997 (0.996 – 0.998)	0.996 (0.993 – 0.997)	**0.003**	0.997 (0.995 – 0.998)	0.158	**0.004**
Native blood T1 (ms)	1480 (1453 – 1541)	1507 (1476 – 1545)	0.161	1513 (1462 – 1562)	0.328	0.808
Post-contrast myocardial T1 (ms)	496±25	498±38	0.820	495±30	0.960	0.498
Post-contrast myocardial R^2	0.998 (0.997 – 0.998)	0.996 (0.992 – 0.998)	**0.001**	0.997 (0.996 – 0.998)	0.074	**0.001**
Post-contrast blood T1 (ms)	356 (338 – 383)	370 (355 – 407)	0.199	377 (345 – 390)	0.328	**0.032**
Haematocrit (%)	42.6±3.5	43.5±2.9	0.273	42.6±3.1	0.997	**0.018**
ECV (%)	26.3±2.8	27.2±2.0	0.211	27.1±2.2	0.242	0.588

Table 8: T1-mapping data in patients with AF pre-ablation, by CMR rhythm

	AF during CMR (n=28)	**SR during CMR (n=24)**	**p value**
Native myocardial T1 (ms)	956 (931 – 984)	937 (924 – 961)	0.180
Native myocardial R^2	0.994 (0.990 – 0.996)	0.996 (0.994 – 0.998)	**0.004**
Native blood T1 (ms)	1509 (1473 – 1573)	1511 (1484 – 1534)	0.956
Post-contrast myocardial T1 (ms)	491±39	503±35	0.251
Post-contrast myocardial R^2	0.993 (0.988 – 0.995)	0.998 (0.997 – 0.998)	**<0.001**
Post-contrast blood T1 (ms)	363 (354 – 398)	379 (356 – 415)	0.123
Haematocrit (%)	43.8 ± 3.8	43.1 ± 2.6	0.100
ECV (%)	27.2 ± 2.1	27.3 ± 2.1	0.969

There were no significant differences between patients with AF and controls in SR in either native myocardial T1 values (median 946 ms, IQR 925–975 ms versus median 933 ms, IQR 917–972 ms; p=0.22; **Figure 25A**) or post-contrast myocardial T1 values (497±38 ms versus 496±25 ms, p=0.92). Similarly, haematocrit (0.43±0.03 versus 0.43±0.03, p=0.31) and ECV (27±2% versus 26±3%, p=0.20; **Figure 25B**) were similar between groups. In a repeat analysis excluding individuals with LGE, there remained no significant differences between patients with AF and controls in SR in myocardial native T1, post-contrast T1 or ECV (all p=ns; **Table 9**).

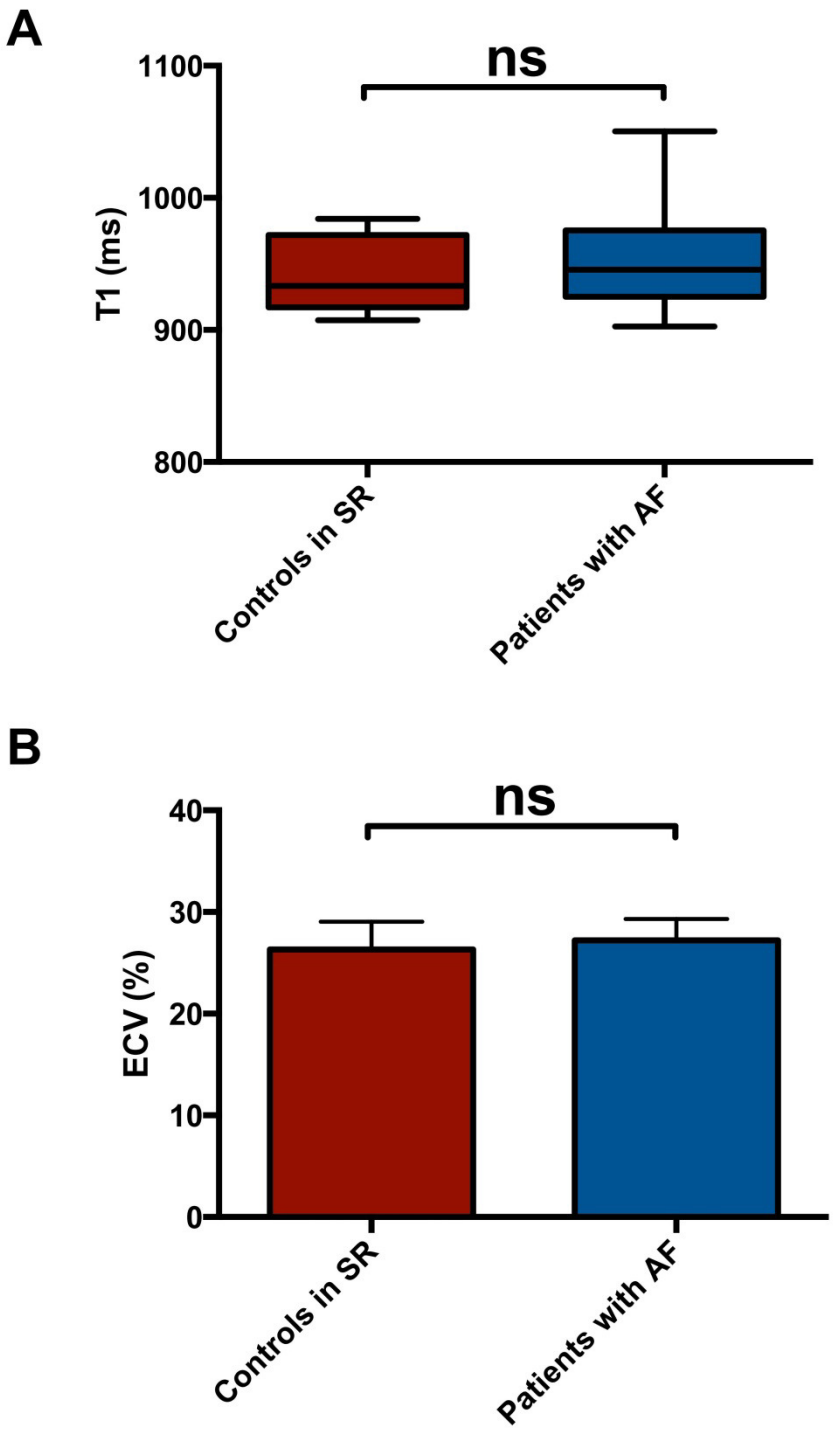


Figure 25: Native myocardial T1 and ECV in controls in SR and patients with AF pre-ablation. *(**A**) Native myocardial T1 and (**B**) ECV in controls in SR (n=19) and patients with AF pre-ablation (n=52). There are no significant differences between the groups in either parameter (p=0.217 and p=0.201, respectively).*

Table 9: Left ventricular indices and T1 mapping data in patients and controls without late gadolinium enhancement

	Patients with AF (n=44)	**Controls in SR (n=16)**	**p value**
LV end-diastolic volume (mL)	148±39	135±28	0.225
LV end-systolic volume (mL)	62±25	43±14	**<0.001**
LVEF (%)	59 (51–65)	69 (65–72)	**<0.001**
Peak systolic circumferential strain (%)	-14 (-11 to -18)	-17 (-16 to -19)	**0.007**
LV mass index (g/m^2)	61±12	56±12	0.136
LV mass/end-diastolic volume (g/mL)	0.88±0.19	0.86±0.13	0.725
Plasma NT-proBNP (pg/ml)	498 (145–1014)	47 (31–98)	**<0.001**
Native myocardial T1 (ms)	955 (931 – 976)	932 (918 – 969)	0.128
Post-contrast myocardial T1 (ms)	498±39	499±25	0.910
ECV (%)	27.2±2.1	26.3±2.7	0.162

Native myocardial T1 and ECV were similar between persistent AF and paroxysmal AF patients (respectively: median 957 ms versus median 938 ms, p=0.12, and 27±2% versus 27±2%, p=0.97; **Table 10**). There were also no

differences in these parameters between patients in AF during CMR and patients in SR during CMR (both p=ns; **Table 8**).

Table 10: T1-mapping data in patients with AF pre-ablation, by AF type

	Paroxysmal AF (n=27)	**Persistent AF (n=25)**	**p value**
Native myocardial T1 (ms)	938 (923 – 962)	957 (932 – 984)	0.122
Native myocardial R^2	0.996 (0.994 – 0.997)	0.995 (0.991 – 0.996)	0.068
Native blood T1 (ms)	1516 (1495 – 1558)	1496 (1470 – 1531)	0.126
Post-contrast myocardial T1 (ms)	507±34	486±39	**0.041**
Post-contrast myocardial R^2	0.997 (0.995 – 0.998)	0.992 (0.988 – 0.996)	**<0.001**
Post-contrast blood T1 (ms)	381 (364 – 417)	357 (335 – 388)	**0.016**
Haematocrit (%)	42.9 ± 3.3	44.1 ± 3.1	0.173
ECV (%)	27.2 ± 2.3	27.2 ± 1.9	0.969

Finally, there were no differences in myocardial native T1, post-contrast T1 or ECV between patients receiving angiotensin-converting enzyme (ACE) inhibitors / angiotensin II receptor blockers (ARB) (n=23) versus the remainder of patients not receiving such medications (all p=ns).

5.4.3 Outcomes after ablation

Ablation was undertaken in 50 patients, with no significant complications – planned ablation was cancelled for clinical reasons in 2 patients. By the follow-up visit (at a median of 7 months post-ablation [IQR 7 – 9 months]), 9 patients (18%) underwent an attempt at electrical cardioversion and 3 patients (6%) underwent a second ablation procedure as a result of recurrence of AF or a left atrial tachycardia. Four patients (8%) declined to attend the follow-up visit and one patient did not receive gadolinium at follow-up due to a prior intolerance to this agent, meaning that complete and paired pre- and post-ablation data were available in 45 patients.

Pre- and post-ablation intra-scan rhythms were: SR-SR (n=21); AF-SR (n=18); AF-AF (n=4); and SR-AF (n=2). Holter-determined AF burden was significantly lower than before ablation (median 0%, IQR, 0%–0% post-ablation versus 48%, IQR, 0.7%–100% pre-ablation, $p<0.001$).

5.4.4 Post-ablation left ventricular indices and tissue characterisation

Restoration of sinus rhythm and/or reduction in AF burden following ablation was associated with a small but significant improvement in LVEF in the entire cohort (pre-ablation median 62%, IQR 53-65% versus post-ablation median 65%, IQR 59-68%; $p=0.006$). In keeping with the reduction in AF burden and improvement in LV function, plasma NT-proBNP concentrations also fell significantly (pre-ablation median 313 pg/ml, IQR 130–803 pg/ml

versus post-ablation median 97 pg/ml, IQR 56–252 pg/ml; p<0.001). The changes in both LVEF and NT-proBNP were largely driven by the AF-SR sub-group (n=18) in whom both parameters improved significantly post-ablation (p=0.008 and p<0.001, respectively; **Figure 26A** and **Figure 26B**). Despite these favourable changes in LV function and NT-proBNP concentrations, there was no associated change in either native myocardial T1 or ECV in this sub-group (both p=ns, **Figure 26C** and **Figure 26D**).

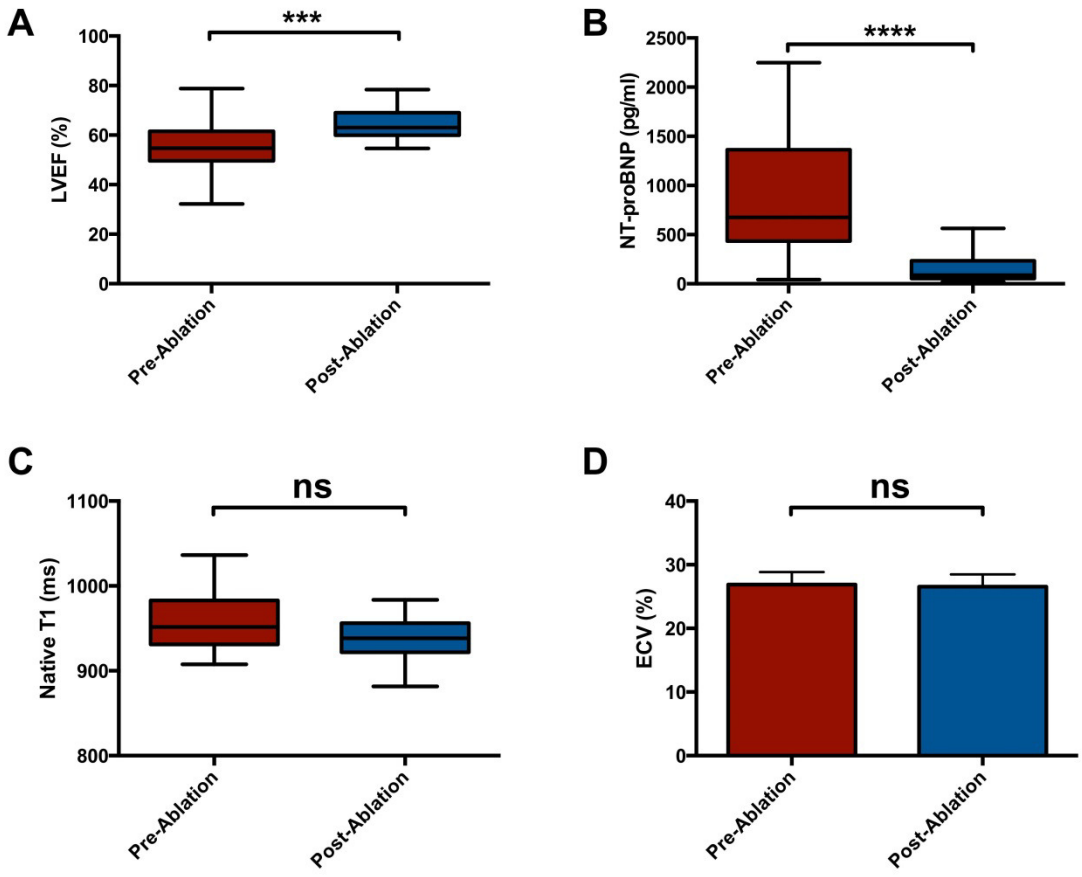


Figure 26: Pre- and post-ablation LVEF, NT-proBNP, native myocardial T1 and ECV in patients in AF during the pre-ablation CMR and in SR during the post-ablation CMR. *Pre-ablation and post-ablation results for (**A**) LVEF, (**B**) NT-proBNP, (**C**) native myocardial T1, and (**D**) ECV in patients in AF during pre-ablation CMR and in SR during post-ablation CMR. Note the significant improvement in LVEF and NT-proBNP post-ablation (p=0.008 and p<0.001, respectively), but no change in native myocardial T1 and ECV (p=0.102 and p=0.499, respectively).*

As expected from these findings, there was also no change in native myocardial T1 or ECV when considering the entire cohort post-ablation (respectively: pre-ablation median native T1 945 ms versus post-ablation 944 ms, p=0.266; pre-ablation ECV 27±2% versus post-ablation 27±2%, p=0.588; **Table 7**).

5.5 Discussion

This is the first study to prospectively address the important question of whether diffuse myocardial fibrosis (DMF) contributes to LV dysfunction in AF. The study design is unique in several aspects, such as the exclusion of significant cardiovascular comorbidities in the AF patient group, the inclusion of control subjects fully matched for baseline characteristics (rather than completely healthy individuals), the presence of a post-ablation follow-up CMR evaluation, and use of a systolic T1-mapping sequence that can handle tachyarrhythmia and generate robust T1-maps[159].

The main finding is absence of evidence of significant DMF in patients with lone AF, despite mildly reduced LV function and elevated plasma NT-proBNP concentration compared to matched controls in SR. Additionally, recovery of SR post-ablation from AF pre-ablation did not affect LV T1 biomarkers, in contrast with favourable changes seen in the functional parameters. These novel data demonstrate that DMF is not critical to LV systolic dysfunction in AF.

5.5.1 Diffuse ventricular fibrosis in AF

Histological data from AF patients are scarce - one small series of 14 patients with AF refractory to initial medical therapy suggested abnormal histology in all cases (including cardiomyopathic changes, myocarditis, and nonspecific necrosis and fibrosis)[33]. However, this was a select group of young patients (mean age 37) with a clinical indication for left ventricular endomyocardial biopsy, and therefore not representative of typical AF patients seen in the clinic.

There are also limited data investigating DMF in patients with AF using CMR. Ling et al. reported only post-contrast T1 values in 67 patients with paroxysmal and persistent AF scheduled for catheter ablation, and in a control group of 23 healthy volunteers[46]. Patients with AF had lower post-contrast T1 values compared to controls, consistent with the presence of DMF, which was also independently associated with ageing and systolic dysfunction. A follow-up study based on an overlapping cohort of patients from the same institution demonstrated that lower post-contrast T1 values were associated with recurrence of AF after catheter ablation[160]. Importantly, isolated post-contrast T1 values are confounded by haematocrit, gadolinium dose and renal clearance, and current guidelines recommend against reporting of post-contrast T1 in isolation[45]. A separate study by Neilan et al. examined the relationship between LV ECV measured before catheter ablation and freedom from AF after ablation in a cohort of patients with both AF and hypertension[47]. They found that AF patients had increased ECV compared to healthy controls, and that ECV was the

strongest predictor of recurrent AF (each 10% increase in ECV associated with a 29% increased risk of recurrent AF). Importantly, these and other previous studies[157, 158] included patients with significant cardiovascular comorbidities in addition to AF, undertook imaging at only a single (pre-ablation) timepoint, and compared results with "healthy" (rather than "matched") control subjects. As a result, these study designs were unable to determine whether the DMF identified was related to AF *per se*, or whether the association may have been confounded by other factors.

The present cohort of patients was, if anything, older than those in the Ling[46], McLellan[160], and Neilan[47] studies (mean age 63 years in this study, versus mean age 57-58 years in the prior studies), had a considerable median time since first AF diagnosis of nearly 4 years, and had reduced LVEF and elevated plasma NT-proBNP concentrations compared to matched control subjects. Despite all these indications of significant AF exposure and abnormal LV function, there was no excess in T1 markers of DMF compared to the control group, which was very well-matched for all baseline characteristics including age, gender, body mass index, and arterial blood pressure. LV tissue characteristics were also similar in patients with paroxysmal and persistent AF, despite the latter having a greater AF burden, lower LVEF and higher plasma NT-proBNP concentration. These data argue against a direct relationship between AF and abnormal LV tissue characteristics, and instead suggest that underlying comorbidities (such as congestive heart failure, coronary artery

disease, and diabetes mellitus) may predispose to both AF and diffuse ventricular fibrosis. This latter possibility requires confirmation in future prospective studies that include patients with comorbidities with and without AF, and patients with AF with and without comorbidities.

5.5.2 T1-mapping in AF

Patients with AF present technical challenges to CMR imaging due to the frequently fast and irregular RR-interval[45]. There has historically been limited experience of applying quantitative mapping techniques in patients with tachyarrhythmia, and some previous studies have either excluded patients not in SR at the time of imaging[47] or failed to report intra-scan rhythms[46]. A significant strength of the present work is the universal use of systolic ShMOLLI, meaning that high-quality T1-maps could be acquired even when patients were in AF during the CMR scan. Subsequent to the original description of systolic readout T1-mapping for application in tachyarrhythmia[159], the findings were independently replicated using a MOLLI sequence[161]. Importantly, the segmental rejection rate of 17.8% in the present study compares favourably to the 26.3% segmental rejection rate reported using various MOLLI sampling schemes in patients with AF[161].

In addition to the innovative use of systolic T1-mapping, several further techniques were employed to optimise data quality and increase robustness of the results. Firstly, artefacts were carefully excluded using R^2 maps of goodness-of-fit and visual inspection of raw images, as the diagnostic performance of

mapping techniques depends heavily on image quality. Secondly, image analysis was undertaken in a blinded fashion and in a randomized order by an operator not involved with data collection. Finally, an automated algorithm systematically modified manually drawn endocardial and epicardial contours towards the centreline of the myocardium, minimising contamination of the myocardial sample by partial volume effects. Each of these methods acted to remove potential sources of bias, as reduced image quality in the presence of arrhythmia is an important confounder that must be carefully considered and accounted for in imaging studies involving patients with AF.

5.5.3 Clinical implications and future directions

These results indicate that patients with AF and no significant comorbidities do not have more imaging markers of DMF than matched control subjects in SR, despite impaired LV function and elevated plasma NT-proBNP concentration. Whilst the reduction in LVEF and the increase in plasma NT-proBNP in patients with AF were relatively subtle, population-based data demonstrate that borderline changes in both these parameters are highly clinically relevant, being associated with an increased risk of heart failure and death[162] and an increased risk of major cardiovascular events[163], respectively. Additionally, this study demonstrates that T1 markers of DMF are unchanged post-ablation, even in the sub-group of patients in whom LV function improves.

These novel data have important clinical implications. Firstly, they indicate that, in lone AF, small areas of LV fibrosis or scarring are not critical to

the pathophysiology of subtle LV dysfunction; instead, alternative mechanisms (including impaired myocardial energetics[164]) that act independently of LV tissue characteristics are likely to be responsible, in combination with haemodynamic effects, such as absence of active atrial emptying and an irregular RR interval, in those individuals with a rhythm of AF at the time of assessment. The lack of significant fibrosis suggests that LV dysfunction in patients with lone AF is likely to be reversible, if the underlying mechanism or mechanisms are successfully identified and treated. Secondly, these data should be interpreted in the context of previous investigations showing that DMF in patients with AF and cardiovascular comorbidity is associated with treatment resistance and recurrence of AF following ablation[47, 160]. Clinical trials of novel therapeutic strategies are likely to benefit from screening patients for absence of LV fibrosis at baseline, thereby selecting a population with the best chance of a successful response to treatment. The present data are highly relevant as they indicate that LV function is not a surrogate for DMF in patients with lone AF. CMR could therefore play a role in phenotyping and selection of patients prior to inclusion in a clinical trial.

5.5.4 Limitations

T1-mapping was undertaken in a mid-ventricular short-axis plane, rather than attempting whole-heart coverage. This approach has the advantage of reducing partial volume effects seen in more apical slices, but would be insensitive to disease processes preferentially affecting the base or apex of the heart. Despite

this theoretical possibility, a previous study demonstrated that ECV is similar in basal, mid-ventricular and apical short-axis planes in patients with AF[47].

Whilst patients with controlled hypertension and AF were included in the study, there was no evidence of hypertensive heart disease with normal LV mass index in patients and controls. The inclusion of patients with controlled hypertension is unlikely to have affected the results, as a previous CMR study demonstrated that only patients with LV hypertrophy had evidence of DMF[165]. Some patients with AF were treated with angiotensin converting enzyme (ACE) inhibitors or angiotensin II receptor blockers (ARB), which may have anti-fibrotic effects and could have resulted in a reduction in ECV compared to control subjects, who were not treated with these agents. However, no differences in T1 markers of DMF were detected between those patients receiving and not receiving such medications.

5.6 **Conclusion**

In lone AF, early LV dysfunction is not attributable to diffuse myocardial fibrosis. These data strongly argue against a direct relationship between AF and DMF, and instead suggest that underlying comorbidities predispose to both AF and LV fibrosis. Subtle LV dysfunction in lone AF patients may be reversible with appropriate and targeted therapeutic strategies initiated prior to the development of adverse LV remodelling.

Chapter 6

Myocardial perfusion in atrial fibrillation

6.1 Abstract

6.1.1 Introduction

Atrial fibrillation (AF) is associated with non-ST elevation myocardial infarction, while patients with AF and no obstructive coronary artery disease can present with symptoms and objective evidence of cardiac ischaemia. The aim of this study was to investigate myocardial perfusion in patients with "lone" AF and no significant cardiovascular comorbidities, to determine the presence and degree of coronary microvascular dysfunction and its relationship with left ventricular (LV) function.

6.1.2 Methods

Patients with lone paroxysmal/persistent AF underwent cardiac magnetic resonance (1.5 Tesla) for evaluation of LV strain, and myocardial perfusion with absolute quantification of myocardial blood flow (MBF) at baseline and during adenosine stress, before (n=49) and 6-9 months after (n=40) catheter ablation.

Analyses were blinded, and results compared with those from matched controls in sinus rhythm (SR; n=25).

6.1.3 Results

Patients with AF pre-ablation had significantly impaired systolic strain indices (all $p<0.001$ vs. controls), reduced baseline MBF (1.21±0.24 mL/min/g.(mmHg.bpm/10^4)$^{-1}$ versus 1.34±0.28 mL/min/g.(mmHg.bpm/10^4)$^{-1}$, $p=0.044$) and stress MBF (2.29±0.48 mL/min/g versus 2.73±0.37 mL/min/g, $p<0.001$). Baseline MBF correlated with systolic and diastolic strain indices (r 0.382-0.517, all $p\leq0.001$). Despite a significant reduction in AF burden after ablation ($p=0.001$), baseline and stress MBF were unchanged compared to pre-ablation in paired analyses (n=33, p=ns).

6.1.4 Conclusion

Baseline and stress myocardial perfusion are significantly impaired in the absence of epicardial coronary artery disease in patients with AF, and do not normalize after ablation. Lower baseline MBF is also linked to impaired LV systolic and diastolic function, indicating that coronary microvascular dysfunction may be an important pathophysiological mechanism in patients with lone AF.

6.2 Introduction

Atrial fibrillation (AF) is a major cause of morbidity and healthcare resource utilisation, and represents a growing worldwide epidemic[112]. Recent

large-scale prospective cohort data have demonstrated a clear association between AF and incident myocardial infarction in individuals without baseline coronary heart disease, independent of conventional atherosclerotic risk factors and other demographic characteristics[6]. The association is exclusive to non ST-elevation myocardial infarction[166], implicating an underlying pathophysiology of oxygen supply-demand imbalance rather than complete thrombotic coronary occlusion. Clinicians are also familiar with patients with acute onset of AF presenting with chest pain and objective evidence of cardiac ischaemia or necrosis, such as 'rate-related' ST depression or Troponin release, in the absence of significant epicardial coronary artery disease[54, 167]. Despite these intriguing observations, no previous study has systematically investigated myocardial perfusion and function in patients with AF.

Cardiac magnetic resonance (CMR) is a validated, non-invasive, and accurate method for detection of inducible myocardial hypoperfusion[168], including in patients with microvascular dysfunction without obstructive CAD[169-171]. This study tested the hypothesis that microcirculatory dysfunction and impaired myocardial perfusion are present in patients with AF but no significant epicardial coronary artery disease or other cardiovascular comorbidities, and that these findings would relate to the subtle reduction in left ventricular (LV) function that is present even when the ventricular rate is well controlled (Chapter 3). Adenosine stress/rest CMR was used to evaluate myocardial perfusion reserve (MPR), and a model-independent and fully

quantitative technique to determine baseline and stress myocardial blood flow (MBF). The relationship between myocardial perfusion and LV function was examined both before and after catheter ablation, to assess the effect of restoration of sinus rhythm (SR) and reduction in AF burden.

6.3 Methods

6.3.1 Study Population

Detailed inclusion and exclusion criteria are provided in Chapter 2: General Methods. Briefly, patients undergoing first-time catheter ablation of symptomatic paroxysmal or persistent AF were screened for eligibility. Individuals with significant epicardial coronary artery disease or other significant cardiovascular comorbidities, contraindications to CMR, or contraindications to administration of gadolinium or adenosine were not enrolled. Matched control subjects in SR were recruited via poster advertising.

All subjects avoided potential adenosine antagonisers (e.g. caffeine) for ≥24 h before CMR scans.

6.3.2 Study Protocol

Patients underwent pre-ablation assessment at up to 4 weeks prior to the procedure, and were then invited for an identical follow-up visit at between 6 and 9 months post-ablation. Controls were studied at a single timepoint.

6.3.3 Cardiac Magnetic Resonance Protocol and Analysis

Full details of the cardiac MR imaging protocol, including pulse sequence parameters and detailed description of analysis methods are contained in Chapter 2.

6.3.4 Statistical Analysis

Power calculations were based on prior data demonstrating baseline MBF of 0.95±0.19 mL/min/mL in AF patients and 1.14±0.22 mL/min/mL in matched controls, and adenosine-stress induced MBF of 2.07±0.80 mL/min/mL in AF patients and 3.33±0.78 mL/min/mL in matched controls[57]. We calculated that inclusion of at least 48 patients and 24 controls (2:1 ratio) would give >90% power to detect a difference of ≥15% in baseline MBF between patients and controls (2-sided α=0.05). We also calculated that paired analysis of 30 patients before and after ablation would give >90% power to detect a change of ≥25% in adenosine-stress induced MBF (2-sided α=0.05, between group correlation=0.5).

Statistical analyses were performed using IBM SPSS Statistics for Windows, version 20.0 (IBM Corp., Armonk, NY, USA) and GraphPad Prism version 6 (GraphPad Software, San Diego, California, USA). Normality of data was assessed using Kolmogorov-Smirnov tests. Normally-distributed data were compared using t tests (paired when appropriate) and 1-way ANOVA. Non-normally-distributed unpaired data were compared using the Mann-Whitney U test or the Kruskal-Wallis test, and non-normally-distributed paired data were

compared using the Wilcoxon signed-rank test. The Chi-square test was used to compare proportions. The Pearson r was used to report correlations between parameters. All tests were 2 tailed, and P values < 0.05 (after Bonferroni adjustment for multiple comparisons when appropriate) were considered significant. Data are shown as mean ± SD or median and interquartile range (IQR), as appropriate.

6.4 Results

A total of 74 subjects were included: 49 patients with AF (25 paroxysmal, 24 persistent), and 25 matched control subjects in SR. Patients and controls were well-matched for all characteristics, including age, gender, body mass index, heart rate, and arterial blood pressure (see **Table 11**).

Table 11: Baseline characteristics of the study groups

	Patients with AF (n=49)	Controls in SR (n=25)	p value
Age, years	67 (57–70)	64 (63–66)	0.60
Male, n (%)	37 (76)	19 (76)	0.96
BMI, kg/m^2	28±5	27±3	0.36
Pulse, bpm	60 (54–78)	66 (60–68)	0.98
SBP, mmHg	130 (124–146)	137 (124–155)	0.36
DBP, mmHg	81±12	80±11	0.86
ACEI / ARB, n (%)	22 (45)	1 (4)	-
Beta-blocker / Sotalol, n (%)	33 (67)	0 (0)	-
Flecainide, n (%)	12 (24)	0 (0)	-
Digoxin, n (%)	7 (14)	0 (0)	-
Amiodarone, n (%)	4 (8)	0 (0)	-

6.4.1 Pre-ablation LV function, hemodynamic data, and perfusion reserve

Compared to controls, patients with AF had significantly impaired LV systolic function as measured by tissue-tracking derived peak systolic circumferential strain and peak systolic radial strain (both p<0.001), and impaired diastolic function by peak diastolic radial strain rate (p=0.039; **Table 12**).

Table 12: Left ventricular strain indices in the study groups

	Patients with AF (n=49)	Controls in SR (n=25)	p value
Peak systolic circumferential strain, %	-16±3	-19±2	**<0.001**
Peak systolic radial strain, %	31±9	40±6	**<0.001**
Peak diastolic radial strain rate, s^{-1}	-2.0±0.6	-2.2±0.4	**0.039**

Baseline and stress hemodynamic data are shown in **Table 13**. Patients in SR during CMR had significantly lower baseline HR and RPP than patients in AF during CMR and a trend to lower baseline RPP than controls (p<0.001 and p=0.069, respectively; **Table 13**), likely due to the effects of medications (**Table 11**). Stress RPP was significantly lower in patients compared to controls, regardless of the patients' intra-scan rhythm (**Table 13**). The difference in RPP between baseline and stress (delta RPP) was significantly lower in patients in AF during CMR compared to the other two groups (p<0.001 for both; **Table 13**). Positive splenic switch-off (i.e. evidence of adequate adenosine stress) was present in 88% of scans in patients with AF compared to 92% of scans in controls in SR (p=0.58), and all subjects experienced at least one adenosine-related symptom (e.g. chest tightness, dyspnoea, flushing). There were no visual perfusion defects in any study subject on stress or rest perfusion imaging, consistent with the exclusion of obstructive epicardial coronary disease in the study population.

Table 13: Haemodynamic and myocardial blood flow indices in patients pre-ablation and controls

	1 Patients in SR during CMR (n=24)	2 Patients in AF during CMR (n=25)	3 Controls in SR (n=25)	p value (1 vs 2)	p value (1 vs 3)	p value (2 vs 3)
Baseline HR, bpm	55±7	76±23	64±11	**<0.001**	0.132	**0.022**
Baseline systolic BP, mmHg	137±16	139±20	142±18	1.000	1.000	1.000
Baseline RPP, bpm.mmHg	7500±1300	10500±3300	9100±2400	**<0.001**	0.069	0.145
Stress HR, bpm	75 (66 – 79)	75 (64 – 90)	96 (84 – 101)	1.000	**0.004**	**0.014**
Stress systolic BP, mmHg	132±17	138±21	138±16	0.715	1.000	1.000
Stress RPP, bpm.mmHg	10000±2900	10700±2600	12800±2600	1.000	**0.004**	**0.040**
Delta RPP, bpm.mmHg	2500±2100	200±1600	3300±1900	**<0.001**	0.565	**<0.001**
Baseline MBF, mL/min/g.(mmHg.bpm/10^4)$^{-1}$	1.30±0.19	1.09±0.25	1.34±0.28	**0.016**	1.000	**0.003**
Stress MBF, mL/min/g	2.22±0.34	2.36±0.60	2.73±0.37	0.919	**0.001**	**0.024**
Quantitative MPR, index	1.74±0.38	2.28±0.71	2.11±0.44	**0.004**	**0.047**	0.844

6.4.2 Absolute myocardial blood flow is impaired in patients with AF pre-ablation

Absolute MBF quantification could be undertaken successfully at the pre-ablation timepoint in 42 patients with AF and 25 controls in SR. Rejection of all myocardial segments due to poor fitting quality occurring in 6 patients (12%) in AF during CMR and 1 patient (2%) in SR during CMR. In the remaining subjects, a total of 549 segments were rejected out of the total available 2412 segments (23% rejection rate). Absolute (uncorrected) baseline MBF was correlated with baseline RPP in all subjects ($r = 0.622$, $p<0.001$), with a similar correlation in patients ($r=0.602$, $p<0.001$).

Compared to controls, patients (with or without AF at the time of the scan) had significantly lower corrected baseline and stress MBF (**Figure 27A, Figure 27B**). The lower corrected baseline MBF was driven mainly by patients in AF during the CMR scan (**Figure 27C**), whereas impaired stress MBF was seen in all patients, irrespective of the intrascan rhythm (**Figure 27D**). Quantitative myocardial perfusion reserve (calculated as stress MBF divided by corrected baseline MBF) was "pseudo-normal" in patients in AF during CMR, due to significant impairment in both baseline and stress MBF compared to controls (**Table 13**).

The impairment in corrected baseline MBF and stress MBF in patients compared to controls remained significant when subjects without splenic switch-off were excluded from analysis (respectively: 1.21±0.26

mL/min/g.(mmHg.bpm/10^4)$^{-1}$ versus 1.38±0.26 mL/min/g.(mmHg.bpm/10^4)$^{-1}$ for baseline MBF, p=0.016, and 2.33±0.37 mL/min/g versus 2.74±0.36 mL/min/g for stress MBF, p<0.001). There were also no significant differences in either corrected baseline MBF or stress MBF between patients receiving and those not receiving beta-blocker or angiotensin-converting enzyme inhibitor/angiotensin II receptor blocker medications (p=ns for all comparisons).

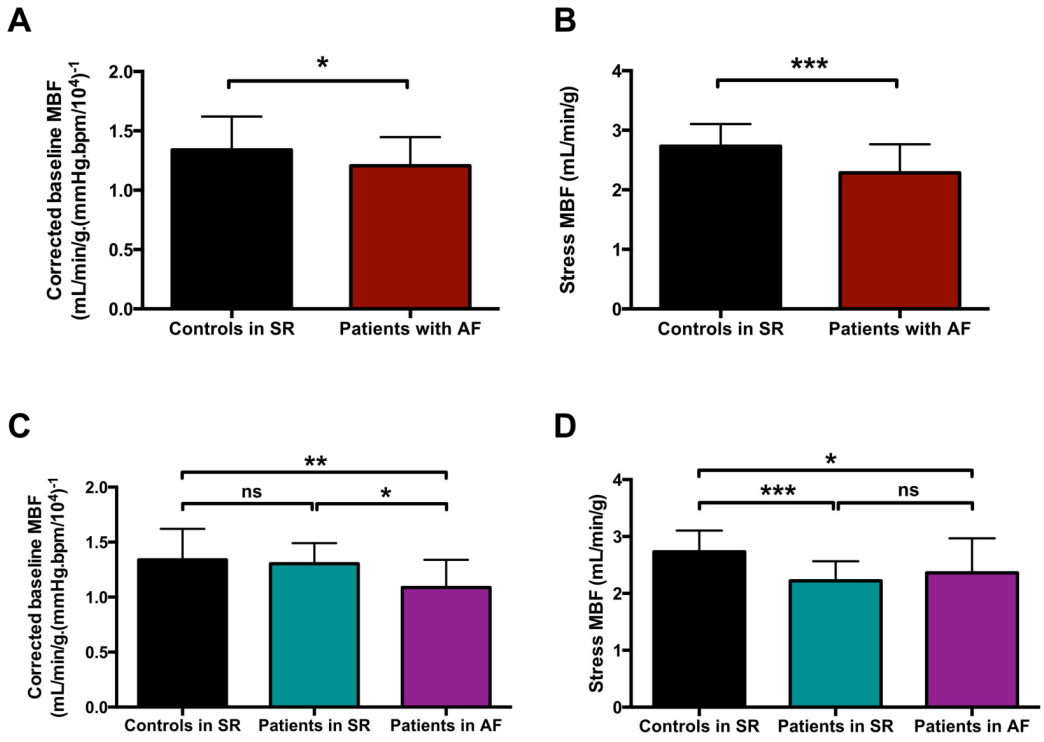


Figure 27: Myocardial blood flow indices pre-ablation. *Compared to matched control subjects in sinus rhythm (SR), patients with atrial fibrillation (AF) pre-ablation have significantly lower corrected baseline myocardial blood flow (MBF) (**A**) and adenosine-stress induced MBF (**B**). Compared to controls, the reduction in corrected baseline MBF in patients is driven mainly by patients with a rhythm of AF at the time of CMR imaging (**C**), whereas stress MBF is impaired in patients irrespective of the rhythm at the time of imaging (**D**). Data are presented as mean ± SD.*

6.4.3 Relationship between LV myocardial blood flow and function

Corrected baseline MBF was positively correlated with peak systolic radial strain (**Figure 28A**), and inversely correlated with peak systolic circumferential strain and peak diastolic radial strain rate (**Figure 28B** and **Figure 28C**, respectively) - i.e. the direction of correlation supported an association between higher corrected baseline MBF and better LV function in each case (all $p \leq 0.001$). Stress MBF showed a weak inverse correlation with peak diastolic strain rate ($r = -0.283$, $p = 0.020$), but no significant correlation with peak systolic radial strain, or peak systolic circumferential strain (both p=ns; **Figure 29**).

Representative examples of the results of functional imaging and absolute MBF quantification are shown in **Figure 30**.

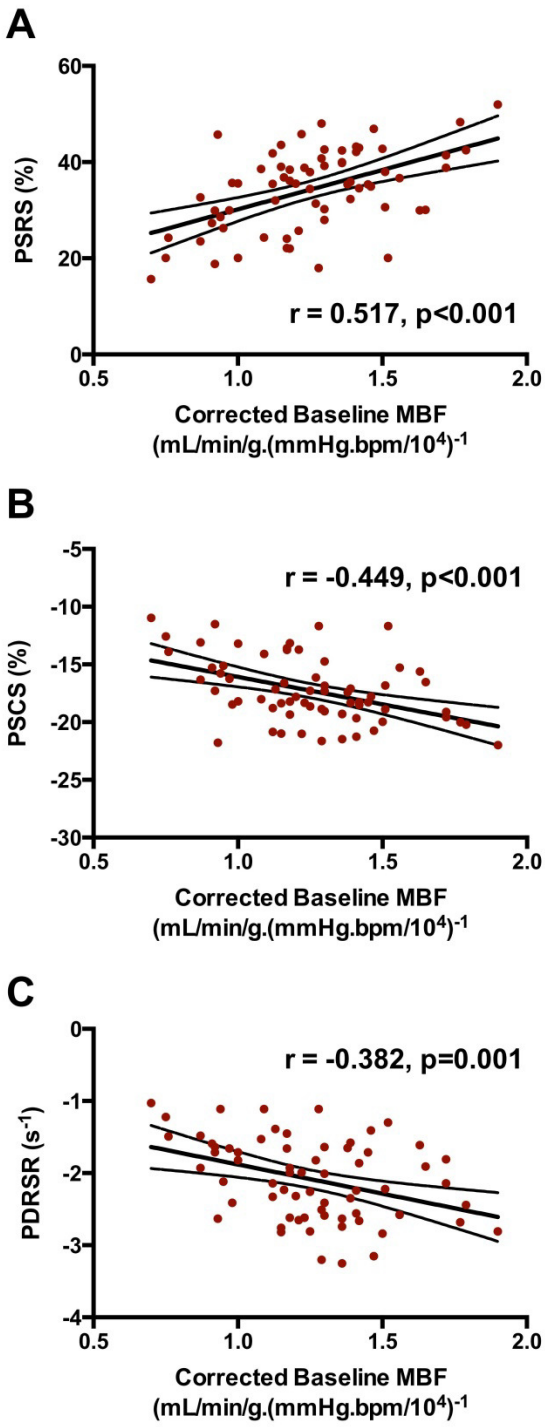


Figure 28: Relationships between baseline myocardial blood flow and indices of left ventricular function. *Relationships between corrected baseline myocardial blood flow (MBF) and peak systolic radial strain (PSRS;* ***A****), peak systolic circumferential strain (PSCS;* ***B****), and peak diastolic radial strain rate (PDRSR;* ***C****) in patients with atrial fibrillation pre-ablation and control subjects in sinus rhythm. Pearson r and the respective p values for the associations are shown in each case. Lines of best-fit and 95% confidence bands are also shown.*

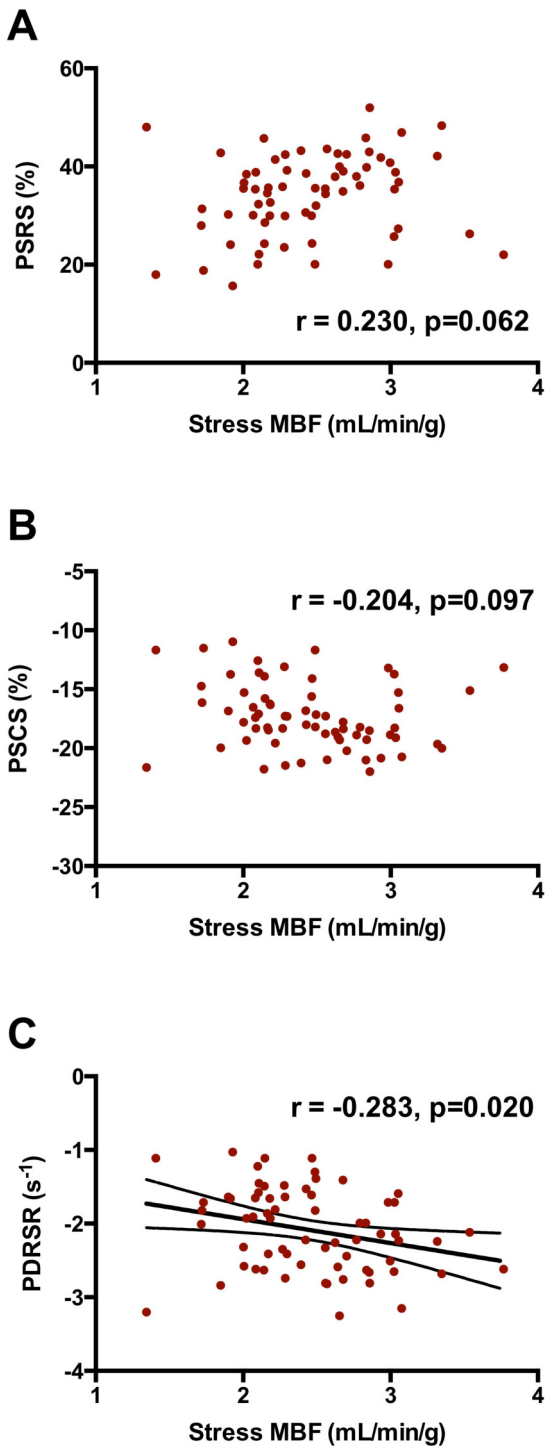


Figure 29: Relationships between stress myocardial blood flow and indices of left ventricular function. *Relationships between stress myocardial blood flow (MBF) and peak systolic radial strain (PSRS; **A**), peak systolic circumferential strain (PSCS; **B**), and peak diastolic radial strain rate (PDRSR; **C**). Pearson r and the respective p values for the associations are shown in each case. Lines of best-fit and 95% confidence bands are also shown for significant associations.*

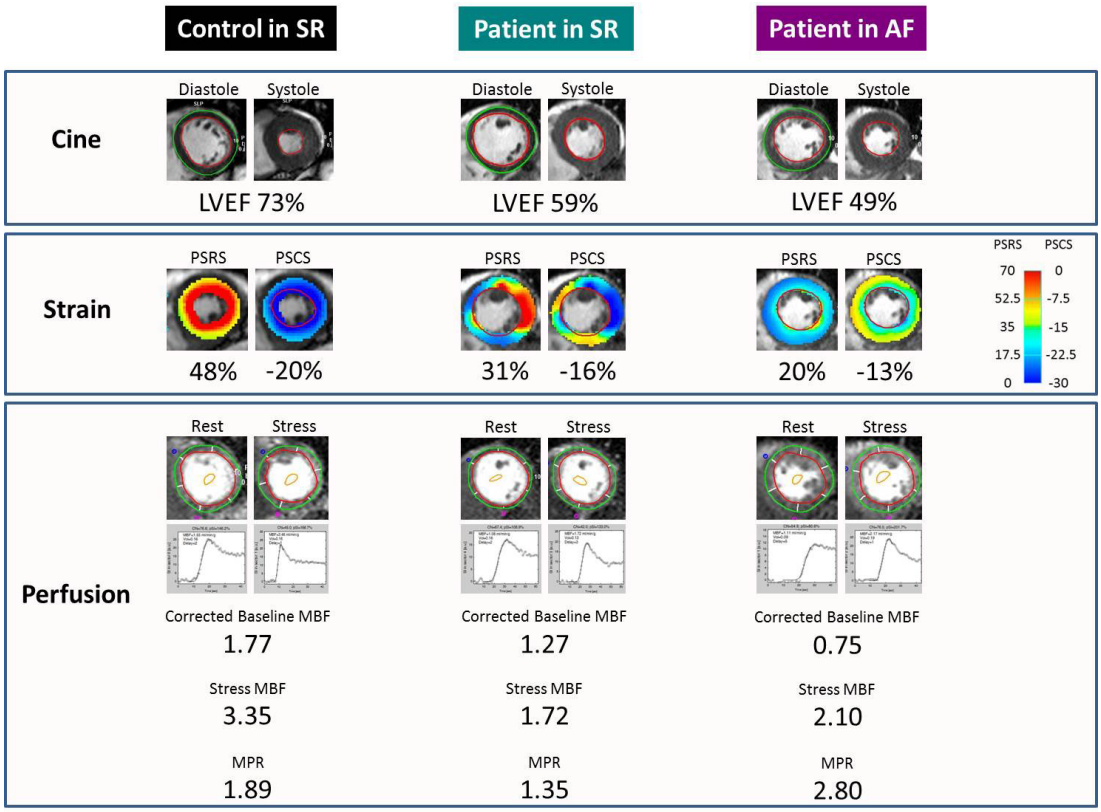


Figure 30: Representative examples of the results of functional and perfusion imaging. *Representative examples of functional imaging and perfusion imaging from a control subject in sinus rhythm (SR), a patient with a history of atrial fibrillation (AF) but in SR during imaging, and a patient in AF during imaging.* ***Top panel*** *shows end-diastolic and end-systolic frames from a single left ventricular (LV) short axis slice, with manually-placed endocardial (red) and epicardial (green) contours. The LV ejection fraction (LVEF) calculated from volumetric analysis of the entire short axis stack is shown. Note lower LVEF in both patients, compared to the control subject in SR. The normal range for LVEF by CMR is 57-81%[120].* ***Middle panel*** *shows the end-systolic frame from a single LV short axis slice, with colour overlays representing pixel-wise peak systolic radial strain (PSRS) and peak systolic circumferential strain (PSCS). Scale bars for PSRS and PSCS are shown – note that the most positive values (red colour) indicate the best function for PSRS, but the most negative values (blue colour) indicate the best function for PSCS. Overall average PSRS and PSCS from global analysis of the stack of short axis images are also shown. Note impaired PSRS and PSCS in both patients, compared to the control subject in SR.* ***Bottom panel*** *shows a single frame during first-pass of contrast through the LV and into the coronary arteries at baseline and peak adenosine stress, with manually-placed endocardial (red), epicardial (green), and LV blood-pool (orange) contours. The model-independent fitting of the tissue response in a single representative myocardial segment under each condition is also shown, as are corrected baseline and stress myocardial blood flow (MBF), and derived myocardial perfusion reserve (MPR). Note lower corrected baseline and stress MBF in both patients, compared to the control in SR. MPR results are difficult to interpret and potentially misleading due to significant differences in baseline and stress MBF. MPR values are a dimensionless index, corrected baseline MBF values are mL/min/g.(mmHg.bpm/104)-1, and stress MBF values are mL/min/g.*

6.4.4 MBF is unaffected despite reduction in AF burden after ablation

Paired pre- and post-ablation MBF and MPR results were available in 33 patients. Within this group, 29 patients (88%) were in SR at the post-ablation CMR scan, and overall there was a significant reduction in Holter-determined AF burden (post-ablation median 0%, IQR 0-0.1%, versus pre-ablation median 11.2%, IQR 0-100%; p=0.001). Despite recovery of SR and reduction in AF burden, corrected baseline and stress MBF were unchanged compared to pre-ablation in paired analyses (both p=ns; **Figure 31**).

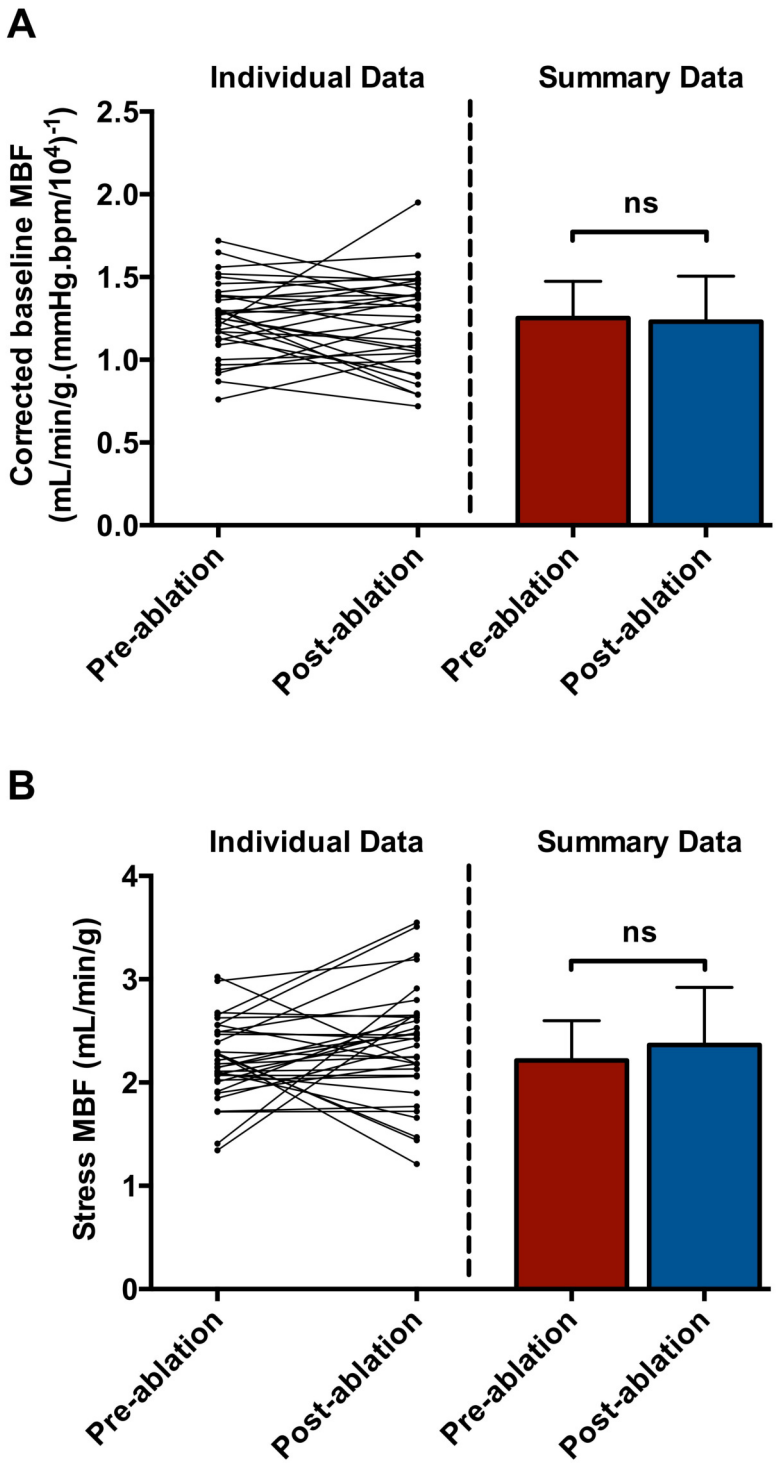


Figure 31: Paired pre- and post-ablation myocardial blood flow. *Individual (left panels) and summary (right panels) results from paired pre- and post-ablation analysis of corrected baseline myocardial blood flow (MBF; **A**) and stress MBF (**B**) in patients with AF (n=33). Neither parameter changes significantly (p=0.59 for corrected baseline MBF and p=0.16 for stress MBF).*

Across all post-ablation patients in whom absolute MBF could be determined (n=40), corrected baseline MBF was positively correlated with peak systolic radial strain, and inversely correlated with peak systolic circumferential strain and peak diastolic radial strain rate (all p≤0.002; **Figure 32**). The correlations with all strain parameters remained significant when analysis was restricted to patients in SR at this timepoint (n=35, all p≤0.006; **Figure 33**), demonstrating that the relationship between baseline MBF and LV function was not significantly affected by rhythm at the time of CMR.

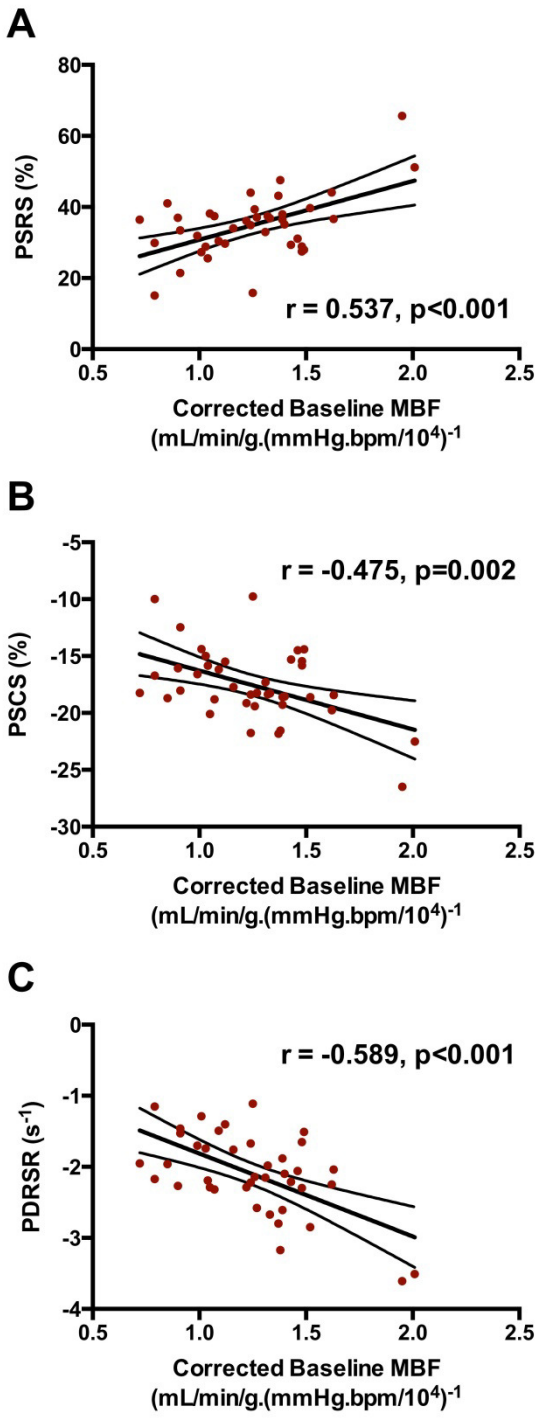


Figure 32: Relationships between baseline myocardial blood flow and indices of left ventricular function after ablation. *Relationships between corrected baseline myocardial blood flow (MBF) and peak systolic radial strain (PSRS; **A**), peak systolic circumferential strain (PSCS; **B**), and peak diastolic radial strain rate (PDRSR; **C**) after ablation. Pearson r and the respective p values for the associations are shown in each case. Lines of best-fit and 95% confidence bands are also shown for significant associations.*

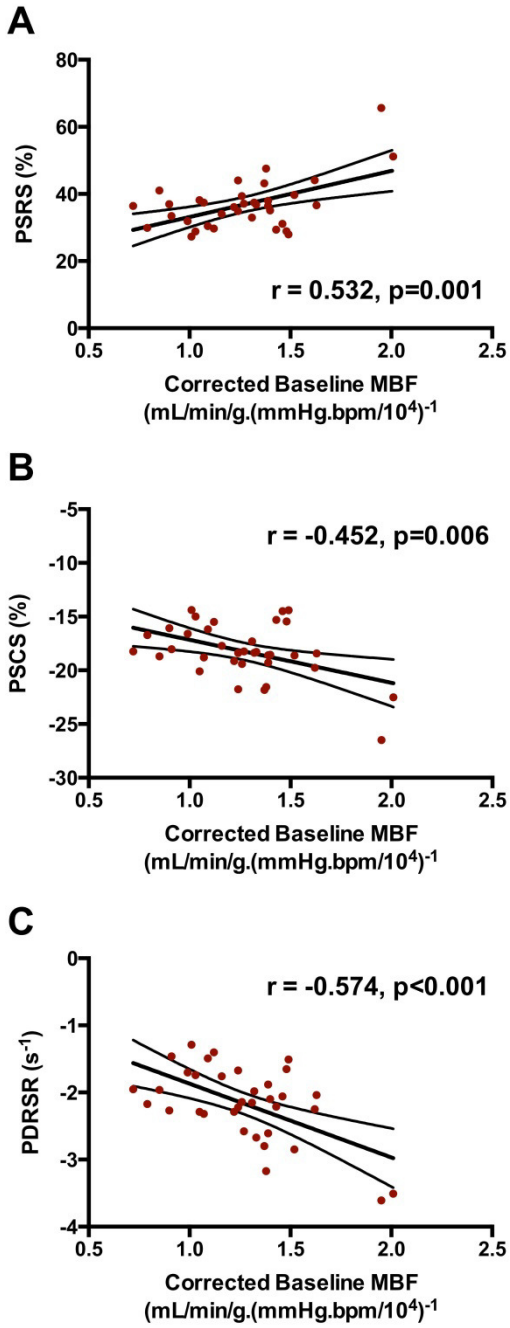


Figure 33: Relationships between baseline myocardial blood flow and indices of left ventricular function in patients in sinus rhythm during the post-ablation CMR scan. *Relationships between corrected baseline myocardial blood flow (MBF) and peak systolic radial strain (PSRS; **A**), peak systolic circumferential strain (PSCS; **B**), and peak diastolic radial strain rate (PDRSR; **C**) in patients in sinus rhythm during the post-ablation CMR scan. Pearson r and the respective p values for the associations are shown in each case. Lines of best-fit and 95% confidence bands are also shown for significant associations.*

6.5 Discussion

This prospective study used advanced CMR techniques to quantify myocardial perfusion at baseline and under conditions of adenosine stress in patients with a diagnosis of AF and no obstructive epicardial coronary disease or other significant comorbidities and in matched controls in SR. As well as showing reduced baseline and stress myocardial blood flow (MBF) in patients with AF compared to controls, these data indicate for the first time that reduced baseline MBF is associated with impairment in strain parameters of LV function. The reduction in baseline and stress MBF, and the association between reduced baseline MBF and impaired LV function, persisted after ablation despite a significant reduction in AF burden. These novel data imply: that lone AF is associated with coronary microvascular dysfunction, that the resultant reduction in MBF is at least partially responsible for subtle LV systolic and diastolic dysfunction, and that ablation alone is insufficient to normalise coronary microvascular function in this group of patients.

6.5.1 Myocardial perfusion in patients with AF

Previous data on myocardial perfusion in patients with AF are limited. One study used positron emission tomography to investigate perfusion and perfusion reserve in 25 male patients with persistent AF and no obstructive epicardial coronary artery disease, and 13 matched male control subjects in SR[57]. Patients with AF had markedly reduced MBF at baseline, and adenosine-

induced hyperaemic MBF was similarly impaired. A small subgroup (10 patients) was investigated again following successful cardioversion to SR. Baseline MBF normalised, and hyperaemic flow and coronary vascular resistance improved significantly from baseline, although these latter parameters remained impaired compared to control subjects.

The present data support the previous findings of impaired baseline and stress MBF in patients with AF compared with matched control subjects in SR, and importantly, extend investigation to females and patients with paroxysmal AF. However, no significant change in baseline or stress MBF was detected following catheter ablation, suggesting that improvements in these parameters previously reported in a very small number of patients following cardioversion[57] may have been due to the play of chance. Moreover, our results are consistent with the previously reported absence of significant differences in myocardial perfusion reserve between patients with AF and matched control subjects in SR[57]. This is not surprising as in patients with hypertrophic or dilated cardiomyopathy (and no obstructive coronary artery disease)[172, 173], stress MBF has been shown to be superior to perfusion reserve for uncovering coronary microvascular dysfunction and predicting adverse cardiac events[174].

Of note, patients with AF in this study had significantly different stress RPP to controls in SR, with patients in AF at the time of imaging showing very limited changes in HR and SBP in response to adenosine. In healthy individuals, intravenous adenosine infusion increases heart rate by reducing

parasympathetic tone and augmenting cardiac sympathetic input to the sinoatrial node, which together override the direct negative chronotropic effect of adenosine[175]. The present findings of blunted changes in HR, SBP, and RPP in response to adenosine in patients with AF compared to matched controls in SR have been noted previously[57]; these differences may reflect the fact that the atrioventricular node (rather than the sinoatrial node) is the main determinant of HR in AF. Nevertheless, adenosine stress CMR remains an accurate clinical diagnostic tool in patients with AF[176]. Indeed, the coronary hyperaemic effects of adenosine are known to be largely independent of changes in cardiac haemodynamics, and the historical use of RPP to demonstrate adequacy of adenosine stress has been questioned[106]. Importantly, rates of splenic switch-off[101] - a recently identified and validated technique for the identification of inadequate stress - were similar between patients with AF and controls in SR in the present study. A sensitivity analysis that excluded subjects without splenic switch-off did not affect the results, confirming that the results are reliable and not confounded by the blunted changes in haemodynamic parameters in patients with AF.

6.5.2 Impaired LV perfusion and function in AF

This study adds unique insight regarding the functional significance of abnormalities in myocardial blood flow in patients with AF. There are highly significant and moderately strong correlations between baseline MBF and strain parameters of LV function, suggesting that reduced baseline MBF could be at

least partially responsible for LV dysfunction in this group of patients. Moreover, the relationship between reduced baseline MBF and indices of LV function was also present after ablation, including in patients who had successfully recovered SR at the time of the scan and had a significant reduction in AF burden on Holter monitoring. These findings imply that the reduction in baseline MBF is not a direct effect of the arrhythmia itself; instead, microvascular dysfunction is more likely to reflect underlying systemic disease or coronary endothelial dysfunction[10]. This paradigm may initially appear inconsistent with results from a mechanistic study in a pig pacing model of AF, where AF induction was associated with a rapid deterioration in microvascular coronary function[56]. However, rapid ventricular rates and reduced duration of diastole could have been the primary driver of impaired myocardial perfusion under those experimental conditions. Importantly, microvascular dysfunction could also affect left atrial perfusion, which was shown to be reduced in previous mechanistic[59] and clinical[177] studies; thus, subclinical supply-demand ischaemia could contribute to the substrate that initiates and maintains AF.

Whilst stress MBF was also impaired in patients with AF compared to controls, this parameter was not correlated with indices of LV systolic function. This may be because all LV functional parameters were measured at baseline, and logically a reduction in stress MBF would be expected to be more important in determining exercise capacity or other parameters of functional cardiac reserve. Interestingly, reduced exercise capacity and functional status are

closely related to the risk of developing AF and precede the onset of the arrhythmia[178]. Future studies are needed to test the hypothesis that impaired stress MBF may underlie the reduction of exercise capacity in individuals at risk of AF.

6.5.3 Clinical implications and future directions

The present findings of impaired baseline and stress MBF in the absence of obstructive epicardial coronary disease, and the links to subtle impairment in LV function, point to an important pathophysiological role for coronary microvascular dysfunction in patients with AF. Coronary microvascular dysfunction is under-recognized, under-diagnosed, and linked to an increased incidence of adverse cardiac events[179]. Aggressive risk factor control and lifestyle modification have been advocated in the management of this condition, as high quality clinical trials demonstrating efficacy of specific pharmacological agents are currently lacking[179]. Intriguingly, a very similar treatment strategy has proven highly efficacious in reducing symptoms and inducing beneficial reverse cardiac remodelling in patients with AF[133].

These results should also be interpreted in the context of the other findings in this well-characterised cohort of patients with lone AF, including impaired LV energetics that persist despite successful ablation, suggesting that apparently lone AF may actually be the consequence (rather than the cause) of an occult cardiomyopathy (see Chapter 3). It is possible that coronary microvascular dysfunction is part of, or even responsible for, the same

underlying disease process. Future studies are needed to determine whether global risk factor management (beyond ablation alone) may improve both myocardial energetics and perfusion in patients with AF. Such a link would provide further evidence for the mechanistic importance of coronary microvascular and energetic dysfunction in AF, and confirm their validity as therapeutic targets. In this context, the lack of ventricular structural remodelling (including LV dilatation, hypertrophy, concentric remodelling, and late gadolinium enhancement – see Chapter 3) and diffuse LV fibrosis (see Chapter 5) in this cohort is particularly pertinent, raising the possibility that subtle LV dysfunction could be entirely reversible if the underlying causes are rapidly identified and successfully targeted.

6.5.4 Limitations

As expected, prescription of beta-blockers and angiotensin-converting enzyme inhibitors/angiotensin II receptor blockers was much more common in patients with AF than in control subjects in SR. A decision was made not to withdraw medications prior to scans, to avoid patients attending with uncontrolled ventricular rate. In any case, the confounding effect of medication use is likely to be very small as there were no significant differences in corrected baseline or stress MBF between patients receiving and not receiving beta-blockers or angiotensin-converting enzyme inhibitors/angiotensin II receptor blockers.

6.6 Conclusion

Baseline and stress myocardial perfusion are significantly impaired in patients with AF and no significant epicardial coronary artery disease, both before and after catheter ablation, and lower baseline blood flow is related to a reduction in LV performance. These novel findings imply that coronary microvascular dysfunction, perhaps due to underlying systemic disease or abnormal coronary endothelial function, is an important pathophysiological mechanism in lone AF which may be, at least partially, responsible for LV dysfunction.

Chapter 7

General conclusions

In conclusion, this Thesis has provided novel insights into LV function in patients with AF, its relationship with myocardial energetics, blood flow and fibrosis, and the effect of catheter ablation and restoration of SR on these parameters. The main findings of this Thesis are:

1. Patients with AF have subtle impairment in LV systolic function compared to matched control subjects in SR, despite a similar ventricular rate and absence of significant cardiovascular comorbidities. This impairment in function has been demonstrated by multiple parameters including LV ejection fraction and multiple strain parameters derived from both MR cine and MR tagging approaches. Myocardial energetic impairment, a characteristic and early feature of cardiomyopathy, is present in patients with AF and is completely unchanged following ablation despite a significant and sustained reduction in AF burden.
2. There is a subtle, but significant, improvement in LV systolic function following ablation. This is driven exclusively by the sub-group of patients that recover SR at the post-ablation assessment having had a rhythm of

AF at the pre-ablation assessment, rather than patients with a significant reduction in AF burden over time but who happen to be in SR at both pre- and post-ablation assessments. Much of the overall improvement is also seen within 24 hours of ablation, and is likely to be due to altered haemodynamics in association with the change of rhythm rather than beneficial cardiac remodelling over time.

3. Similarly, restoration of sinus rhythm and reduction in AF burden both lead to a significant reduction in left atrial volume after ablation. Restoration of sinus rhythm post-ablation led to modest improvement, but not normalisation, in left atrial emptying fraction. Overall, there is no significant effect of ablation on left atrial emptying fraction in this cohort of patients, with atrial function remaining significantly impaired compared to control subjects several months following ablation, when myocardial stunning is expected to have dissipated.

4. Baseline and stress myocardial perfusion are significantly impaired before and after catheter ablation in patients with AF and no significant epicardial coronary artery disease, and lower baseline blood flow is related to a reduction in LV performance. Coronary microvascular dysfunction is likely to be an important pathophysiological mechanism in lone AF, and at least partially responsible for LV dysfunction.

5. Left ventricular dysfunction in lone AF is not attributable to diffuse myocardial fibrosis or focal scarring. This strongly argues against a direct

causal relationship between AF and ventricular fibrosis; underlying comorbidities may underlie both fibrosis and AF in those patients in whom these conditions co-exist. The absence of significant LV scarring and adverse LV remodelling suggest that subtle LV dysfunction in lone AF patients may be reversible, if the underlying causes can be successfully targeted and reversed with appropriate therapeutic strategies that are initiated prior to the development of structural LV remodelling.

Additionally, this Thesis has also established and validated systolic T1-mapping as a method for extending the clinical applicability of advanced MR tissue characterisation to individuals with challenging rhythms. This technique may also aid the investigation of thinner myocardial segments, which could have relevant applications in other diseases such as dilated cardiomyopathy.

There are a number of research directions for future studies based on this work. The following concepts may be of greatest interest, in view of the clinical relevance and therapeutic potential:

1. Identification of the contribution of stress-induced energetic dysfunction, including reduced creatinine kinase flux, and reduced stress myocardial blood flow to left ventricular performance and functional capacity during exercise in patients with AF.
2. Investigation of the impact of combined aggressive risk factor control and lifestyle modification, including weight loss and regular physical

activity, on the structural, functional and metabolic cardiovascular phenotype in patients with AF.

Finally, the concept of sophisticated imaging in patients with AF could also be used to improve mechanistic understanding and reduce clinical uncertainty more broadly. For example, advanced magnetic resonance imaging allows detailed and comprehensive investigation of pathophysiologic mechanisms associated with ischaemic brain injury, including biomarkers of atrial cardiopathy (e.g. left atrial stasis, fibrosis, and function) and carotid plaque characterisation (e.g. identification of complex thrombogenic plaques).

Overall, advanced imaging approaches offer the possibility of a more individualised approach to the treatment of patients with AF, as well as the primary and secondary prevention of cardiovascular complications including stroke and heart failure in high-risk patients (with and without AF).

Bibliography

1. Kirchhof P, Benussi S, Kotecha D, Ahlsson A, Atar D, Casadei B, Castella M, Diener HC, Heidbuchel H, Hendriks J, Hindricks G, Manolis AS, Oldgren J, Popescu BA, Schotten U, Van Putte B, Vardas P, Agewall S, Camm J, Baron Esquivias G, Budts W, Carerj S, Casselman F, Coca A, De Caterina R, Deftereos S, Dobrev D, Ferro JM, Filippatos G, Fitzsimons D, Gorenek B, Guenoun M, Hohnloser SH, Kolh P, Lip GY, Manolis A, McMurray J, Ponikowski P, Rosenhek R, Ruschitzka F, Savelieva I, Sharma S, Suwalski P, Tamargo JL, Taylor CJ, Van Gelder IC, Voors AA, Windecker S, Zamorano JL and Zeppenfeld K. 2016 ESC Guidelines for the management of atrial fibrillation developed in collaboration with EACTS. *European heart journal*. 2016;37:2893-2962.
2. Go AS, Hylek EM, Phillips KA, Chang Y, Henault LE, Selby JV and Singer DE. Prevalence of diagnosed atrial fibrillation in adults: national implications for rhythm management and stroke prevention: the AnTicoagulation and Risk Factors in Atrial Fibrillation (ATRIA) Study. *JAMA : the journal of the American Medical Association*. 2001;285:2370-5.
3. Kannel WB, Abbott RD, Savage DD and McNamara PM. Epidemiologic features of chronic atrial fibrillation: the Framingham study. *The New England journal of medicine*. 1982;306:1018-22.
4. Marijon E, Le Heuzey JY, Connolly S, Yang S, Pogue J, Brueckmann M, Eikelboom J, Themeles E, Ezekowitz M, Wallentin L, Yusuf S and Investigators R-L. Causes of death and influencing factors in patients with atrial fibrillation: a competing-risk analysis from the randomized evaluation of long-term anticoagulant therapy study. *Circulation*. 2013;128:2192-201.
5. Lin HJ, Wolf PA, Kelly-Hayes M, Beiser AS, Kase CS, Benjamin EJ and D'Agostino RB. Stroke severity in atrial fibrillation. The Framingham Study. *Stroke; a journal of cerebral circulation*. 1996;27:1760-4.
6. Soliman EZ, Safford MM, Muntner P, Khodneva Y, Dawood FZ, Zakai NA, Thacker EL, Judd S, Howard VJ, Howard G, Herrington DM and Cushman M. Atrial fibrillation and the risk of myocardial infarction. *JAMA internal medicine*. 2014;174:107-14.
7. Benjamin EJ, Wolf PA, D'Agostino RB, Silbershatz H, Kannel WB and Levy D. Impact of atrial fibrillation on the risk of death: the Framingham Heart Study. *Circulation*. 1998;98:946-52.
8. Nattel S, Burstein B and Dobrev D. Atrial remodeling and atrial fibrillation: mechanisms and implications. *Circulation Arrhythmia and electrophysiology*. 2008;1:62-73.

9. Cha YM, Redfield MM, Shen WK and Gersh BJ. Atrial fibrillation and ventricular dysfunction: a vicious electromechanical cycle. *Circulation*. 2004;109:2839-43.
10. Wijesurendra RS and Casadei B. Atrial fibrillation: effects beyond the atrium? *Cardiovascular research*. 2015;105:238-47.
11. Tops LF, Den Uijl DW, Delgado V, Marsan NA, Zeppenfeld K, Holman E, van der Wall EE, Schalij MJ and Bax JJ. Long-term improvement in left ventricular strain after successful catheter ablation for atrial fibrillation in patients with preserved left ventricular systolic function. *Circulation Arrhythmia and electrophysiology*. 2009;2:249-57.
12. Reant P, Lafitte S, Bougteb H, Sacher F, Mignot A, Douard H, Blanc P, Hocini M, Clementy J, Haissaguerre M, Roudaut R and Jais P. Effect of catheter ablation for isolated paroxysmal atrial fibrillation on longitudinal and circumferential left ventricular systolic function. *The American journal of cardiology*. 2009;103:232-7.
13. Reant P, Lafitte S, Jais P, Serri K, Weerasooriya R, Hocini M, Pillois X, Clementy J, Haissaguerre M and Roudaut R. Reverse remodeling of the left cardiac chambers after catheter ablation after 1 year in a series of patients with isolated atrial fibrillation. *Circulation*. 2005;112:2896-903.
14. Anter E, Jessup M and Callans DJ. Atrial fibrillation and heart failure: treatment considerations for a dual epidemic. *Circulation*. 2009;119:2516-25.
15. Maisel WH and Stevenson LW. Atrial fibrillation in heart failure: epidemiology, pathophysiology, and rationale for therapy. *The American journal of cardiology*. 2003;91:2D-8D.
16. Dries DL, Exner DV, Gersh BJ, Domanski MJ, Waclawiw MA and Stevenson LW. Atrial fibrillation is associated with an increased risk for mortality and heart failure progression in patients with asymptomatic and symptomatic left ventricular systolic dysfunction: a retrospective analysis of the SOLVD trials. Studies of Left Ventricular Dysfunction. *Journal of the American College of Cardiology*. 1998;32:695-703.
17. Kober L, Swedberg K, McMurray JJ, Pfeffer MA, Velazquez EJ, Diaz R, Maggioni AP, Mareev V, Opolski G, Van de Werf F, Zannad F, Ertl G, Solomon SD, Zelenkofske S, Rouleau JL, Leimberger JD and Califf RM. Previously known and newly diagnosed atrial fibrillation: a major risk indicator after a myocardial infarction complicated by heart failure or left ventricular dysfunction. *European journal of heart failure*. 2006;8:591-8.
18. Swedberg K, Olsson LG, Charlesworth A, Cleland J, Hanrath P, Komajda M, Metra M, Torp-Pedersen C and Poole-Wilson P. Prognostic relevance of atrial fibrillation in patients with chronic heart failure on long-term treatment with beta-blockers: results from COMET. *European heart journal*. 2005;26:1303-8.
19. Wyse DG, Waldo AL, DiMarco JP, Domanski MJ, Rosenberg Y, Schron EB, Kellen JC, Greene HL, Mickel MC, Dalquist JE, Corley SD and Atrial Fibrillation Follow-up Investigation of Rhythm Management I. A comparison of rate control and rhythm control in patients with atrial fibrillation. *The New England journal of medicine*. 2002;347:1825-33.

20. Van Gelder IC, Hagens VE, Bosker HA, Kingma JH, Kamp O, Kingma T, Said SA, Darmanata JI, Timmermans AJ, Tijssen JG, Crijns HJ and Rate Control versus Electrical Cardioversion for Persistent Atrial Fibrillation Study G. A comparison of rate control and rhythm control in patients with recurrent persistent atrial fibrillation. *The New England journal of medicine*. 2002;347:1834-40.
21. Roy D, Talajic M, Nattel S, Wyse DG, Dorian P, Lee KL, Bourassa MG, Arnold JM, Buxton AE, Camm AJ, Connolly SJ, Dubuc M, Ducharme A, Guerra PG, Hohnloser SH, Lambert J, Le Heuzey JY, O'Hara G, Pedersen OD, Rouleau JL, Singh BN, Stevenson LW, Stevenson WG, Thibault B, Waldo AL, Atrial F and Congestive Heart Failure I. Rhythm control versus rate control for atrial fibrillation and heart failure. *The New England journal of medicine*. 2008;358:2667-77.
22. Haissaguerre M, Jais P, Shah DC, Takahashi A, Hocini M, Quiniou G, Garrigue S, Le Mouroux A, Le Metayer P and Clementy J. Spontaneous initiation of atrial fibrillation by ectopic beats originating in the pulmonary veins. *The New England journal of medicine*. 1998;339:659-66.
23. European Heart Rhythm A, European Association for Cardio-Thoracic S, Camm AJ, Kirchhof P, Lip GY, Schotten U, Savelieva I, Ernst S, Van Gelder IC, Al-Attar N, Hindricks G, Prendergast B, Heidbuchel H, Alfieri O, Angelini A, Atar D, Colonna P, De Caterina R, De Sutter J, Goette A, Gorenek B, Heldal M, Hohloser SH, Kolh P, Le Heuzey JY, Ponikowski P and Rutten FH. Guidelines for the management of atrial fibrillation: the Task Force for the Management of Atrial Fibrillation of the European Society of Cardiology (ESC). *European heart journal*. 2010;31:2369-429.
24. Catheter Ablation vs Anti-arrhythmic Drug Therapy for Atrial Fibrillation Trial (CABANA). http://clinicaltrials.gov/ct2/show/NCT00911508 (accessed 25/04/2016).
25. Clark DM, Plumb VJ, Epstein AE and Kay GN. Hemodynamic effects of an irregular sequence of ventricular cycle lengths during atrial fibrillation. *Journal of the American College of Cardiology*. 1997;30:1039-45.
26. Iles L, Pfluger H, Phrommintikul A, Cherayath J, Aksit P, Gupta SN, Kaye DM and Taylor AJ. Evaluation of diffuse myocardial fibrosis in heart failure with cardiac magnetic resonance contrast-enhanced T1 mapping. *Journal of the American College of Cardiology*. 2008;52:1574-80.
27. Ling LH, Khammy O, Byrne M, Amirahmadi F, Foster A, Li G, Zhang L, dos Remedios C, Chen C and Kaye DM. Irregular rhythm adversely influences calcium handling in ventricular myocardium: implications for the interaction between heart failure and atrial fibrillation. *Circulation Heart failure*. 2012;5:786-93.
28. Phillips E and Levine SA. Auricular fibrillation without other evidence of heart disease; a cause of reversible heart failure. *The American journal of medicine*. 1949;7:478-89.
29. Trulock KM, Narayan SM and Piccini JP. Rhythm Control in Heart Failure Patients With Atrial Fibrillation: Contemporary Challenges Including the Role of Ablation. *Journal of the American College of Cardiology*. 2014;64:710-721.

30. Bosch RF and Nattel S. Cellular electrophysiology of atrial fibrillation. *Cardiovascular research*. 2002;54:259-69.
31. Deckers JW, Hare JM and Baughman KL. Complications of transvenous right ventricular endomyocardial biopsy in adult patients with cardiomyopathy: a seven-year survey of 546 consecutive diagnostic procedures in a tertiary referral center. *Journal of the American College of Cardiology*. 1992;19:43-7.
32. Hauck AJ, Kearney DL and Edwards WD. Evaluation of postmortem endomyocardial biopsy specimens from 38 patients with lymphocytic myocarditis: implications for role of sampling error. *Mayo Clinic proceedings*. 1989;64:1235-45.
33. Frustaci A, Caldarulo M, Buffon A, Bellocci F, Fenici R and Melina D. Cardiac biopsy in patients with "primary" atrial fibrillation. Histologic evidence of occult myocardial diseases. *Chest*. 1991;100:303-6.
34. Grogan M, Smith HC, Gersh BJ and Wood DL. Left ventricular dysfunction due to atrial fibrillation in patients initially believed to have idiopathic dilated cardiomyopathy. *The American journal of cardiology*. 1992;69:1570-3.
35. Packer DL, Bardy GH, Worley SJ, Smith MS, Cobb FR, Coleman RE, Gallagher JJ and German LD. Tachycardia-induced cardiomyopathy: a reversible form of left ventricular dysfunction. *The American journal of cardiology*. 1986;57:563-70.
36. Dosdall DJ, Ranjan R, Higuchi K, Kholmovski E, Angel N, Li L, Macleod R, Norlund L, Olsen A, Davies CJ and Marrouche NF. Chronic atrial fibrillation causes left ventricular dysfunction in dogs but not goats: experience with dogs, goats, and pigs. *American journal of physiology Heart and circulatory physiology*. 2013;305:H725-31.
37. Ling LH, Taylor AJ, Ellims AH, Iles LM, McLellan AJ, Lee G, Kumar S, Lee G, Teh A, Medi C, Kaye DM, Kalman JM and Kistler PM. Sinus rhythm restores ventricular function in patients with cardiomyopathy and no late gadolinium enhancement on cardiac magnetic resonance imaging who undergo catheter ablation for atrial fibrillation. *Heart Rhythm*. 2013;10:1334-9.
38. Hunter RJ, Berriman TJ, Diab I, Kamdar R, Richmond L, Baker V, Goromonzi F, Sawhney V, Duncan E, Page SP, Ullah W, Unsworth B, Mayet J, Dhinoja M, Earley MJ, Sporton S and Schilling RJ. A randomized controlled trial of catheter ablation versus medical treatment of atrial fibrillation in heart failure (the CAMTAF trial). *Circulation Arrhythmia and electrophysiology*. 2014;7:31-8.
39. Prabhu S, Taylor AJ, Costello BT, Kaye DM, McLellan AA, Voskoboinik A, Sugumar H, Lockwood SM, Stokes MB, Pathik B, Nalliah CJ, Wong GR, Azzopardi SM, Gutman S, Lee G, Layland J, Mariani JA, Ling LH, Kalman JM and Kistler PM. Catheter Ablation Versus Medical Rate control in Atrial Fibrillation and Systolic Dysfunction (CAMERA-MRI). *Journal of the American College of Cardiology*. 2017.
40. Zhu P, Zhang Y, Jiang P, Wang Z, Wang J, Yin X and Hou Y. Effects of radiofrequency catheter ablation on left ventricular structure and function in patients with atrial fibrillation: a meta-analysis. *Journal of interventional cardiac*

electrophysiology : an international journal of arrhythmias and pacing. 2014;40:137-45.
41. Lutomsky BA, Rostock T, Koops A, Steven D, Mullerleile K, Servatius H, Drewitz I, Ueberschar D, Plagemann T, Ventura R, Meinertz T and Willems S. Catheter ablation of paroxysmal atrial fibrillation improves cardiac function: a prospective study on the impact of atrial fibrillation ablation on left ventricular function assessed by magnetic resonance imaging. *Europace*. 2008;10:593-9.
42. Daoud EG, Weiss R, Bahu M, Knight BP, Bogun F, Goyal R, Harvey M, Strickberger SA, Man KC and Morady F. Effect of an irregular ventricular rhythm on cardiac output. *The American journal of cardiology*. 1996;78:1433-6.
43. Van Gelder IC, Crijns HJ, Blanksma PK, Landsman ML, Posma JL, Van Den Berg MP, Meijler FL and Lie KI. Time course of hemodynamic changes and improvement of exercise tolerance after cardioversion of chronic atrial fibrillation unassociated with cardiac valve disease. *The American journal of cardiology*. 1993;72:560-6.
44. Kobayashi Y, Yazawa T, Baba T, Mukai H, Inoue S, Takeyama Y and Niitani H. Clinical, electrophysiological, and histopathological observations in supraventricular tachycardia. *Pacing and clinical electrophysiology : PACE*. 1988;11:1154-67.
45. Moon JC, Messroghli DR, Kellman P, Piechnik SK, Robson MD, Ugander M, Gatehouse PD, Arai AE, Friedrich MG, Neubauer S, Schulz-Menger J and Schelbert EB. Myocardial T1 mapping and extracellular volume quantification: a Society for Cardiovascular Magnetic Resonance (SCMR) and CMR Working Group of the European Society of Cardiology consensus statement. *J Cardiovasc Magn Reson*. 2013;15:92.
46. Ling LH, Kistler PM, Ellims AH, Iles LM, Lee G, Hughes GL, Kalman JM, Kaye DM and Taylor AJ. Diffuse ventricular fibrosis in atrial fibrillation: noninvasive evaluation and relationships with aging and systolic dysfunction. *Journal of the American College of Cardiology*. 2012;60:2402-8.
47. Neilan TG, Mongeon FP, Shah RV, Coelho-Filho O, Abbasi SA, Dodson JA, McMullan CJ, Heydari B, Michaud GF, John RM, Blankstein R, Jerosch-Herold M and Kwong RY. Myocardial extracellular volume expansion and the risk of recurrent atrial fibrillation after pulmonary vein isolation. *JACC Cardiovascular imaging*. 2014;7:1-11.
48. Avitall B, Bi J, Mykytsey A and Chicos A. Atrial and ventricular fibrosis induced by atrial fibrillation: evidence to support early rhythm control. *Heart Rhythm*. 2008;5:839-45.
49. Ling LH, Kalman JM, Ellims AH, Iles LM, Medi C, Sherratt C, Kaye DM, Hare JL, Kistler PM and Taylor AJ. Diffuse ventricular fibrosis is a late outcome of tachycardia-mediated cardiomyopathy after successful ablation. *Circulation Arrhythmia and electrophysiology*. 2013;6:697-704.
50. Yeh YH, Kuo CT, Chang GJ, Qi XY, Nattel S and Chen WJ. Nicotinamide Adenine Dinucleotide Phosphate Oxidase 4 Mediates the Differential Responsiveness of Atrial Versus Ventricular Fibroblasts to Transforming

Growth Factor-beta. *Circulation Arrhythmia and electrophysiology*. 2013;6:790-8.
51. Halperin HR and Nazarian S. Atrial fibrillation and diffuse left ventricular fibrosis, a causal association? *Journal of the American College of Cardiology*. 2012;60:2409-10.
52. Neilan TG, Shah RV, Abbasi SA, Farhad H, Groarke JD, Dodson JA, Coelho-Filho O, McMullan CJ, Heydari B, Michaud GF, John RM, van der Geest R, Steigner ML, Blankstein R, Jerosch-Herold M and Kwong RY. The incidence, pattern, and prognostic value of left ventricular myocardial scar by late gadolinium enhancement in patients with atrial fibrillation. *Journal of the American College of Cardiology*. 2013;62:2205-14.
53. Wong TC, Piehler K, Meier CG, Testa SM, Klock AM, Aneizi AA, Shakesprere J, Kellman P, Shroff SG, Schwartzman DS, Mulukutla SR, Simon MA and Schelbert EB. Association between extracellular matrix expansion quantified by cardiovascular magnetic resonance and short-term mortality. *Circulation*. 2012;126:1206-16.
54. Parwani AS, Boldt LH, Huemer M, Wutzler A, Blaschke D, Rolf S, Mockel M and Haverkamp W. Atrial fibrillation-induced cardiac troponin I release. *International journal of cardiology*. 2013;168:2734-7.
55. van den Bos EJ, Constantinescu AA, van Domburg RT, Akin S, Jordaens LJ and Kofflard MJ. Minor elevations in troponin I are associated with mortality and adverse cardiac events in patients with atrial fibrillation. *European heart journal*. 2011;32:611-7.
56. Bukowska A, Hammwohner M, Sixdorf A, Schild L, Wiswedel I, Rohl FW, Wolke C, Lendeckel U, Aderkast C, Bochmann S, Chilukoti RK, Mostertz J, Bramlage P and Goette A. Dronedarone prevents microcirculatory abnormalities in the left ventricle during atrial tachypacing in pigs. *British journal of pharmacology*. 2012;166:964-80.
57. Range FT, Schafers M, Acil T, Schafers KP, Kies P, Paul M, Hermann S, Brisse B, Breithardt G, Schober O and Wichter T. Impaired myocardial perfusion and perfusion reserve associated with increased coronary resistance in persistent idiopathic atrial fibrillation. *European heart journal*. 2007;28:2223-30.
58. Kochiadakis GE, Skalidis EI, Kalebubas MD, Igoumenidis NE, Chrysostomakis SI, Kanoupakis EM, Simantirakis EN and Vardas PE. Effect of acute atrial fibrillation on phasic coronary blood flow pattern and flow reserve in humans. *European heart journal*. 2002;23:734-41.
59. van Bragt KA, Nasrallah HM, Kuiper M, Luiken JJ, Schotten U and Verheule S. Atrial supply-demand balance in healthy adult pigs: coronary blood flow, oxygen extraction, and lactate production during acute atrial fibrillation. *Cardiovascular research*. 2014;101:9-19.
60. Goette A, Bukowska A, Dobrev D, Pfeiffenberger J, Morawietz H, Strugala D, Wiswedel I, Rohl FW, Wolke C, Bergmann S, Bramlage P, Ravens U and Lendeckel U. Acute atrial tachyarrhythmia induces angiotensin II type 1

receptor-mediated oxidative stress and microvascular flow abnormalities in the ventricles. *European heart journal*. 2009;30:1411-20.
61. Freestone B, Chong AY, Nuttall S and Lip GY. Impaired flow mediated dilatation as evidence of endothelial dysfunction in chronic atrial fibrillation: relationship to plasma von Willebrand factor and soluble E-selectin levels. *Thrombosis research*. 2008;122:85-90.
62. Skalidis EI, Zacharis EA, Tsetis DK, Pagonidis K, Chlouverakis G, Yarmenitis S, Hamilos M, Manios EG and Vardas PE. Endothelial cell function during atrial fibrillation and after restoration of sinus rhythm. *The American journal of cardiology*. 2007;99:1258-62.
63. Guazzi M, Belletti S, Lenatti L, Bianco E and Guazzi MD. Effects of cardioversion of atrial fibrillation on endothelial function in hypertension or diabetes. *European journal of clinical investigation*. 2007;37:26-34.
64. Freestone B, Chong AY, Blann AD and Lip GY. The effects of direct current cardioversion for persistent atrial fibrillation on indices of endothelial damage/dysfunction. *Thrombosis research*. 2006;118:479-85.
65. Shin SY, Na JO, Lim HE, Choi CU, Choi JI, Kim SH, Kim EJ, Park SW, Rha SW, Park CG, Seo HS, Oh DJ and Kim YH. Improved endothelial function in patients with atrial fibrillation through maintenance of sinus rhythm by successful catheter ablation. *Journal of cardiovascular electrophysiology*. 2011;22:376-82.
66. Lim HS, Willoughby SR, Schultz C, Gan C, Alasady M, Lau DH, Leong DP, Brooks AG, Young GD, Kistler PM, Kalman JM, Worthley MI and Sanders P. Effect of atrial fibrillation on atrial thrombogenesis in humans: impact of rate and rhythm. *Journal of the American College of Cardiology*. 2013;61:852-60.
67. Reilly SN, Jayaram R, Nahar K, Antoniades C, Verheule S, Channon KM, Alp NJ, Schotten U and Casadei B. Atrial sources of reactive oxygen species vary with the duration and substrate of atrial fibrillation: implications for the antiarrhythmic effect of statins. *Circulation*. 2011;124:1107-17.
68. Healey JS, Connolly SJ, Gold MR, Israel CW, Van Gelder IC, Capucci A, Lau CP, Fain E, Yang S, Bailleul C, Morillo CA, Carlson M, Themeles E, Kaufman ES, Hohnloser SH and Investigators A. Subclinical atrial fibrillation and the risk of stroke. *The New England journal of medicine*. 2012;366:120-9.
69. Kim YM, Guzik TJ, Zhang YH, Zhang MH, Kattach H, Ratnatunga C, Pillai R, Channon KM and Casadei B. A myocardial Nox2 containing NAD(P)H oxidase contributes to oxidative stress in human atrial fibrillation. *Circulation research*. 2005;97:629-36.
70. Purohit A, Rokita AG, Guan X, Chen B, Koval OM, Voigt N, Neef S, Sowa T, Gao Z, Luczak ED, Stefansdottir H, Behunin AC, Li N, El-Accaoui RN, Yang B, Swaminathan PD, Weiss RM, Wehrens XH, Song LS, Dobrev D, Maier LS and Anderson ME. Oxidized Ca(2+)/calmodulin-dependent protein kinase II triggers atrial fibrillation. *Circulation*. 2013;128:1748-57.
71. Shan J, Xie W, Betzenhauser M, Reiken S, Chen BX, Wronska A and Marks AR. Calcium leak through ryanodine receptors leads to atrial fibrillation in 3

mouse models of catecholaminergic polymorphic ventricular tachycardia. *Circulation research*. 2012;111:708-17.
72. Cai H, Li Z, Goette A, Mera F, Honeycutt C, Feterik K, Wilcox JN, Dudley SC, Jr., Harrison DG and Langberg JJ. Downregulation of endocardial nitric oxide synthase expression and nitric oxide production in atrial fibrillation: potential mechanisms for atrial thrombosis and stroke. *Circulation*. 2002;106:2854-8.
73. Goette A, Bukowska A, Lendeckel U, Erxleben M, Hammwohner M, Strugala D, Pfeiffenberger J, Rohl FW, Huth C, Ebert MP, Klein HU and Rocken C. Angiotensin II receptor blockade reduces tachycardia-induced atrial adhesion molecule expression. *Circulation*. 2008;117:732-42.
74. Goette A, Bukowska A, Lillig CH and Lendeckel U. Oxidative Stress and Microcirculatory Flow Abnormalities in the Ventricles during Atrial Fibrillation. *Frontiers in physiology*. 2012;3:236.
75. Nattel S and Harada M. Atrial Remodeling and Atrial Fibrillation: Recent Advances and Translational Perspectives. *Journal of the American College of Cardiology*. 2014.
76. Simon JN, Duglan D, Casadei B and Carnicer R. Nitric oxide synthase regulation of cardiac excitation-contraction coupling in health and disease. *Journal of molecular and cellular cardiology*. 2014.
77. Voigt N, Li N, Wang Q, Wang W, Trafford AW, Abu-Taha I, Sun Q, Wieland T, Ravens U, Nattel S, Wehrens XH and Dobrev D. Enhanced sarcoplasmic reticulum Ca2+ leak and increased Na+-Ca2+ exchanger function underlie delayed afterdepolarizations in patients with chronic atrial fibrillation. *Circulation*. 2012;125:2059-70.
78. Mihm MJ, Yu F, Carnes CA, Reiser PJ, McCarthy PM, Van Wagoner DR and Bauer JA. Impaired myofibrillar energetics and oxidative injury during human atrial fibrillation. *Circulation*. 2001;104:174-80.
79. Ausma J, Coumans WA, Duimel H, Van der Vusse GJ, Allessie MA and Borgers M. Atrial high energy phosphate content and mitochondrial enzyme activity during chronic atrial fibrillation. *Cardiovascular research*. 2000;47:788-96.
80. Ausma J, Wijffels M, Thone F, Wouters L, Allessie M and Borgers M. Structural changes of atrial myocardium due to sustained atrial fibrillation in the goat. *Circulation*. 1997;96:3157-63.
81. Neubauer S. The failing heart--an engine out of fuel. *The New England journal of medicine*. 2007;356:1140-51.
82. Bottomley PA, Panjrath GS, Lai S, Hirsch GA, Wu K, Najjar SS, Steinberg A, Gerstenblith G and Weiss RG. Metabolic rates of ATP transfer through creatine kinase (CK Flux) predict clinical heart failure events and death. *Science translational medicine*. 2013;5:215re3.
83. Neubauer S, Horn M, Cramer M, Harre K, Newell JB, Peters W, Pabst T, Ertl G, Hahn D, Ingwall JS and Kochsiek K. Myocardial phosphocreatine-to-ATP ratio is a predictor of mortality in patients with dilated cardiomyopathy. *Circulation*. 1997;96:2190-6.

84. Grothues F, Smith GC, Moon JC, Bellenger NG, Collins P, Klein HU and Pennell DJ. Comparison of interstudy reproducibility of cardiovascular magnetic resonance with two-dimensional echocardiography in normal subjects and in patients with heart failure or left ventricular hypertrophy. *The American journal of cardiology*. 2002;90:29-34.
85. Hudsmith LE and Neubauer S. Detection of myocardial disorders by magnetic resonance spectroscopy. *Nature clinical practice*. 2008;5 Suppl 2:S49-56.
86. Nagel E, Klein C, Paetsch I, Hettwer S, Schnackenburg B, Wegscheider K and Fleck E. Magnetic resonance perfusion measurements for the noninvasive detection of coronary artery disease. *Circulation*. 2003;108:432-7.
87. White SK, Sado DM, Flett AS and Moon JC. Characterising the myocardial interstitial space: the clinical relevance of non-invasive imaging. *Heart*. 2012;98:773-9.
88. Popovic ZB and Klein AL. Cracking the mysteries of diastolic function in atrial fibrillation: new technology for an old problem. *JACC Cardiovascular imaging*. 2009;2:1157-8.
89. Kusunose K, Yamada H, Nishio S, Tomita N, Niki T, Yamaguchi K, Koshiba K, Yagi S, Taketani Y, Iwase T, Soeki T, Wakatsuki T, Akaike M and Sata M. Clinical utility of single-beat E/e' obtained by simultaneous recording of flow and tissue Doppler velocities in atrial fibrillation with preserved systolic function. *JACC Cardiovascular imaging*. 2009;2:1147-56.
90. Tyler DJ, Emmanuel Y, Cochlin LE, Hudsmith LE, Holloway CJ, Neubauer S, Clarke K and Robson MD. Reproducibility of 31P cardiac magnetic resonance spectroscopy at 3 T. *NMR in biomedicine*. 2009;22:405-13.
91. Purvis LAB CW, Biasiolli L, Robson MD, Rodgers CT. Linewidth constraints in Matlab AMARES using per-metabolite T2 and per-voxel ΔB0. *In Proceedings of the 22nd Annual Meeting of ISMRM-ESMRMB, Milan, Italy, 2014 Abstract 2885*. 2014.
92. Rodgers CT, Clarke WT, Snyder C, Vaughan JT, Neubauer S and Robson MD. Human cardiac ^{31}P magnetic resonance spectroscopy at 7 tesla. *Magnetic Resonance in Medicine*. 2014;72:304-315.
93. Dodson JA, Neilan TG, Shah RV, Farhad H, Blankstein R, Steigner M, Michaud GF, John R, Abbasi SA, Jerosch-Herold M and Kwong RY. Left atrial passive emptying function determined by cardiac magnetic resonance predicts atrial fibrillation recurrence after pulmonary vein isolation. *Circulation Cardiovascular imaging*. 2014;7:586-92.
94. Kramer CM, Barkhausen J, Flamm SD, Kim RJ, Nagel E and Society for Cardiovascular Magnetic Resonance Board of Trustees Task Force on Standardized P. Standardized cardiovascular magnetic resonance (CMR) protocols 2013 update. *J Cardiovasc Magn Reson*. 2013;15:91.
95. Piechnik SK, Ferreira VM, Dall'Armellina E, Cochlin LE, Greiser A, Neubauer S and Robson MD. Shortened Modified Look-Locker Inversion recovery (ShMOLLI) for clinical myocardial T1-mapping at 1.5 and 3 T within a 9 heartbeat breathhold. *J Cardiovasc Magn Reson*. 2010;12:69.

96. Ferreira VM, Piechnik SK, Dall'Armellina E, Karamitsos TD, Francis JM, Choudhury RP, Friedrich MG, Robson MD and Neubauer S. Non-contrast T1-mapping detects acute myocardial edema with high diagnostic accuracy: a comparison to T2-weighted cardiovascular magnetic resonance. *J Cardiovasc Magn Reson*. 2012;14:42.
97. Piechnik SK, Ferreira VM, Lewandowski AJ, Ntusi NA, Banerjee R, Holloway C, Hofman MB, Sado DM, Maestrini V, White SK, Lazdam M, Karamitsos T, Moon JC, Neubauer S, Leeson P and Robson MD. Normal variation of magnetic resonance T1 relaxation times in the human population at 1.5 T using ShMOLLI. *J Cardiovasc Magn Reson*. 2013;15:13.
98. White SK, Sado DM, Fontana M, Banypersad SM, Maestrini V, Flett AS, Piechnik SK, Robson MD, Hausenloy DJ, Sheikh AM, Hawkins PN and Moon JC. T1 mapping for myocardial extracellular volume measurement by CMR: bolus only versus primed infusion technique. *JACC Cardiovascular imaging*. 2013;6:955-62.
99. Lawton JS, Cupps BP, Knutsen AK, Ma N, Brady BD, Reynolds LM and Pasque MK. Magnetic resonance imaging detects significant sex differences in human myocardial strain. *Biomedical engineering online*. 2011;10:76.
100. Yilmaz A, Athanasiadis A, Mahrholdt H, Voehringer M, Ong P, Hill S, Kispert EM, Seebo M and Sechtem U. Diagnostic value of perfusion cardiovascular magnetic resonance in patients with angina pectoris but normal coronary angiograms assessed by intracoronary acetylcholine testing. *Heart*. 2010;96:372-9.
101. Manisty C, Ripley DP, Herrey AS, Captur G, Wong TC, Petersen SE, Plein S, Peebles C, Schelbert EB, Greenwood JP and Moon JC. Splenic Switch-off: A Tool to Assess Stress Adequacy in Adenosine Perfusion Cardiac MR Imaging. *Radiology*. 2015;276:732-40.
102. Jerosch-Herold M, Swingen C and Seethamraju RT. Myocardial blood flow quantification with MRI by model-independent deconvolution. *Med Phys*. 2002;29:886-97.
103. Petersen SE, Jerosch-Herold M, Hudsmith LE, Robson MD, Francis JM, Doll HA, Selvanayagam JB, Neubauer S and Watkins H. Evidence for microvascular dysfunction in hypertrophic cardiomyopathy: new insights from multiparametric magnetic resonance imaging. *Circulation*. 2007;115:2418-25.
104. Czernin J, Muller P, Chan S, Brunken RC, Porenta G, Krivokapich J, Chen K, Chan A, Phelps ME and Schelbert HR. Influence of age and hemodynamics on myocardial blood flow and flow reserve. *Circulation*. 1993;88:62-9.
105. Selvanayagam JB, Jerosch-Herold M, Porto I, Sheridan D, Cheng AS, Petersen SE, Searle N, Channon KM, Banning AP and Neubauer S. Resting myocardial blood flow is impaired in hibernating myocardium: a magnetic resonance study of quantitative perfusion assessment. *Circulation*. 2005;112:3289-96.
106. Mishra RK, Dorbala S, Logsetty G, Hassan A, Heinonen T, Schelbert HR, Di Carli MF and investigators R. Quantitative relation between hemodynamic changes during intravenous adenosine infusion and the magnitude of coronary

hyperemia: implications for myocardial perfusion imaging. *Journal of the American College of Cardiology*. 2005;45:553-8.
107. Dall'Armellina E, Piechnik SK, Ferreira VM, Si QL, Robson MD, Francis JM, Cuculi F, Kharbanda RK, Banning AP, Choudhury RP, Karamitsos TD and Neubauer S. Cardiovascular magnetic resonance by non contrast T1-mapping allows assessment of severity of injury in acute myocardial infarction. *J Cardiovasc Magn Reson*. 2012;14:15.
108. Nagueh SF, Appleton CP, Gillebert TC, Marino PN, Oh JK, Smiseth OA, Waggoner AD, Flachskampf FA, Pellikka PA and Evangelisa A. Recommendations for the evaluation of left ventricular diastolic function by echocardiography. *Eur J Echocardiogr*. 2009;10:165-93.
109. Scherr D, Dalal D, Henrikson CA, Spragg DD, Berger RD, Calkins H and Cheng A. Prospective comparison of the diagnostic utility of a standard event monitor versus a "leadless" portable ECG monitor in the evaluation of patients with palpitations. *Journal of interventional cardiac electrophysiology : an international journal of arrhythmias and pacing*. 2008;22:39-44.
110. Kaleschke G, Hoffmann B, Drewitz I, Steinbeck G, Naebauer M, Goette A, Breithardt G and Kirchhof P. Prospective, multicentre validation of a simple, patient-operated electrocardiographic system for the detection of arrhythmias and electrocardiographic changes. *Europace*. 2009;11:1362-8.
111. Calkins H, Kuck KH, Cappato R, Brugada J, Camm AJ, Chen SA, Crijns HJ, Damiano RJ, Jr., Davies DW, DiMarco J, Edgerton J, Ellenbogen K, Ezekowitz MD, Haines DE, Haissaguerre M, Hindricks G, Iesaka Y, Jackman W, Jalife J, Jais P, Kalman J, Keane D, Kim YH, Kirchhof P, Klein G, Kottkamp H, Kumagai K, Lindsay BD, Mansour M, Marchlinski FE, McCarthy PM, Mont JL, Morady F, Nademanee K, Nakagawa H, Natale A, Nattel S, Packer DL, Pappone C, Prystowsky E, Raviele A, Reddy V, Ruskin JN, Shemin RJ, Tsao HM and Wilber D. 2012 HRS/EHRA/ECAS Expert Consensus Statement on Catheter and Surgical Ablation of Atrial Fibrillation: recommendations for patient selection, procedural techniques, patient management and follow-up, definitions, endpoints, and research trial design. *Europace*. 14:528-606.
112. Chugh SS, Havmoeller R, Narayanan K, Singh D, Rienstra M, Benjamin EJ, Gillum RF, Kim YH, McAnulty JH, Jr., Zheng ZJ, Forouzanfar MH, Naghavi M, Mensah GA, Ezzati M and Murray CJ. Worldwide epidemiology of atrial fibrillation: a Global Burden of Disease 2010 Study. *Circulation*. 2014;129:837-47.
113. Wijffels MC, Kirchhof CJ, Dorland R and Allessie MA. Atrial fibrillation begets atrial fibrillation. A study in awake chronically instrumented goats. *Circulation*. 1995;92:1954-68.
114. Carnes CA, Chung MK, Nakayama T, Nakayama H, Baliga RS, Piao S, Kanderian A, Pavia S, Hamlin RL, McCarthy PM, Bauer JA and Van Wagoner DR. Ascorbate attenuates atrial pacing-induced peroxynitrite formation and electrical remodeling and decreases the incidence of postoperative atrial fibrillation. *Circulation research*. 2001;89:E32-8.

115. Schotten U, Verheule S, Kirchhof P and Goette A. Pathophysiological mechanisms of atrial fibrillation: a translational appraisal. *Physiological reviews*. 2011;91:265-325.
116. Levy S. Epidemiology and classification of atrial fibrillation. *Journal of cardiovascular electrophysiology*. 1998;9:S78-82.
117. Wyse DG, Van Gelder IC, Ellinor PT, Go AS, Kalman JM, Narayan SM, Nattel S, Schotten U and Rienstra M. Lone atrial fibrillation: does it exist? *Journal of the American College of Cardiology*. 2014;63:1715-23.
118. Hudsmith LE and Neubauer S. Magnetic resonance spectroscopy in myocardial disease. *JACC Cardiovascular imaging*. 2009;2:87-96.
119. Faul F, Erdfelder E, Lang AG and Buchner A. G*Power 3: a flexible statistical power analysis program for the social, behavioral, and biomedical sciences. *Behav Res Methods*. 2007;39:175-91.
120. Hudsmith LE, Petersen SE, Francis JM, Robson MD and Neubauer S. Normal human left and right ventricular and left atrial dimensions using steady state free precession magnetic resonance imaging. *J Cardiovasc Magn Reson*. 2005;7:775-82.
121. Verdecchia P, Schillaci G, Borgioni C, Ciucci A, Battistelli M, Bartoccini C, Santucci A, Santucci C, Reboldi G and Porcellati C. Adverse prognostic significance of concentric remodeling of the left ventricle in hypertensive patients with normal left ventricular mass. *Journal of the American College of Cardiology*. 1995;25:871-8.
122. Dweck MR, Joshi S, Murigu T, Gulati A, Alpendurada F, Jabbour A, Maceira A, Roussin I, Northridge DB, Kilner PJ, Cook SA, Boon NA, Pepper J, Mohiaddin RH, Newby DE, Pennell DJ and Prasad SK. Left ventricular remodeling and hypertrophy in patients with aortic stenosis: insights from cardiovascular magnetic resonance. *J Cardiovasc Magn Reson*. 2012;14:50.
123. Cavassila S, Deval S, Huegen C, van Ormondt D and Graveron-Demilly D. Cramer-Rao bounds: an evaluation tool for quantitation. *NMR in biomedicine*. 2001;14:278-83.
124. Lim HS, Schultz C, Dang J, Alasady M, Lau DH, Brooks AG, Wong CX, Roberts-Thomson KC, Young GD, Worthley MI, Sanders P and Willoughby SR. Time course of inflammation, myocardial injury, and prothrombotic response after radiofrequency catheter ablation for atrial fibrillation. *Circulation Arrhythmia and electrophysiology*. 2014;7:83-9.
125. Hsieh MH, Chiou CW, Wen ZC, Wu CH, Tai CT, Tsai CF, Ding YA, Chang MS and Chen SA. Alterations of heart rate variability after radiofrequency catheter ablation of focal atrial fibrillation originating from pulmonary veins. *Circulation*. 1999;100:2237-43.
126. Kottkamp H. Fibrotic atrial cardiomyopathy: a specific disease/syndrome supplying substrates for atrial fibrillation, atrial tachycardia, sinus node disease, AV node disease, and thromboembolic complications. *Journal of cardiovascular electrophysiology*. 2012;23:797-9.

127. Schotten U, Dobrev D, Platonov PG, Kottkamp H and Hindricks G. Current controversies in determining the main mechanisms of atrial fibrillation. *J Intern Med*. 2016;279:428-38.
128. McGann C, Akoum N, Patel A, Kholmovski E, Revelo P, Damal K, Wilson B, Cates J, Harrison A, Ranjan R, Burgon NS, Greene T, Kim D, Dibella EV, Parker D, Macleod RS and Marrouche NF. Atrial fibrillation ablation outcome is predicted by left atrial remodeling on MRI. *Circulation Arrhythmia and electrophysiology*. 2014;7:23-30.
129. Konrad T, Theis C, Mollnau H, Sonnenschein S, Ocete BQ, Bock K, Munzel T and Rostock T. Primary Persistent Atrial Fibrillation: A Distinct Arrhythmia Subentity of an Ablation Population. *Journal of cardiovascular electrophysiology*. 2015;26:1289-94.
130. Kottkamp H. Human atrial fibrillation substrate: towards a specific fibrotic atrial cardiomyopathy. *European heart journal*. 2013;34:2731-8.
131. Smith CS, Bottomley PA, Schulman SP, Gerstenblith G and Weiss RG. Altered creatine kinase adenosine triphosphate kinetics in failing hypertrophied human myocardium. *Circulation*. 2006;114:1151-8.
132. Hirsch GA, Bottomley PA, Gerstenblith G and Weiss RG. Allopurinol acutely increases adenosine triphospate energy delivery in failing human hearts. *Journal of the American College of Cardiology*. 2012;59:802-8.
133. Abed HS, Wittert GA, Leong DP, Shirazi MG, Bahrami B, Middeldorp ME, Lorimer MF, Lau DH, Antic NA, Brooks AG, Abhayaratna WP, Kalman JM and Sanders P. Effect of weight reduction and cardiometabolic risk factor management on symptom burden and severity in patients with atrial fibrillation: a randomized clinical trial. *JAMA : the journal of the American Medical Association*. 2013;310:2050-60.
134. Pathak RK, Middeldorp ME, Lau DH, Mehta AB, Mahajan R, Twomey D, Alasady M, Hanley L, Antic NA, McEvoy RD, Kalman JM, Abhayaratna WP and Sanders P. Aggressive Risk Factor Reduction Study for Atrial Fibrillation and Implications for the Outcome of Ablation: The ARREST-AF Cohort Study. *Journal of the American College of Cardiology*. 2014;64:2222-31.
135. Hundley WG, Meshack BM, Willett DL, Sayad DE, Lange RA, Willard JE, Landau C, Hillis LD and Peshock RM. Comparison of quantitation of left ventricular volume, ejection fraction, and cardiac output in patients with atrial fibrillation by cine magnetic resonance imaging versus invasive measurements. *The American journal of cardiology*. 1996;78:1119-23.
136. Ugander M, Bagi PS, Oki AJ, Chen B, Hsu LY, Aletras AH, Shah S, Greiser A, Kellman P and Arai AE. Myocardial edema as detected by pre-contrast T1 and T2 CMR delineates area at risk associated with acute myocardial infarction. *JACC Cardiovascular imaging*. 2012;5:596-603.
137. Karamitsos TD, Piechnik SK, Banypersad SM, Fontana M, Ntusi NB, Ferreira VM, Whelan CJ, Myerson SG, Robson MD, Hawkins PN, Neubauer S and Moon JC. Noncontrast T1 mapping for the diagnosis of cardiac amyloidosis. *JACC Cardiovascular imaging*. 2013;6:488-97.

138. Bull S, White SK, Piechnik SK, Flett AS, Ferreira VM, Loudon M, Francis JM, Karamitsos TD, Prendergast BD, Robson MD, Neubauer S, Moon JC and Myerson SG. Human non-contrast T1 values and correlation with histology in diffuse fibrosis. *Heart*. 2013;99:932-7.
139. Sado DM, White SK, Piechnik SK, Banypersad SM, Treibel T, Captur G, Fontana M, Maestrini V, Flett AS, Robson MD, Lachmann RH, Murphy E, Mehta A, Hughes D, Neubauer S, Elliott PM and Moon JC. Identification and assessment of Anderson-Fabry disease by cardiovascular magnetic resonance noncontrast myocardial T1 mapping. *Circulation Cardiovascular imaging*. 2013;6:392-8.
140. Scholz TD, Fleagle SR, Parrish FC, Breon T and Skorton DJ. Effect of tissue fat and water content on nuclear magnetic resonance relaxation times of cardiac and skeletal muscle. *Magnetic resonance imaging*. 1990;8:605-11.
141. Kellman P and Hansen MS. T1-mapping in the heart: accuracy and precision. *J Cardiovasc Magn Reson*. 2014;16:2.
142. Ferreira VM, Piechnik SK, Dall'Armellina E, Karamitsos TD, Francis JM, Ntusi N, Holloway C, Choudhury RP, Kardos A, Robson MD, Friedrich MG and Neubauer S. Native T1-mapping detects the location, extent and patterns of acute myocarditis without the need for gadolinium contrast agents. *J Cardiovasc Magn Reson*. 2014;16:36.
143. Dass S, Suttie JJ, Piechnik SK, Ferreira VM, Holloway CJ, Banerjee R, Mahmod M, Cochlin L, Karamitsos TD, Robson MD, Watkins H and Neubauer S. Myocardial tissue characterization using magnetic resonance noncontrast t1 mapping in hypertrophic and dilated cardiomyopathy. *Circulation Cardiovascular imaging*. 2012;5:726-33.
144. Mahmod M, Piechnik SK, Levelt E, Ferreira VM, Francis JM, Lewis A, Pal N, Dass S, Ashrafian H, Neubauer S and Karamitsos TD. Adenosine stress native T1 mapping in severe aortic stenosis: evidence for a role of the intravascular compartment on myocardial T1 values. *J Cardiovasc Magn Reson*. 2014;16:92.
145. Messroghli DR, Greiser A, Frohlich M, Dietz R and Schulz-Menger J. Optimization and validation of a fully-integrated pulse sequence for modified look-locker inversion-recovery (MOLLI) T1 mapping of the heart. *Journal of magnetic resonance imaging : JMRI*. 2007;26:1081-6.
146. Kawel N, Nacif M, Zavodni A, Jones J, Liu S, Sibley CT and Bluemke DA. T1 mapping of the myocardium: intra-individual assessment of the effect of field strength, cardiac cycle and variation by myocardial region. *J Cardiovasc Magn Reson*. 2012;14:27.
147. Reiter U, Reiter G, Dorr K, Greiser A, Maderthaner R and Fuchsjager M. Normal diastolic and systolic myocardial T1 values at 1.5-T MR imaging: correlations and blood normalization. *Radiology*. 2014;271:365-72.
148. Gregg DE and Sabiston DC, Jr. Effect of cardiac contraction on coronary blood flow. *Circulation*. 1957;15:14-20.
149. Wijesurendra RS, Liu A, Casadei B, Robson MD, Neubauer S, Ferreira VM and Piechnik SK. Systolic ShMOLLI T1-mapping is feasible in tachyarrhythmia, with improved image quality compared to diastolic readout. *Journal of Cardiovascular Magnetic Resonance*. 2015;17:1-2.

150. Tessa C, Diciotti S, Landini N, Lilli A, Del Meglio J, Salvatori L, Giannelli M, Greiser A, Vignali C and Casolo G. Myocardial T1 and T2 mapping in diastolic and systolic phase. *The international journal of cardiovascular imaging*. 2015.
151. Kellman P and Arai AE. Imaging sequences for first pass perfusion --a review. *J Cardiovasc Magn Reson*. 2007;9:525-37.
152. Motwani M, Fairbairn TA, Larghat A, Mather AN, Biglands JD, Radjenovic A, Greenwood JP and Plein S. Systolic versus diastolic acquisition in myocardial perfusion MR imaging. *Radiology*. 2012;262:816-23.
153. Kawel-Boehm N, Dellas Buser T, Greiser A, Bieri O, Bremerich J and Santini F. In-vivo assessment of normal T1 values of the right-ventricular myocardium by cardiac MRI. *The international journal of cardiovascular imaging*. 2014;30:323-8.
154. Patel NJ, Deshmukh A, Pant S, Singh V, Patel N, Arora S, Shah N, Chothani A, Savani GT, Mehta K, Parikh V, Rathod A, Badheka AO, Lafferty J, Kowalski M, Mehta JL, Mitrani RD, Viles-Gonzalez JF and Paydak H. Trends of Hospitalization for Atrial Fibrillation in the United States, 2000 Through 2010: Implications for Healthcare Planning. *Circulation*. 2014.
155. Mann DL. Mechanisms and models in heart failure: A combinatorial approach. *Circulation*. 1999;100:999-1008.
156. Ambale-Venkatesh B and Lima JA. Cardiac MRI: a central prognostic tool in myocardial fibrosis. *Nat Rev Cardiol*. 2015;12:18-29.
157. Kato S, Foppa M, Roujol S, Basha T, Berg S, Kissinger KV, Goddu B, Manning WJ and Nezafat R. Left ventricular native T1 time and the risk of atrial fibrillation recurrence after pulmonary vein isolation in patients with paroxysmal atrial fibrillation. *International journal of cardiology*. 2016;203:848-54.
158. Montgomery JA, Abdallah W, Yoneda ZT, Brittain E, Aznaurov SG, Parvez B, Adkins K, Whalen SP, Estrada JC, Shen S, Crossley GH, Kanagasundram A, Saavedra P, Ellis CR, Lawson M, Darbar D and Shoemaker MB. Measurement of diffuse ventricular fibrosis with myocardial T1 in patients with atrial fibrillation. *J Arrhythm*. 2016;32:51-6.
159. Ferreira VM, Wijesurendra RS, Liu A, Greiser A, Casadei B, Robson MD, Neubauer S and Piechnik SK. Systolic ShMOLLI myocardial T1-mapping for improved robustness to partial-volume effects and applications in tachyarrhythmias. *J Cardiovasc Magn Reson*. 2015;17:77.
160. McLellan AJ, Ling LH, Azzopardi S, Ellims AH, Iles LM, Sellenger MA, Morton JB, Kalman JM, Taylor AJ and Kistler PM. Diffuse ventricular fibrosis measured by T(1) mapping on cardiac MRI predicts success of catheter ablation for atrial fibrillation. *Circulation Arrhythmia and electrophysiology*. 2014;7:834-40.
161. Zhao L, Li S, Ma X, Greiser A, Zhang T, An J, Bai R, Dong J and Fan Z. Systolic MOLLI T1 mapping with heart-rate-dependent pulse sequence sampling scheme is feasible in patients with atrial fibrillation. *J Cardiovasc Magn Reson*. 2016;18:13.

162. Tsao CW, Lyass A, Larson MG, Cheng S, Lam CS, Aragam JR, Benjamin EJ and Vasan RS. Prognosis of Adults With Borderline Left Ventricular Ejection Fraction. *JACC Heart Fail*. 2016;4:502-10.
163. Kara K, Lehmann N, Neumann T, Kalsch H, Mohlenkamp S, Dykun I, Broecker-Preuss M, Pundt N, Moebus S, Jockel KH, Erbel R and Mahabadi AA. NT-proBNP is superior to BNP for predicting first cardiovascular events in the general population: the Heinz Nixdorf Recall Study. *International journal of cardiology*. 2015;183:155-61.
164. Wijesurendra RS, Liu A, Eichhorn C, Ariga R, Levelt E, Clarke WT, Rodgers CT, Karamitsos TD, Bashir Y, Ginks M, Rajappan K, Betts T, Ferreira VM, Neubauer S and Casadei B. Lone Atrial Fibrillation Is Associated With Impaired Left Ventricular Energetics That Persists Despite Successful Catheter Ablation. *Circulation*. 2016;134:1068-1081.
165. Treibel TA, Zemrak F, Sado DM, Banypersad SM, White SK, Maestrini V, Barison A, Patel V, Herrey AS, Davies C, Caulfield MJ, Petersen SE and Moon JC. Extracellular volume quantification in isolated hypertension - changes at the detectable limits? *J Cardiovasc Magn Reson*. 2015;17:74.
166. Soliman EZ, Lopez F, O'Neal WT, Chen LY, Bengtson L, Zhang ZM, Loehr L, Cushman M and Alonso A. Atrial Fibrillation and Risk of ST-Segment Elevation versus Non-ST Segment Elevation Myocardial Infarction: The Atherosclerosis Risk in Communities (ARIC) Study. *Circulation*. 2015.
167. Pradhan R, Chaudhary A and Donato AA. Predictive accuracy of ST depression during rapid atrial fibrillation on the presence of obstructive coronary artery disease. *Am J Emerg Med*. 2012;30:1042-7.
168. Rieber J, Huber A, Erhard I, Mueller S, Schweyer M, Koenig A, Schiele TM, Theisen K, Siebert U, Schoenberg SO, Reiser M and Klauss V. Cardiac magnetic resonance perfusion imaging for the functional assessment of coronary artery disease: a comparison with coronary angiography and fractional flow reserve. *European heart journal*. 2006;27:1465-71.
169. Panting JR, Gatehouse PD, Yang GZ, Grothues F, Firmin DN, Collins P and Pennell DJ. Abnormal subendocardial perfusion in cardiac syndrome X detected by cardiovascular magnetic resonance imaging. *The New England journal of medicine*. 2002;346:1948-53.
170. Lanza GA, Buffon A, Sestito A, Natale L, Sgueglia GA, Galiuto L, Infusino F, Mariani L, Centola A and Crea F. Relation between stress-induced myocardial perfusion defects on cardiovascular magnetic resonance and coronary microvascular dysfunction in patients with cardiac syndrome X. *Journal of the American College of Cardiology*. 2008;51:466-72.
171. Thomson LE, Wei J, Agarwal M, Haft-Baradaran A, Shufelt C, Mehta PK, Gill EB, Johnson BD, Kenkre T, Handberg EM, Li D, Sharif B, Berman DS, Petersen JW, Pepine CJ and Bairey Merz CN. Cardiac magnetic resonance myocardial perfusion reserve index is reduced in women with coronary microvascular dysfunction. A National Heart, Lung, and Blood Institute-sponsored study from the Women's Ischemia Syndrome Evaluation. *Circulation Cardiovascular imaging*. 2015;8.

172. Neglia D, Michelassi C, Trivieri MG, Sambuceti G, Giorgetti A, Pratali L, Gallopin M, Salvadori P, Sorace O, Carpeggiani C, Poddighe R, L'Abbate A and Parodi O. Prognostic role of myocardial blood flow impairment in idiopathic left ventricular dysfunction. *Circulation*. 2002;105:186-93.
173. Cecchi F, Olivotto I, Gistri R, Lorenzoni R, Chiriatti G and Camici PG. Coronary microvascular dysfunction and prognosis in hypertrophic cardiomyopathy. *The New England journal of medicine*. 2003;349:1027-35.
174. Camici PG, d'Amati G and Rimoldi O. Coronary microvascular dysfunction: mechanisms and functional assessment. *Nat Rev Cardiol*. 2015;12:48-62.
175. Rongen GA, Brooks SC, Pollard MJ, Ando S, Dajani HR, Notarius CF and Floras JS. Effect of adenosine on heart rate variability in humans. *Clin Sci (Lond)*. 1999;96:597-604.
176. Greulich S, Steubing H, Birkmeier S, Grun S, Bentz K, Sechtem U and Mahrholdt H. Impact of arrhythmia on diagnostic performance of adenosine stress CMR in patients with suspected or known coronary artery disease. *J Cardiovasc Magn Reson*. 2015;17:94.
177. Skalidis EI, Hamilos MI, Karalis IK, Chlouverakis G, Kochiadakis GE and Vardas PE. Isolated atrial microvascular dysfunction in patients with lone recurrent atrial fibrillation. *Journal of the American College of Cardiology*. 2008;51:2053-7.
178. Ramkumar S, Yang H, Wang Y, Nolan M, Negishi K, Sanders P and Marwick TH. Relation of Functional Status to Risk of Development of Atrial Fibrillation. *The American journal of cardiology*. 2017;119:572-578.
179. Dean J, Cruz SD, Mehta PK and Merz CN. Coronary microvascular dysfunction: sex-specific risk, diagnosis, and therapy. *Nat Rev Cardiol*. 2015;12:406-14.